


Doctoral Dissertation
Doctoral Program in Computer and Control Engineering (34.th cycle)

Model-based and data-based frequency domain design of fixed structure robust controller: a polynomial optimization approach

Abdul Salam
* * * * *

Supervisor
Prof. Diego Regruto Tomalino

Politecnico di Torino
2022

This thesis is licensed under a Creative Commons License, Attribution - Noncommercial-NoDerivative Works 4.0 International: see www.creativecommons.org. The text may be reproduced for non-commercial purposes, provided that credit is given to the original author.

I hereby declare that, the contents and organisation of this dissertation constitute my own original work and does not compromise in any way the rights of third parties, including those relating to the security of personal data.

. . . . . .

Abdul Salam

Turin, 2022

This thesis is dedicated to my late mother, Bibi Khursheed, my wife, Zardana Haq, my son, Abdul Muiz and my daughters, Ayesha and Hareem.

Acknowledgements

This Ph.D. has been an unequivocally metamorphic experience for me, and I could not have accomplished it without the encouragement, support, and guidance of many amazing people in my life. First of all, I would like to thank the Department of Computer and Control Engineering of Politecnico di Torino for providing an excellent research environment and all the necessary facilities to accomplish my doctoral work. I express my deepest gratitude to my advisors, Prof. Vito Cerone and Prof. Diego Regruto, for their time and excellent guidance. I want to pay special thanks to Dr. Valentino Razza and my colleague Dr. Talal Abdalla for their thoughtful questions and comments that prompted me to broaden my research from various perspectives.

I express my deepest gratitude to my late mother for her unconditional love, unwavering commitment to my personal and professional growth, and for inspiring me to pursue my dreams. I wish to thank my brother and sisters for their immense love and unrelenting support throughout my life. Finally, I would also like to say a heartfelt thanks to my wife for persuading me to go abroad for a Ph.D. in unfavorable circumstances and for taking care of our kids while I was away.

Summary

This research is focused on the development of new methods and algorithms for solving polynomial optimization problems arising in the framework of robust control. More specifically, the main objective of the research is to exploit powerful tools and recent mathematical results in polynomial optimization to effectively address some problems widely recognized to be complex ones and/or partially addressed in the past by means of other less effective tools, with particular reference to the problem of fixed-order/fixed-structure (FOFS) robust controller design. The thesis is divided into three parts: the first two parts focus on model-based and direct data-driven design of the FOFS robust controller, which is the main topic of this thesis. Part III is focused on the application of convex relaxation technique for the computation of frequency response envelope for linear-time-invariant (LTI) single-input single-output (SISO) plants affected by parametric uncertainty. The results provided in part III are useful in the context of frequency domain robust controller design. Although the last part of the thesis is not directly focused on the design of FOFS controller, but it represents another interesting application of convex-relaxation techniques in the context of robust frequency domain control.

- **Design of model-based FOFS mixed sensitivity H_∞ controllers for LTI SISO plants.**
  Several methods are available in the literature for designing full-order H_∞ controllers (e.g., Riccati equations approach and linear matrix inequalities approach). The main limitation of such methods is that the obtained controllers often have high order that is challenging to implement in typical industrial settings. To overcome such limitations, many authors in the past have proposed the mixed-sensitivity H_∞ FOFS control design. The main scientific challenge posed by the formulation of the FOFS H_∞ control problem is the non-convexity of the optimization problem required to be solved to design the controller. Existing techniques essentially rely on local optimization algorithms that can typically trap in local minima of the underlying nonconvex optimization problem, possibly leading to control systems that do not satisfy all the assigned requirements.

  In this dissertation, we propose the design of FOFS robust H_∞ controllers,

both for continuous-time (CT) and discrete-time (DT) systems, by using convex relaxation algorithms assuming that the model of the given plant is known. First, we define the feasible controller parameter set, which is the set of the controller parameters that guarantee robust stability of the closed-loop system and the achievement of the nominal performance requirements. Then, we compute a convex relaxation of the nonconvex feasible controller parameter set and formulate the original H_∞ controller design problem as the non-emptiness test of the feasible controller parameter set.

We present three algorithms for the convex relaxation of the feasible controller parameter set. The first algorithm exploits the celebrated Putinar's positivstellensatz, the second algorithm uses a generalization of the S-procedure, and the third algorithm employs a moment relaxation-based exchange method for the convex relaxation of the feasible controller parameter set.

- **Direct data-driven FOFS mixed-sensitivity H_∞ control design for LTI SISO plants using frequency domain experimental data.**
  In industrial settings, low order/fixed structure controllers are typically preferred to meet stringent constraints in terms of computational resources. Furthermore, in many cases, an accurate mathematical model of the plant to be controlled is either not available or difficult to derive through a simple (not expensive) procedure. This limitation motivates the development of data-driven controller design methodologies that allows the user to design controllers directly from a set of input-output data experimentally collected from the plant. In the context of data-driven design, parametric uncertainties and unmodeled dynamics (for LTI systems) do not come into play since a mathematical model of the plant is not required. Therefore, the only source of uncertainty comes from the measurement process. This fact suggests that the controller design problem can suitably be reformulated in terms of system identification problem by directly identifying the controller from the available input-output data. Although several contributions are proposed in recent years about direct data-driven controller design based on time-domain data, only a few authors have considered the case of frequency domain data. Most of the existing frequency-domain methods use local optimization algorithms for designing FOFS direct data-driven controllers. However, these algorithms can typically trap in local minima.

  This dissertation proposes the convex relaxation-based algorithms for designing the robust direct data-driven mixed-sensitivity H_∞ FOFS controllers. For a given controller structure and/or order and a set of frequency-domain input-output data, we first define a feasible controller parameter set which is the set of controller parameters that guarantee closed-loop stability and satisfy the H_∞-norm of performance constraints. Then we reformulate the original

problem as a polynomial optimization problem and compute the controller parameters by relaxing the non-convex feasible controller parameter set through convex relaxation methods. We also derive the necessary and sufficient conditions for closed stability in the direct data-driven framework. Finally, we extend this methodology to systems subjected to frequency-domain uncertainties. Two types are uncertainties are considered in this work (i) unstructured uncertainty described by the frequency domain transfer function and (ii) unknown but bounded uncertainty affecting the experimentally collected input-output data.

- **Computation of Bode envelope bounds for LTI SISO systems affected by parametric uncertainty.**
  When a plant's model is developed from the first principles of physics or identified from the input-output data, uncertainty in each parameter is provided typically as an interval, and correlation between the parameters is either implicitly ignored or described in terms of linear or multilinear relationships only. Several techniques for computing the Bode envelope bounds of an uncertain system have been proposed in the past. These methods typically rely on an interval, linear, or multilinear description of the parametric uncertainty and, as a result, produce conservative Bode envelope bounds.

  In this dissertation, we propose a new approach for computing the Bode envelopes bounds that can account for possible nonlinear correlations between different uncertain parameters. In the proposed method, based on the description of the parametric uncertainty implicitly provided by the feasible parameter set, a suitable polynomial optimization problem is formulated whose global optima can be approximated arbitrarily well using the convex semi-definite program (SDP) relaxation.

Contents

List of Tables

List of Figures

Chapter 1

Introduction

1.1 General introduction to the control systems design

The control system is an integral part of our modern society. It has numerous applications ranging from simple household washing machines to complex systems like aircraft and modern rockets. In fact, control system theory can be applied to electrical, mechanical, chemical, social, financial, and biological systems. To provide a general overview of the control system, consider the following control scheme where r_t is the reference signal, e_t is the error signal, u_t is the control signal, d_{it} is the input disturbance, d_{ot} is the output disturbance and y_t is the output.

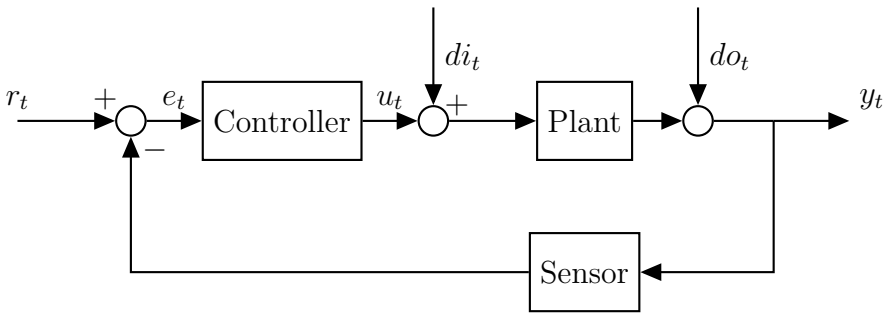

Figure 1.1: A basic control system

In control system design, the plant is represented by its mathematical model. The mathematical model of a real system is developed by two methods. The first method relies on physical laws to construct the mathematical models whereas the second method uses experimental data to develop mathematical models. Sensors are the measuring devices used in the feedback loop to monitor the value of the output variable. The feedback control system uses various types of sensors for

different applications. Some examples of sensors include potentiometers, current sensors, motion sensors, temperature sensors, and flow sensors. The objective of the control system is to track the reference and reject the disturbance while keeping the closed-loop system stable.

In the classical control system, a mathematical model of the plant is represented in the frequency domain. Classical controllers are then designed by using graphical tools such as bode plots and Nyquist plots. Modern control design methods utilize the state-space representation of the plant model. By optimizing the specified objective function, these approaches can efficiently solve complex control problems. Modern control systems are very attractive due to their ability to design for both performance and cost. The major drawback of these methods is the assumption that the plant's model is known to be exact. The real-world systems are subjected to uncertainties, and controllers designed using classical and modern control approaches may not provide optimal performance in the presence of uncertainty.

Robust control is the branch of the control system that explicitly deals with uncertainties. Some of the popular examples of robust control methods are loop shaping, H_∞ control, parametric robust control, quantitative feedback theory, and sliding mode control. H_∞ control is one of the first methods proposed for solving the problem of robustness. This elegant approach is highly developed and many control system problems can be formulated in H_∞ framework. Here, we provide a basic review of mixed sensitivity H_∞ control.

1.2 Mixed sensitivity H_∞ control

In this section, we provide a review of some of the basics of H_∞ mixed sensitivity control theory. Consider a transfer function $C(\epsilon)$ defined in a generic variable ϵ. For CT systems, $\epsilon = s$ and for DT systems $\epsilon = z$. For CT systems, the frequency response is obtained by replacing $\epsilon = j\omega$. Similarly, frequency response of a DT system is computed by substituting $\epsilon = e^{j\omega T_s}$, where T_s is the sampling time.

Now consider the feedback control system shown in Figure 1.2, where $G_n(\epsilon)$ is the nominal plant, $K(\epsilon)$ is the controller, $r_t \in \mathbb{R}$ is the reference signal, $u_t \in \mathbb{R}$ is the control input, $y_t \in \mathbb{R}$ is the measured output and $z_1 \in \mathbb{R}^{n_1}$ and $z_2 \in \mathbb{R}^{n_2}$ are the controlled outputs associated to the assigned performance requirements.

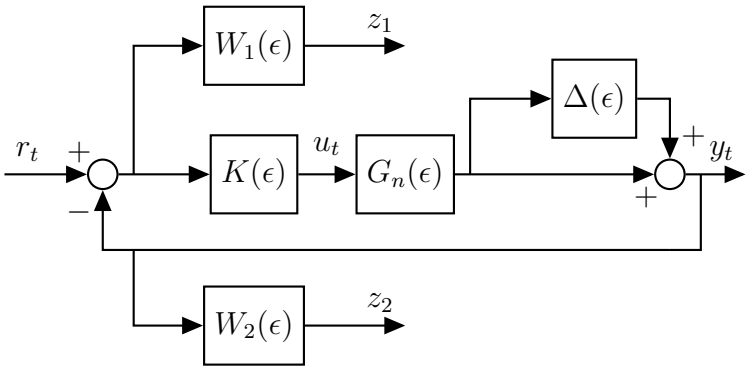

Figure 1.2: Block diagram of feedback system.

The uncertain model of the plant $G(\epsilon)$ is described by

$$G(\epsilon) = G_n(\epsilon)(1 + \Delta(\epsilon)) \tag{1.1}$$

where $\Delta(\epsilon) \in \mathbb{C}$ is unstructured multiplicative uncertainty, which is bounded by a frequency domain weighting filter $W_u(\epsilon)$, i.e.,

$$|\Delta(\epsilon)| \leq |W_u(\epsilon)|, \forall \omega \in \Omega \tag{1.2}$$

such that $\Omega = [0, +\infty)$ for CT systems and $\Omega = \left[0, \frac{\pi}{T_s}\right]$ for DT systems.

For a given nominal plant $G_n(\epsilon)$ and a controller $K(\epsilon)$, the nominal loop transfer function is defined as

$$L_n(\epsilon) = K(\epsilon)G_n(\epsilon). \tag{1.3}$$

Similarly, the nominal sensitivity function $S_n(\epsilon)$ and complementary sensitivity function $T_n(\epsilon)$ are defined as

$$S_n(\epsilon) = (1 + L_n(\epsilon))^{-1} \tag{1.4}$$

and

$$T_n(\epsilon) = L_n(\epsilon)(1 + L_n(\epsilon))^{-1}. \tag{1.5}$$

In figure 1.2, $W_1(\epsilon)$ and $W_2(\epsilon)$ are suitable weighting filters that are designed according to both time-domain and frequency-domain performance requirements (for details, see e.g., [92]). The closed-loop system achieves the nominal performances if

$$\begin{aligned} \|S_n(\epsilon)W_1(\epsilon)\|_\infty &\leq 1 \\ \|T_n(\epsilon)W_2(\epsilon)\|_\infty &\leq 1 \end{aligned} \tag{1.6}$$

where $\|\cdot\|_\infty$ is the H_∞ norm of a dynamical system, which, for a generic SISO system $H(\epsilon)$, is

$$\|H(\epsilon)\|_\infty = \sup_{\omega\in\Omega} |H(j\omega)|. \tag{1.7}$$

Now, we review some definitions and results about feedback systems properties.

Definition 1. *A feedback system is said to be well-posed if all closed-loop transfer functions, defined from any exogenous input to all internal signals, are well-defined and proper (see, e.g.,[85]).*

Result 1. *A necessary and sufficient condition for well-posedness is that $S_n(\epsilon)$ exists and is proper, i.e., $1+K(\epsilon)G_n(\epsilon)$ is not strictly proper. A stronger condition for well-posedness is that either $K(\epsilon)$ or $G_n(\epsilon)$ be strictly proper transfer functions (see, e.g., [95]).*

Definition 2. *A well-posed feedback system is internally stable if, and only if, all the transfer functions from any input to any output are BIBO stable (see, e.g., [85]).*

Result 2. *The feedback system is internally stable if and only if: (i) the nominal sensitivity function $S_n(\epsilon)$ is BIBO stable (ii) there are no zero/pole cancellations in $\Re[s] \geq 0$ for CT systems and on or outside unit circle in DT systems while forming the loop transfer functions [85], where $\Re[.]$ stands for real of $[.]$.*

Definition 3. *A feedback system is robustly stable if the controller $K(\epsilon)$ makes the system internally stable for all possible uncertain plants.*

Result 3. *By applying the small gain theorem (see, e.g., [85]), the system shown in Figure 1.2 is robustly stable if the nominal sensitivity function $S_n(\epsilon)$ is stable and*

$$\|T_n(\epsilon)W_u(\epsilon)\|_\infty \leq 1. \tag{1.8}$$

For further details on robust stability, please see [95].

1.3 Parametric robust control

H_∞ control theory is deficient in addressing some issues when parametric uncertainty is considered. Parametric robust control theory efficiently deals with the systems subjected to parametric uncertainty. This branch of the robust control is highly developed and some of its contributions are:

(1) the determination of the stability and stability margins under parametric uncertainty,

(2) the evaluation of H_∞ control performance for the parametric uncertainty set, and

(3) extension of the classical control methods to design controllers for systems that have many uncertain real parameters.

For further details on the parametric robust control, the interested readers are referred to [146] and the references therein.

1.4 Direct data driven control

As discussed earlier, robust control theory emerged to account for uncertainties in the plant's model. However, finding an accurate model which is simple enough for the control system design and finding appropriate bounds for the associated uncertainties can be complex, time-consuming, or costly for many applications. Thus, in such applications, direct data-driven control should be considered where instead of identifying the model of the plant, the controller is directly synthesized from the input-output data. Direct data-driven control theory is maturing very fast and many techniques such as model reference adaptive control, predictive data-driven control, and robust data-driven control are available for solving different control problems.

1.5 Dissertation topics

This dissertation aims to provide the convex relaxation algorithms for different polynomial optimization problems that arise in solving robust control problems. More specifically, we present the convex relaxation algorithms for (i) model-based mixed-sensitivity H_∞ fixed-order/fixed-structure (FOFS) control design for LTI SISO plants, (ii) direct data-driven mixed-sensitivity H_∞ FOFS control design for LTI SISO plants and, (iii) computation of frequency response bounds for LTI SISO systems affected by parametric uncertainty.

This thesis is organized as follows. In Chapter 2, convex relaxation techniques originally proposed for relaxing the nonconvex polynomial optimization problems to convex optimization problems are reviewed. Then, the dissertation is divided into three parts and each part contains its own introduction and conclusion.

Part-I presents the design of robust FOFS H_∞ mixed sensitivity control for LTI SISO plants assuming that the plant model is already available. The problem is formulated as a nonconvex polynomial optimization problem which is then relaxed by three convex relaxation algorithms.

Part II of the thesis provides the design of robust FOFS H_∞ mixed sensitivity control, using data experimentally collected from the LTI SISO plant. The control design problem is formulated as a polynomial optimization problem, which is then relaxed via moment relaxation.

Part-III deals with the computation of the Bode envelopes for the uncertain LTI systems subjected to parametric uncertainty. The problem is formulated as a polynomial optimization problem, which is then relaxed to an SDP via convex relaxation.

Chapter 2

Positive polynomials and convex relaxation of polynomial optimization problems

In this chapter, we review some of the elementary results on the sum-of-squares (SOS) representation of positive polynomials and moment relaxation of polynomial optimization problems. These results are used throughout the thesis for designing FOFS H_∞ controllers and computation of Bode envelopes for parametric uncertain plants. A detail discussion on the SOS decomposition and moment relaxation can be found in [27], [104] and [111].

2.1 SOS representation of positive polynomials

Testing the positivity of a polynomial is a common problem in control system theory. However, checking the non-negativity of a polynomial is generally NP-hard, especially when the degree of the polynomial is higher than four (see e. g., [89]). On the other hand, testing whether a polynomial is an SOS can be formulated as an SDP, which can be solved in polynomial time. We will show in this section that if a non-negative polynomial has an SOS representation, it can be computed by solving an SDP.

Suppose $\mathbb{R}[x]$ denotes the ring of polynomials in $x = (x_1, x_2, \ldots, x_n)$. A polynomial $f(x) \in \mathbb{R}[x]$ is said to be positive if $f(x) > 0$ for every $x \in \mathbb{R}^n$. On the other hand, $f(x) \in \mathbb{R}[x]$ is said to be SOS, if there exist $g_1(x), \ldots, g_k(x) \in \mathbb{R}[x]$, such that:

$$f(x) = \sum_{i=1}^{k} g_i^2(x). \tag{2.1}$$

If a polynomial $f(x)$ is SOS then it is always positive. However, the converse

of this is not always true, that is, a positive polynomial does not always have an SOS decomposition. For univariate polynomials, the relationship between non-negativity and the SOS decomposition is provided by the following result.

Result 4. *An even degree polynomial in a single variable is non-negative, if and only if, it can be represented as an SOS of other polynomials.*

The proof of result 4 can be found in [104].

By the end of 19^{th} century, it was known that all the one variable positive polynomials and two variables, degree two positive polynomials have the SOS decomposition. In 1900, Hilbert hypothesized that every positive polynomial could be written as an SOS of rational functions. This was later proved by E. Artin in 1926.

Result 5. *(Artin's Theorem)*
Suppose, $\mathbb{R}[x]$ denote the ring of real polynomials $\mathbb{R}[x_1, x_2, x_3, \ldots, x_n]$. Suppose $f(x) \in \mathbb{R}[x]$ is non-negative, then there exist a non-zero $h(x) \in \mathbb{R}[x]$ such that $h^2(x)f(x)$ is SOS.

The proof can be found in [35].

It is important to note that the certificate of non-negativity provided by the Artin always exists if we relax the condition that the certificate must be in the polynomial ring $\mathbb{R}[x]$, that is, we must allow denominators.

2.1.1 SOS decomposition and semi-definite optimization

Consider an even degree polynomial $g(x) \in \mathbb{R}[x]_{2d}$. Suppose $\boldsymbol{v}_d(x)$ is the vector of all the monomials of degree less than or equal to d, given by

$$\boldsymbol{v}_d(x) = \left(1, x_1, \ldots, x_n, x_1^2, x_1x_2, \ldots, x_{n-1}x_n, x_n^2 \ldots, x_1^d, \ldots, x_n^d\right)^T \in \mathbb{R}^{\ell_d} \tag{2.2}$$

where $\ell_d = \binom{n+d}{d}$. The polynomial $f(x)$ can be expressed as a quadratic form in the monomial vector $\boldsymbol{v}_d(x)$ thanks to the following result.

Result 6. *A polynomial $f(x) \in \mathbb{R}[x]_{2d}$ has a SOS decomposition if, and only if, there exists a real symmetric and positive semi-definite matrix $Q \in \mathbb{R}^{\ell_d \times \ell_d}$, such that $f(x) = \boldsymbol{v}_d(x)^T Q \boldsymbol{v}_d(x)$, for all $x \in \mathbb{R}^n$ (see [104] for a detailed proof).*

Thus, the problem of checking whether a polynomial $f(x)$ is SOS is equivalent to the problem of finding a symmetric positive definite matrix $Q \in R^{\ell_d \times \ell_d}$.

Construction of an equivalent SDP for computing the SOS decomposition of $f(x)$ in result 6 is difficult when the degree of $f(x)$ is high. However, some MATLAB tools such as YALMIP [78] and SOSTOOLS [131] are available that can automatically compute the SOS decomposition of polynomials that have a large degree. These tools use SeDumi [153] and Mosek [115] SDP solver for computing the SOS decomposition.

Example 1. *Consider the following polynomial in two variables x_1 and x_2.*

$$f(x_1, x_2) = x_1^4 + 2x_2^4 - 2x_1x_2^3. \tag{2.3}$$

we want to check whether $f(x_1, x_2)$ has SOS decomposition using result 6. For this purpose, we write $f(x_1, x_2)$ in the following form.

$$\begin{aligned} f(x_1, x_2) &= \begin{bmatrix} x_1^2 \\ x_2^2 \\ x_1x_2 \end{bmatrix}^T \begin{bmatrix} q_{11} & q_{12} & q_{13} \\ q_{12} & q_{22} & q_{23} \\ q_{13} & q_{23} & q_{33} \end{bmatrix} \begin{bmatrix} x_1^2 \\ x_2^2 \\ x_1x_2 \end{bmatrix} \\ &= q_{11}x_1^4 + q_{22}x_2^4 + (q_{33} + 2q_{12})x_1^2x_2^2 + 2q_{13}x_1^3x_2 + 2q_{23}x_1x_2^3 \end{aligned} \tag{2.4}$$

From equations (2.3)-(2.4), we can write the following inequalities.

$$q_{11} = 1, \quad q_{22} = 2, \quad q_{33} + 2q_{12} = 0, \quad q_{13} = 0, \quad q_{23} = -1 \tag{2.5}$$

By using semidefinite programming, a positive semidefinite matrix Q that fulfills the above linear equalities can be found. One such solution is given by:

$$Q = H^TH = \begin{bmatrix} 1 & -1 & 0 \\ -1 & 2 & -1 \\ 0 & -1 & 2 \end{bmatrix} \tag{2.6}$$

where,

$$H = \begin{bmatrix} 1 & -1 & 0 \\ 0 & 1 & -1 \\ 0 & 0 & 1 \end{bmatrix}.$$

Thus, SOS decomposition of $f(x_1, x_2)$ is given by:

$$f(x_1, x_2) = (x_1^2 - x_2^2)^2 + (x_2^2 - x_1x_2)^2 + (x_1x_2)^2. \tag{2.7}$$

2.2 Positive polynomials over a compact semi-algebraic set

In this section, we provide results for the positivity of a polynomial $f(x) \in \mathbb{R}[x]$ over a semialgebraic set

$$\Phi = \{x \in \mathbb{R}^n : q_1(x) \geq 0, q_2(x) \geq 0, \ldots, q_m(x) \geq 0\} \tag{2.8}$$

where, $q_1(x), q_2(x), \ldots, q_m(x) \in \mathbb{R}[x]$.

The preordering generated by the set Φ is:

$$PO(\Phi) = \left\{ \sum_{J \subseteq \{1,\ldots,m\}} \sigma_J q_J : \sigma_J \in \Sigma[x] \right\} \tag{2.9}$$

where $q_J = \prod_{\nu \in J} q_\nu(x)$ and $\Sigma[x]$ is the set of SOS polynomials. The quadratic module generated by the set Φ is given by:

$$Q(\Phi) = \left\{ \sigma_0 + \sum_{\nu=1}^{m} \sigma_\nu q_\nu : \sigma_\nu \in \Sigma[x] \right\}. \tag{2.10}$$

It is worth mentioning that both $PO(\Phi)$ and $Q(\Phi)$ are convex cones.

One of the important theorem for the positivity of $f(x)$ over a semialgebraic set Φ is Schmüdgen's positivstellensatz.

Result 7. *(Schmüdgen's positivstellensatz [104])*
Suppose the set Φ in equation (2.8) is a compact set. If $f > 0$ on Φ then $f \in PO(\Phi)$, that is,

$$f(x) = \sum_{J \subseteq \{1,\ldots,m\}} \sigma_J q_J \tag{2.11}$$

Although Schmüdgen's positivstellensatz is a powerful result, the number of terms in equation (2.11) is exponential in the number of polynomials in set (2.8). In contrast to Schmüdgen's theorem, Putinar's positivstellensatz, stated below, provides the positivity of a polynomial over a semialgebraic set with a considerable computational improvement under the assumption that the the semialgebraic set is compact and archimedean.

Result 8. *(Putinar's positivstellensatz [114]) Consider a compact semi-algebraic set given in equation (2.8). It is also assumed that the set Φ is archimedean. For $f \in \mathbb{R}[x]$, a sufficient condition for $f > 0$ on Φ is $f \in Q(\Phi)$, that is,*

$$\begin{aligned} &f(x) = \sigma_0(x) + \sum_{\nu=1}^{m} \sigma_\nu(x) q_\nu(x), \\ &\text{for some } \sigma_\nu(x) \in \Sigma[x]. \end{aligned} \tag{2.12}$$

The compact set Φ is archimedean if all the inequalities in the set Φ are linear or

$$q_k = M - ||x||^2 \geq 0 \tag{2.13}$$

where q_k is one of the polynomial constraints in Φ and M is a large positive number.

In equation (2.12), by putting a-priori bound on the degree of SOS polynomials, the positivity of $f(x)$ on Φ can be solved by an SDP.

Suppose $f \in \mathbb{R}[x]_d$ where $\mathbb{R}[x]_d$ denotes the vector space of polynomials up to degree d. Suppose, $r \geq d$ then the truncated quadratic module associated with the set Φ is given by:

$$Q(\Phi)_{d,r} = \{\sigma_0(x) + \sum_{\nu=1}^{m} \sigma_\nu(x) q_\nu(x), \quad deg(\sigma_0(x)), deg(\sigma_\nu(x) q_\nu(x)) \leq r\} \tag{2.14}$$

where, deg(.) stands for degree of (.).

Result 9. *(Putinar's positivstellensatz with a priori degree bound [104]) Suppose the semi-algebraic set given in equation (2.8) is compact and archimedean. For $f \in \mathbb{R}[x]_d$, if $f > 0$ on Φ then $f \in Q(\Phi)_{d,r}$, that is,*

$$\begin{aligned} f(x) &= \sigma_0(x) + \sum_{\nu=1}^{m} \sigma_\nu(x) q_\nu(x), \\ deg(\sigma_0(x)), deg(\sigma_\nu(x) q_\nu(x)) &\leq r \end{aligned} \tag{2.15}$$

where, $r \geq d$ is the relaxation order.

Putinar's positivstellensatz, stated above, enjoys the following properties:

(i) The result 9 have a degree bound on the SOS polynomials. Therefore, testing whether $f(x)$ is strictly positive on Φ for some SOS polynomial with a degree bound r is equivalent to solving an SDP (see e.g., [104] for details).

(ii) In (2.15), for each $\nu = \{$ 0,1,..., m $\}$, the maximum degree of $\sigma_\nu(x) q_\nu(x)$ is higher than d. However, for SOS decomposition, terms of degree greater than d will cancel out such that the maximum degree of $f(x)$ is d.

(iii) The quality of the estimate by SOS relaxation increases with increasing the degree of the SOS polynomials. However, computational cost increases with the increase in the degree of SOS polynomials.

Although Putinar's positivstellensatz provides a significant reduction in computational complexity compared to the Schmüdgen's positivstellensatz, it may still require SOS polynomials of higher degrees. For example, if the degree of $f(x)$ is 10 and degree of $q_\nu(x)$ is 2 then the minimum degree of $\sigma_\nu(x)$ must be equal to 8. The computational complexity of the positivity test on a semialgebraic set can further be reduced by using the generalized S-procedure which is stated below:

Result 10. *(The generalized S-procedure [157])*
Suppose $\Sigma^t[x]$ is the set of SOS polynomials of given degree t. If there exist SOS polynomials $\sigma_1(x), \sigma_2(x), \ldots, \sigma_v(x) \in \Sigma^t[x]$ such that

$$f(x) - \sum_{\nu=1}^{m} \sigma_\nu(x) q_\nu(x) \;\; \textit{is SOS} \tag{2.16}$$

then $f(x) \geq 0 \; \forall x \in \; \Phi = \{x \in \mathbb{R}^n : q_1(x) \geq 0, q_2(x) \geq 0, \ldots, q_m(x) \geq 0\}$.

Proof. $f(x)$ is positive over the semialgebraic set Φ if:

$$f(x) \geq 0 \tag{2.17}$$

for all x satisfying

$$q_1(x) \geq 0, q_2(x) \geq 0, \ldots, q_m(x) \geq 0. \tag{2.18}$$

Equation (2.17) and equation (2.18) can be equivalently written as the following set containment constraint.

$$\{x \in \mathbb{R}^n : q_1(x) \geq 0, q_2(x) \geq 0, \ldots, q_m(x) \geq 0\} \subseteq \{x \in \mathbb{R}^n : f(x) \geq 0\} \tag{2.19}$$

A sufficient condition for the constraints in the equation (2.19) to hold is the existence of SOS polynomials $\sigma_1(x), \sigma_2(x), \ldots, \sigma_v(x) \in \Sigma^t[x]$ such that

$$f(x) - \sum_{\nu=1}^{m} \sigma_\nu(x) q_\nu(x) \;\; \text{is SOS.} \tag{2.20}$$

To verify that the condition in the equation (2.20) implies that the constraints in the equation (2.17) and equation (2.18) hold, take an arbitrary point x such that:

$$q_1(x) \geq 0, q_2(x) \geq 0, \ldots, q_m(x) \geq 0. \tag{2.21}$$

Since, $\sigma_\nu(x)$ are the SOS polynomials therefore,

$$\sum_{\nu=1}^{m} \sigma_\nu(x) q_\nu(x) \geq 0. \tag{2.22}$$

Hence, $f(x) \geq 0$ according to (2.20) and the constraints in (2.17) and equation (2.18) hold. □

By putting a priori bound on the degree t, we can construct an SDP for computing the SOS decomposition of the polynomial $f(x) - \sum_{\nu=1}^{m} \sigma_\nu(x) q_\nu(x)$. It is important to note that in the generalized S-procedure, Φ is not necessarily archimedean.

2.3 Convex relaxation of polynomial optimization problems

A polynomial optimization problem can be defined as:

$$f^* = \inf_{x \in \Phi} f(x), \tag{2.23}$$

where Φ is a basic closed semi-algebraic set, that is,

$$\Phi = \{x \in \mathbb{R}^n \mid q_1(x) \geq 0, ..., q_m(x) \geq 0\}, \tag{2.24}$$

The optimization problem in (2.23) is in general can be very challenging as:

- $f(x)$ can be nonconvex.
- Φ can be nonconvex and/or disconnected and/or discrete.

In past few decades, many efficient SDP solvers such as SeDumi [153], Mosek [115] and SDPA [88] has been developed. Thus, several efforts have been devoted to relaxing the polynomial optimization problems by a sequence of SDP relaxed problems. In [83], Lasserre proposed moment-SOS convex relaxation of polynomial optimization problems. A MATLAB implementation of moment-SOS relaxation is provided in Yalmip [78]. In this thesis, moment-SOS hierarchy is used to solve the polynomial optimization problems originating from FOFS H_∞ mixed sensitivity control design.

2.3.1 Moment, Riesz functional, moment and localizing matrices

Suppose $\left(h_\alpha(x)\right)_{\alpha \in \mathbb{N}^n_d}$ denotes a basis vector space of $n-$variate polynomial of degree at most d of dimension $\binom{n+d}{d}$ indexed in

$$\mathbb{N}^n_d := \{\alpha \in \mathbb{N}^n : \sum_{k=1}^{n} \alpha_k \leq d\}. \tag{2.25}$$

The polynomial $p(x)$ in terms of monomial $x^\alpha, \alpha \in \mathbb{N}^n_d$, can be written as:

$$p(x) = \sum_{\alpha \in \mathbb{N}^n_d} p_\alpha x^\alpha \tag{2.26}$$

where, p_α are the coefficients of the polynomial $p(x)$.

Definition 4. *(Moment)*
Given a real sequence $y = (y_\alpha)$, $\alpha \in \mathbb{N}^n_d$, if there exists a Borel measure μ supported on Φ then the α moment of the measure μ is given by:

$$y_\alpha = \int_\Phi x_1^{\alpha_1} x_2^{\alpha_2} \dots x_n^{\alpha_n} \, d\mu(x) \qquad \forall \alpha \in \mathbb{N}^n_d. \tag{2.27}$$

Definition 5. *(Riesz functional ([27], [104]))*
Given a sequence $y = (y_\alpha)$, a Riesz functional is a linear functional $L_y : \mathbb{R}[x] \to \mathbb{R}$ such that

$$L_y(p) = \sum_{\alpha \in \mathbb{N}^n_d} p_\alpha y_\alpha \tag{2.28}$$

Example 2. *Consider the following polynomial*

$$p(x) = 1 + 5x_1 + 7x_2^2 + 9x_1x_2, \tag{2.29}$$

the Riesz functional corresponding to $f(x)$ is given by:

$$L_y(p) = y_{00} + 5y_{10} + 7y_{20} + 9y_{11}. \tag{2.30}$$

Definition 6 (Moment Matrix ([27], [104]))**.** *For polynomial $p(x)$ of n variables and degree d, the moment matrix $M_d(y)$ is the Gram matrix associated with the quadratic form $L_y(p^2(x))$, that is,*

$$M_d(y) = \int h_d h_d^T \, \mu(dx) \tag{2.31}$$

The dimension of is $M_d(y)$ is $s(n,d) = \binom{n+d}{d}$.

Example 3. *If n=2 then $M_2(y)$ is given by:*

$$M_2(y) = \begin{bmatrix} y00 & y10 & y01 & y20 & y11 & y02 \\ y10 & y20 & y11 & y30 & y21 & y12 \\ y01 & y11 & y02 & y21 & y12 & y03 \\ y20 & y30 & y21 & y40 & y31 & y22 \\ y11 & y21 & y12 & y31 & y22 & y13 \\ y02 & y12 & y03 & y22 & y13 & y04 \end{bmatrix} \tag{2.32}$$

Definition 7. *(Localizing Moment Matrix)*
Consider a polynomial $q(x) = \sum_{\alpha \in \mathbb{N}^n_d} q_\alpha x^\alpha$ and polynomial $p(x)$ of degree d given in equation (2.26). Then the localizing moment matrix $M_d(qy)$ is the gram matrix associated with $L_y(q(x)p^2(x))$. The localizing matrix can be interpreted as a

linear combination of moment matrices. Suppose, $y_{\alpha(i,j)}$ *be the entry* (i,j) *of the matrix* $M_d(y)$ *then localizing moment matrix associated with the polynomial* $q(x)$ *and moment sequence* y *is given by:*

$$M_d(qy)(i,j) = \sum_{\beta \in \mathbb{N}^n_d} q_\beta y_{\{\alpha(i,j)+\beta\}}, \quad for \;\; i, \;\; j = 1, \ldots, s(n,d) \tag{2.33}$$

Example 4. *Consider a polynomial* $p(x) = 20 + x_1^2 - x_2^2$*. The associated moment matrix and localizing moment matrix of order 1 are given by:*

$$M_1(y) = \begin{bmatrix} 1 & y10 & y01 \\ y10 & y20 & y11 \\ y01 & y11 & y02 \end{bmatrix} \tag{2.34}$$

$$M_1(qy) = \begin{bmatrix} 20 + y20 - y02 & 20y10 + y30 - y12 & 20y01 + y21 - y03 \\ 20y10 + y30 - y12 & 20y20 + y40 - y22 & 20y11 + y31 - y13 \\ 20y01 + y21 - y03 & 20y11 + y31 - y13 & 20y02 + y22 - y04 \end{bmatrix} \tag{2.35}$$

The condition for the existence of measure μ supported on Φ is provided by the following result.

Result 11. *(Riesz-Haviland Theorem)*
For a given real sequence $y = (y_\alpha)$, $\alpha \in \mathbb{N}^n_d$ *and the closed set* Φ*, there exists a finite Borel measure* μ *supported on* Φ *such that*

$$y_\alpha = \int_\Phi x^\alpha \, d\mu \forall \alpha \in \mathbb{N}^n_d, \tag{2.36}$$

if and only if

$$L_y(p) \geq 0 \tag{2.37}$$

for all polynomials $p(x) \in \mathbb{R}[x]_d$ *non-negative on* Φ*.*

2.3.2 Lasserre Moment-SOS hierarchy

The optimization problem in the equation (2.23) can be replaced by the following primal and dual linear programs [104].

$$\begin{aligned} \text{Primal}: \quad & f_M^* = \inf_\mu \int_\Phi f(x) \, d\mu \\ & s.t. \quad \int_\Phi d\mu = 1, \quad \mu \in \mathcal{C}(\Phi)'_+ \end{aligned} \tag{2.38}$$

$$\begin{aligned} \text{Dual}: \quad & f_d^* = \sup_{\lambda \in \mathbb{R}} \lambda \\ & s.t. \quad f(x) - \lambda \in \mathcal{C}(\Phi)_+ \end{aligned} \tag{2.39}$$

In equation (2.39), $\mathcal{C}(\Phi)_+$ is an infinite-dimensional convex cone defined by the set of positive polynomials on Φ. In equation (2.38), $\mathcal{C}(\Phi)'_+$ is the cone of Borel positive measures on Φ and, by Riesz-Haviland theorem, it is topologically dual to $\mathcal{C}(\Phi)_+$.

Suppose, $f(x)$ is an n-variate polynomial of at most degree d. Then, $f(x)$ in terms of monomial $x^\alpha, \alpha \in \mathbb{N}^n_d$, can be written as:

$$f(x) = \sum_{\alpha \in \mathbb{N}^n_d} f_\alpha x^\alpha \tag{2.40}$$

where, f_α are the coefficients of the polynomial $f(x)$.

Given a real sequence $y = (y_\alpha)$, $\alpha \in \mathbb{N}^n_d$, problems in equations ((2.38)-(2.39)) can be rewritten as (see e. g., [27] and [104]):

$$\begin{aligned} & f_M^* = \min_y \sum_{\alpha \in \mathbb{N}^n_d} f_\alpha y_\alpha \\ & s.t. \quad y_0 = 1, \quad y \in P(\Phi)'_d \end{aligned} \tag{2.41}$$

and

$$\begin{aligned} & f_d^* = \sup_{\lambda \in \mathbb{R}} \lambda \\ & s.t. \quad f(x) - \lambda \in P(\Phi)_d \end{aligned} \tag{2.42}$$

where, $P(\Phi)_d$ finite-dimensional convex cone of positive polynomials, that is,

$$P(\Phi)_d = \{p(x) \in \mathbb{R}[x]_d : p(x) = \sum_\alpha p_\alpha x^\alpha \geq 0 \quad \forall \ x \in \Phi\} \subset \mathbb{R}^{\binom{n+d}{d}}. \tag{2.43}$$

By the Riesz-Haviland theorem, its dual is the cone of moments of degree at most d, that is,

$$P(\Phi)'_d = \{y \in \mathbb{R}^{\binom{n+d}{d}} : y_\alpha = \int_\Phi x^\alpha \, d\mu, \ \ \mu \in \mathcal{C}(\Phi)'_+\}. \tag{2.44}$$

The convex cone $P(\Phi)_d$ is generally intractable. By using Putinar's positivstellensatz, we approximate it with the truncated quadratic module $Q(\Phi)_{d,r}$ given in equation (2.14). It is important to note that the $Q(\Phi)_{d,r} \subset P(\Phi)_d$. Thus, this approximation is an inner approximation.

The dual of the quadratic module is given by:

$$Q(\Phi)'_{d,r} = \{y : L_y(p) \geq 0 \ \ \forall p \in Q(\Phi)_{d,r}\} \tag{2.45}$$

$$\begin{aligned} Q(\Phi)'_{d,r} =& \{y : L_y(\sum_{\nu=0}^{m} \sigma_\nu(x) q_\nu(x)) \geq 0,\ \forall \sigma_\nu \in \Sigma^r[x], \nu = 1, \ldots, m\} \\ =& \{y : L_y(q_\nu g^2) \geq 0,\ \forall g \in \mathbb{R}[x],\ \nu = 1, \ldots, m\} \\ =& \{y : M_r(q_\nu y) \geq 0, \nu = 1, \ldots, m\} \end{aligned} \tag{2.46}$$

The matrix $M_r(q_\nu y)$ is called localizing matrix. When $\nu = 0$ and $q_0 = 1$, it is called moment matrix. It is important to note that the $Q(\Phi)'_{d,r} \supset P'(\Phi)_d$. Thus, this is an outer approximation.

Result 12. *(Dual side of the Putinar's Theorem)*
Suppose r_ν is the smallest integer which is greater than or equal to the half the degree of the polynomial q_ν, $\nu = 0,1,\ldots,m$. Suppose, $\tilde{d} = \max\{1, r_1, \ldots, r_m\}$ and $\delta \geq \tilde{d}$ and $M_\delta(y)$ and $M_{\delta - r_\nu}(q_\nu y)$ are the corresponding truncated moments. Then the relaxed version of the problem in (2.41) is given by:

$$\begin{aligned} f^*_\delta = & \min_y \sum_{\alpha \in \mathbb{N}^n_{2\delta}} f_\alpha y_\alpha \\ s.t \quad & y_0 = 1 \\ & M_\delta(y) \geq 0, M_{\delta - r_\nu}(q_\nu y) \geq 0, \quad \nu = 1, \ldots, m. \end{aligned} \tag{2.47}$$

Result 13. *(Global convergence)*
For any $\delta \in \mathbb{N}$: $f^*_\delta \leq f^*_{\delta+1} \leq f^*$ and $\lim_{\delta \to \infty} f^*_\delta = f^*$.

Result 14. *(Certificate of global Convergence)*
For a given relaxation order $\delta \geq \tilde{d}$, if

$$rank\ M_\delta(y) = rank\ M_{\delta - r_\nu}(q_\nu y) \tag{2.48}$$

then $f^*_\delta = f^*$.

2.3.3 Convex relaxation of sparse polynomial optimization problems

In this subsection, we provide a brief overview of the convex relaxation of sparse polynomial optimization problems proposed by Lasserre in [103]. A MATLAB implementation of sparse SDP is available in the software, sparsePOP [67]. Further details on the sparse SDP is available in [68] and [66]. In this thesis, convex relaxation of sparse polynomial optimization problems is used to solve the polynomial optimization problems originating from the computation of bode envelopes of uncertain plants subjected to parametric uncertainty.

For the optimization problem given in (2.23), consider an index set $\{1,2,\ldots,n\}$ which is the union of S, I_s sets.

$$\{1,2,\ldots,n\} = \bigcup_{s=1}^{S} I_s \tag{2.49}$$

Suppose n_s be the number of elements of the set I_s and h_d^s be the canonical basis of polynomials that have degree d and depend only on the variables $x(I_s)$, where

$$x(I_s) = \{x_i | i \in I_s\} \tag{2.50}$$

The moment matrix $M_d(y, I_s)$ associated with the real sequence $y = (y_\alpha)$, $\alpha \in \mathbb{N}_d^n$ is given by:

$$M_d(y, I_s) = \int h_d^s(I_s)(h_d^s(I_s))^T \, \mu(dx) \tag{2.51}$$

The dimension of is $M_d(y, I_s)$ is $s(n_s, d) = \binom{n_s+d}{d}$.

Consider a polynomial $q(x)$ obtained through the basis h_d^s. Suppose, $y_{\alpha(i,j)}$ be the entry (i, j) of the matrix $M_d(y, I_s)$ then localizing moment matrix associated with the polynomial $q(x)$ and moment sequence y is given by:

$$M_d(qy, I_s)(i, j) = \sum_{\beta \in \mathbb{N}_d^{n_s}} q_\beta y_{\{\alpha(i,j)(I_s)+\beta\}}, \quad \text{for } \; i, \; j = 1, \ldots, s(n_s, d) \tag{2.52}$$

Suppose, $sup(\alpha)$ be the support vector α defined as:

$$sup(\alpha) = \{i = 1, \ldots, n : \alpha_i \neq 0\} \tag{2.53}$$

Thus, the moment matrix $M_d(y, I_s)$ and the localizing moment matrix $M_d(qy, I_s)$ contains the moments y_α such that $sup(\alpha) \in I_s$.

The semialgebraic set Φ is archimedean if the condition in equation (2.13) is satisfied. In the case of the variables $x(I_s)$, the archimedean condition is provided by the following equation.

$$||x(I_s)||^2 \leq n_s M \tag{2.54}$$

Thus, for the sparse polynomial optimization problem, we add the following redundant constraints to the semialgebraic set Φ.

$$q_{m+s}(x) = n_s M - ||x(I_s)||^2 \geq 0, \quad s = 1, \ldots, S. \tag{2.55}$$

Now, the optimization problem (2.23) can be rewritten as:

$$f^* = \inf_{x \in \Phi'} f(x), \tag{2.56}$$

where,

$$\Phi' = \{x \in \mathbb{R}^n \mid q_\ell(x), \quad \ell = 1,2, \ldots, m + S\}. \tag{2.57}$$

Suppose, Φ_0 be the index set of the $\Phi^{'}$. Now, we partition the set Φ_0 into S disjoint sets S_r.

$$\Phi_0 = \bigcup_{s=1}^{S} S_r. \tag{2.58}$$

We, further assume that for all $s = 1, \ldots, S$ and for all $\ell \in S_r$, each constraint $q_\ell \geq 0$ in $\Phi^{'}$ depends only on the variables $x(I_s)$. Thus, the objective function $f(x)$ for a sparse polynomial optimization problem can be written as:

$$f(x) = \sum_{s=1}^{S} f_s(x) \tag{2.59}$$

where, each $f_s(x)$ is obtained through canonical basis $h_d^{n_s}$.

Now, we assume, for all $s = 1, \ldots, S-1$, the set I_{S+1} follows the equation (2.60).

$$I_{S+1} \cap \bigcup_{k=1}^{S} I_k \subseteq I_p \quad \text{for} \quad \text{some } p \leq s. \tag{2.60}$$

Under the above assumptions, the convex relaxation of the sparse polynomial optimization is given by:

$$\begin{aligned} & f_{sp}^r = \min_y \sum_{\alpha \in \mathbb{N}^n_{2\delta}} f_\alpha y_\alpha \\ & s.t \\ & \qquad M_\delta(y, I_s) \geq 0, M_{\delta - r_\nu}(q_\nu y, I_s) \geq 0, \quad \nu \in S_r \text{ and } s = 1, \ldots, S. \end{aligned} \tag{2.61}$$

Result 15. *(Global convergence of sparse Polynomial optimization problem) For any $\delta \in \mathbb{N}$: $f_{sp}^{\delta} \leq f_{sp}^{\delta+1} \leq f^*$ and $\lim_{\delta \to \infty} f_{sp}^{\delta} = f^*$.*

Part I

Model based FOFS H_∞ mixed sensitivity control design

Chapter 3

Introduction

Robust control of linear systems is a subject of great interest in the control community since the 1980s. The use of H_∞-norm in the robust control theory has proven critical to progress in this field. H_∞ theory was first introduced by Zames in [54]. Mixed-sensitivity approach was introduced in [62, 112] where constraints on the sensitivity and complementary sensitivity function are defined through the H_∞ norm by selecting suitable frequency domain filters. A deep discussion about the mixed-sensitivity control theory and the selection of appropriate weighting filters can be found in[95, 21] and [61].

Two types of algorithms are commonly used for solving the H_∞ control problem: linear matrix inequalities based algorithms (LMI) (see, e.g., [124, 123]) and algebraic-Riccati equation based algorithms (see, e.g., [94, 76]). Controllers obtained by applying these methods to solve the H_∞ control problem usually have high order. In fact, the controller's order is determined by the plant's order used in the H_∞ control synthesis. Furthermore, these controllers do not have any specific structure. Unfortunately, this is a serious problem as low order-fixed structured controllers are extensively used in numerous industrial applications. This is because the low-order controllers are easy to implement in industrial settings. Moreover, the parameters in the fixed-structured controllers can be linked to the specific performances of the system. For example, integral action provides good disturbance rejection at lower frequencies and zero steady-state error. Similarly, a lead filter can improve the phase of the system in a specific frequency range thus reducing the overshoot. On the other hand, any constraint on the order or structure of the controller makes the H_∞ control design problem non-convex as it introduces bi-linear matrix inequalities (BMIs) instead of LMIs (see, e.g., [12],[107]). Many methods exist in the literature for the design of low-order and/or fixed-structure controllers that are briefly discussed below.

3.1 Existing Methods for design of FOFS controllers

3.1.1 BMIs based algorithms

FOFS controllers can be obtained by solving the BMIs through local and global optimization techniques. Commonly used global algorithms that translate BMIs to LMIs are variable change methods (see, e.g., [23]) and inner convex approximations methods (see, e.g., [132]). The major problem with these algorithms is that they are successful only for specific structures of the controller and thus can not be generalized.

BMIs can be solved locally by many algorithms. Some of most important local algorithms are proposed in ([40, 4, 105, 142]). However, convergence to the global optimal solution is never guaranteed through a local algorithm.

3.1.2 Order reduction methods

Fixed-order controllers can be designed by reducing the order of the plant or the controller (see, e.g., [15, 30, 125]). Reducing the model order results in a conservative uncertainty model. On the other hand, reducing the order of the controller may degrade performance. Furthermore, the order reduction methods can not enforce a specific controller structure.

3.1.3 Interval arithmetic based methods

The commonly used interval arithmetic-based methods are based on quantifier elimination techniques (see, e.g., [56]). Another important contribution is presented in [143] where a branch-and-bound based algorithm is used to compute the inner and outer approximations of the controller parameter set. The main limitation of the interval arithmetic-based methods is that they can only be applied to parametric uncertain plants.

3.1.4 Convex approximation methods for PID controllers

The H_∞ mixed-sensitivity design of PID controllers is well investigated in the literature. Convex optimization techniques have been proposed in [14, 36, 42].

3.1.5 HIFOO and *Hinfstruct*

HIFOO [82] and *Hinfstruct* [121] are perhaps the most important methods for the design of FOFS H_∞ controllers. HIFOO is based on a gradient sampling algorithm and can only be used for the design of fixed-order controllers. A MATLAB

toolbox for the HIFOO is also available ([75]). *Hinfstruct* is based on the Clarke sub-differential approach presented in [45]. Both fixed-order and fixed-structured controllers can be designed through *Hinfstruct* technique. A MATLAB toolbox for *Hinfstruct* technique is also available. Both HIFOO and *Hinfstruct* are based on local optimization techniques. Thus, with these methods, there is no guarantee that the obtained solution is an optimal solution.

3.2 Research Objective

The objective of this research is to provide a global optimization algorithm for solving the model-based FOFS H_∞ mixed sensitivity control problem. Both local and global optimization-based algorithms are available in the literature for solving the FOFS H_∞ mixed sensitivity control problem. The existing global optimization algorithms for solving the FOFS H_∞ control problem are applicable only for specific representations of plants or controllers. On the other hand, local optimization algorithms can trap in a local optimum and may return either a locally infeasible solution or a local solution that violates the constraints. In this part of the thesis, we propose three convex relaxation-based algorithms to solve the FOFS H_∞ mixed sensitivity control problem.

3.2.1 Contribution

The major highlights of this work are:

- The FOFS H_∞ mixed-sensitivity control design problem is formulated as non-convex polynomial feasibility problem in terms of feasible controller parameter set.
- Two single-shot and one iterative convex relaxation-based algorithms are proposed to relax the nonconvex feasible controller parameter set into an SDP. The controller parameters are then computed by solving the SDP using readily available softwares.
- The proposed algorithms doesn't require linear parameterization of the controllers or parametric representation of the uncertain plant.
- The proposed algorithms can be used to design FOFS H_∞ mixed-sensitivity controllers both for CT and DT systems.

The results presented in this section of the thesis are partially published in [164].

Chapter 4

POP formulation of H_∞ mixed sensitivity control

In this chapter, we first present all the necessary class of models and controllers for the design of model based FOFS H_∞ mixed sensitivity controllers. We, then construct the feasible controller parameter set which is the set of controller parameters that guarantees the robust stability and nominal performances. Finally, a polynomial description of the feasible controller parameter set is provided.

4.1 System and controller description

Consider the feedback control system shown in Figure 1.2. We assume that the nominal model of the LTI SISO plant G_n is known and is defined as

$$G_n = \frac{N_g(\epsilon)}{D_g(\epsilon)} \tag{4.1}$$

where $N_g(\epsilon)$ and $D_g(\epsilon)$ are polynomial functions in ϵ. It is important to note that $N_g(\epsilon)$ does not have any root at $s = 0$ for CT systems and $z = 1$ for DT systems. The frequency domain weighting filters $W_1(\epsilon)$ and $W_2(\epsilon)$ are designed according to the time domain performance specifications such as rise time, overshoot, bandwidth etc. It is further assumed that the weighting filter for the unstructured multiplicative uncertainty $W_u(\epsilon)$ is also known.

We assume that the FOFS controller belongs to a class $\mathcal{K}_c$ defined by a n_k-th order transfer function.

$$K(\epsilon, \boldsymbol{p}) = \frac{N_k(\epsilon, \boldsymbol{p})}{D_k(\epsilon, \boldsymbol{p})} = \frac{\sum_{i=0}^{n_k} \beta_i(\boldsymbol{p})\ \epsilon^i}{\epsilon^{n_k} + \sum_{j=0}^{n_k-1} \alpha_j(\boldsymbol{p})\ \epsilon^j} \tag{4.2}$$

where, $\alpha_j(\boldsymbol{p}) \in \mathbb{R}$ and $\beta_i(\boldsymbol{p}) \in \mathbb{R}$, are linear functions in unknown parameter vector $\boldsymbol{p} \in \mathbb{R}^{n_p}$.

Remark 1. *In equation (4.2), we assume that $\alpha_j(\boldsymbol{p})$ and $\beta_i(\boldsymbol{p})$ are linear functions in unknown parameter vector $\boldsymbol{p}$. However, without any modification, the results proposed in this part of the thesis can be applied for $\alpha_j(\boldsymbol{p})$ and $\beta_i(\boldsymbol{p})$ as polynomial functions. However, since we are designing the LTI controller, there is no reason for making the controller structure overly complicated as there will be no effect on the quality of control by considering $\alpha_j(\boldsymbol{p})$ and $\beta_i(\boldsymbol{p})$ linear in unknown parameter vector $\boldsymbol{p}$.*

For unknown parameter vector $\boldsymbol{p}$ and generic variable ϵ, loop-gain, sensitivity and complementary sensitivity functions can be rewritten as given by.

$$L_n(\epsilon, \boldsymbol{p}) = K(\epsilon, \boldsymbol{p})G_n(\epsilon), \tag{4.3}$$

$$S_n(\epsilon, \boldsymbol{p}) = (1 + L_n(\epsilon, \boldsymbol{p}))^{-1} \tag{4.4}$$

and

$$T_n(\epsilon, \boldsymbol{p}) = L_n(\epsilon, \boldsymbol{p})(1 + L_n(\epsilon, \boldsymbol{p}))^{-1} \tag{4.5}$$

4.2 Feasible controller parameter set

In this section, we provide the formal definition of the feasible controller parameter set for achieving robust stability and nominal performance.

From result 3, the feedback system in figure 1.2 is robustly stable if the following two conditions are satisfied.

- The controller $K(\epsilon, \boldsymbol{p})$ internally stabilizes the nominal plant $G_n(\epsilon)$.
- $\|T_n(\epsilon, \boldsymbol{p})W_u(\epsilon)\|_\infty \leq 1$.

For internal stability, we define the following set.

Definition 8. *The stabilizing controller parameter set*

$$\mathcal{S}_p = \{\boldsymbol{p} \in \mathbb{R}^{n_p} | K(\epsilon, \boldsymbol{p}) \text{ internally stabilizes } G_n(\epsilon)\} \tag{4.6}$$

is the set of all the controller parameters that guarantee the internal stability of the feedback control system shown in Figure 1.2.

The emptiness of the set $\mathcal{S}_p$ indicates that the chosen controller class structure $\mathcal{K}_c$ is not adequate to ensure the stability of the nominal plant $G_n(\epsilon)$.

The robust stability set is defined as follows.

Definition 9. *The robust stabilizing controller parameter set*

$$\mathcal{D}_R = \{\boldsymbol{p} \in \mathcal{S}_p | \|T_n(\epsilon, \boldsymbol{p}) W_u(\epsilon)\|_\infty \leq 1\} \tag{4.7}$$

is the set of all the controller parameters which guarantees the internal robust stability of the uncertain plant $G(\epsilon)$.

The emptiness of the set $\mathcal{D}_R$ indicates that the chosen controller structure $\mathcal{K}_c$ is not suitable to provide robust stability of the uncertain plant $G(\epsilon)$.

The closed-loop system achieves nominal performance if

$$\begin{aligned} \|S_n(\epsilon, \boldsymbol{p}) W_1(\epsilon)\|_\infty \leq 1 \\ \|T_n(\epsilon, \boldsymbol{p}) W_2(\epsilon)\|_\infty \leq 1 \end{aligned} \tag{4.8}$$

Now, we introduce the feasible controller parameter set.

Definition 10. *The feasible controller parameter set*

$$\begin{aligned} \mathcal{D}_\mathcal{F} = \{\boldsymbol{p} \in \mathcal{D}_R | \, &\|S_n(\epsilon, \boldsymbol{p}) W_1(\epsilon)\|_\infty \leq 1, \\ &\|T_n(\epsilon, \boldsymbol{p}) W_2(\epsilon)\|_\infty \leq 1\} \end{aligned} \tag{4.9}$$

is the set of controller's parameter $\boldsymbol{p}$ that guarantees robust stability for the plant $G_n(\epsilon)$ subjected to unstructured multiplicative uncertainty bounded by transfer function $W_u(\epsilon)$ and the achievement of the nominal performances defined by the weighting filters $W_1(\epsilon)$ and $W_2(\epsilon)$.

Through (4.8) and (4.9), the set $\mathcal{D}_\mathcal{F}$ can be re-written as

$$\begin{aligned} \mathcal{D}_\mathcal{F} = \{\boldsymbol{p} \in \mathcal{S}_p | \, &\|S_n(\epsilon, \boldsymbol{p}) W_1(\epsilon)\|_\infty \leq 1, \\ &\|T_n(\epsilon, \boldsymbol{p}) \hat{W}_2(\epsilon)\|_\infty \leq 1\Big\} \end{aligned} \tag{4.10}$$

where

$$|\hat{W}_2(j\omega)| = \max\{|W_2(j\omega)|, |W_u(j\omega)|\}, \, \forall \, \omega \in \Omega. \tag{4.11}$$

The fact that the set $\mathcal{D}_\mathcal{F}$ is empty suggests that the selected controller class structure $\mathcal{K}_c$ is not adequate for achieving closed-loop robust stability and desirable closed-loop performance. On the other hand, a large or unbounded set $\mathcal{D}_\mathcal{F}$ indicates that the controller structure is capable of meeting more stringent requirements.

For polynomial representation, we represent set $\mathcal{D}_\mathcal{F}$ as the intersection of two sets, i.e.,

$$\mathcal{D}_\mathcal{F} = \mathcal{S}_p \cap \mathcal{P}_s \tag{4.12}$$

where

$$\begin{aligned} \mathcal{P}_s = \{\boldsymbol{p} \in \mathbb{R}^{n_p} | \, &\|S_n(\epsilon, \boldsymbol{p}) W_1(\epsilon)\|_\infty \leq 1, \\ &\|T_n(\epsilon, \boldsymbol{p}) \hat{W}_2(\epsilon)\|_\infty \leq 1\Big\} \end{aligned} \tag{4.13}$$

4.3 Polynomial description of the set $\mathcal{S}_p$

From result 2, we know that the closed-loop system is internally stable if nominal sensitivity function $S_n(\epsilon, \boldsymbol{p})$ is stable and there is no unstable poles-zero cancellation between the plant and the controller while forming the loop transfer function. First of all, we look at the stability of the $S_n(\epsilon, \boldsymbol{p})$ which is achieved if the numerator of $1 + L_n(\epsilon, \boldsymbol{p})$ have all roots with negative real part (for CT systems) or inside the unit circle (for DT systems). We use Routh's criteria (CT systems) and Jury's test (DT systems) for evaluation of roots of numerator of $1 + L_n(\epsilon, \boldsymbol{p})$.

4.3.1 Routh's stability criterion

Consider the following CT polynomial function.

$$A_p(s) = a_n s^n + a_{n-1} s^{n-1} + \ldots + a_1 s + a_0 \tag{4.14}$$

Routh's Table for the polynomial $A_p(s)$ is provided in Table 4.1 (for details, see e.g.,[120]) .

Table 4.1: Routh's coefficients table.

a_n	a_{n-2}	a_{n-4}	$\ldots$
a_{n-1}	a_{n-3}	a_{n-5}	$\ldots$
b_1	b_2	b_3	$\ldots$
c_1	c_2	c_3	$\ldots$
d_1	d_2	d_3	$\ldots$
$\vdots$	$\vdots$	$\vdots$	$\ddots$

Coefficients in the Routh's Table are given by

$$\begin{aligned} b_1 &= \frac{a_{n-1}a_{n-2} - a_n a_{n-3}}{a_{n-1}} \\ b_2 &= \frac{a_{n-1}a_{n-4} - a_n a_{n-5}}{a_{n-1}} \\ b_3 &= \frac{a_{n-1}a_{n-6} - a_n a_{n-7}}{a_{n-1}} \\ &\vdots \end{aligned} \tag{4.15}$$

$$\begin{aligned} c_1 &= \frac{b_1 a_{n-3} - a_{n-1} b_2}{b_1} \\ c_2 &= \frac{b_1 a_{n-5} - a_{n-1} b_3}{b_1} \\ c_3 &= \frac{b_1 a_{n-7} - a_{n-1} b_4}{b_1} \\ &\vdots \end{aligned} \tag{4.16}$$

$$\begin{aligned} d_1 &= \frac{c_1 b_2 - b_1 c_2}{c_1} \\ d_2 &= \frac{c_1 b_3 - b_1 c_3}{c_1} \\ d_3 &= \frac{c_1 b_4 - b_1 c_4}{c_1} \\ &\vdots \end{aligned} \tag{4.17}$$

We stop if we achieve the coefficients for s^0.

Result 16. *The polynomial function $A_p(s)$ is stable if, and only if, all the coefficients in the first column of the Routh's table have the same sign, that is,*

$$\begin{aligned} &a_n > 0 \\ &a_{n-1} > 0 \\ &b_1 > 0 \\ &c_1 > 0 \\ &\vdots \end{aligned} \tag{4.18}$$

Result 17. *The Routh's stability test can be reformulated into the positivity test of the following polynomials constraints:*

$$\begin{aligned} g_1(\boldsymbol{p}) &= a_n > 0 \\ g_2(\boldsymbol{p}) &= a_{n-1} > 0 \\ g_3(\boldsymbol{p}) &= b_1 a_{n-1} > 0 \\ g_4(\boldsymbol{p}) &= c_1 b_1 > 0 \\ &\vdots \end{aligned} \tag{4.19}$$

4.3.2 Jury's stability criterion

For DT systems, consider the following DT polynomial.

$$A_p(z) = a_n z^n + a_{n-1} z^{n-1} + \ldots + a_1 z + a_0 \tag{4.20}$$

For polynomial $A_p(z)$, jury's co-efficient are given in table 4.2 (for detrails, see e.g., [86]).

Table 4.2: Jury's coefficients table.

Row	z^0	z^1	z^2	z^3	$\ldots$	z^{n-1}	z^n
1	a_0	a_1	a_2	a_3	$\ldots$	a_{n-1}	a_n
2	a_n	a_{n-1}	a_{n-2}	a_{n-3}	$\ldots$	a_1	a_0
3	b_0	b_1	b_2	b_3	$\ldots$	b_{n-1}	
4	b_{n-1}	b_{n-2}	b_{n-3}	b_{n-4}	$\ldots$	b_0	
5	c_0	c_1	c_2	c_3	$\ldots$		
6	c_{n-2}	c_{n-3}	c_{n-4}	c_{n-5}	$\ldots$		
$\vdots$	$\vdots$	$\vdots$	$\vdots$	$\vdots$	$\ldots$		
$2n-3$	q_0	q_1	q_2				

In Table 4.2, the elements of the odd numbered rows are computed as follows.

$$\begin{aligned} b_k &= \begin{vmatrix} a_0 & a_{n-k} \\ a_n & a_k \end{vmatrix} \\ c_k &= \begin{vmatrix} b_0 & b_{n-k-1} \\ b_{n-1} & b_k \end{vmatrix} \\ d_k &= \begin{vmatrix} c_0 & c_{n-k-2} \\ c_{n-2} & c_k \end{vmatrix} \\ &\vdots \end{aligned} \tag{4.21}$$

The even numbered rows contain the elements of the previous row written in reverse order.

Result 18. *The polynomial (4.20) is stable if, and only if all of its roots lie inside*

the unit circle, that is, all of the following conditions are satisfied.

$$\begin{aligned} &A_p(1) > 0 \\ &(-1)^n A_p(-1) > 0 \\ &|a_n| > |a_0| \\ &|b_0| > |b_{n-1}| \\ &|c_0| > |c_{n-2}| \\ &|d_0| > |d_{n-3}| \\ &\vdots \end{aligned} \tag{4.22}$$

Result 19. *The polynomial (4.20) is stable if and only if all the following polynomial positivity constraints are satisfied.*

$$\begin{aligned} g_1(\boldsymbol{p}) &= A_p(1) > 0 \\ g_2(\boldsymbol{p}) &= (-1)^n A_p(-1) > 0 \\ g_3(\boldsymbol{p}) &= |a_n|^2 - |a_0|^2 > 0 \\ g_4(\boldsymbol{p}) &= |b_0|^2 - |b_{n-1}|^2 > 0 \\ g_5(\boldsymbol{p}) &= |c_0|^2 - |c_{n-2}|^2 > 0 \\ g_6(\boldsymbol{p}) &= |d_0|^2 - |d_{n-3}|^2 > 0 \\ &\vdots \end{aligned} \tag{4.23}$$

In case of the CT systems, BIBO stability of $S_n(s, \boldsymbol{p})$ is ensured by applying the result 17 to the numerator of the $1 + L_n(s)$, which is

$$A_p(s, \boldsymbol{p}) = N_k(s, \boldsymbol{p}) N_g(s) + D_k(s, \boldsymbol{p}) D_g(s). \tag{4.24}$$

For CT systems, nominal closed-loop stability is achieved if the second condition in result 2 is also satisfied. If $G_n(s)$ does not have any poles and zeros in the right-half plan, there will be no unstable pole-zero cancellation while forming the loop function. On the other hand, if $G_n(s)$ does have any unstable pole then unstable pole-zero cancellation between the plant and the controller is avoided by considering $N_k(s, \boldsymbol{p})$ to be a stable polynomial which is achieved by applying Routh's criterion to $N_k(s, \boldsymbol{p})$. Similarly, if $G_n(s)$ have any unstable zero then the unstable pole-zero cancellation is avoided by applying Routh's criterion to $D_k(s, \boldsymbol{p})$.

In case of DT systems, BIBO stability of $S_n(z, \boldsymbol{p})$ is obtained by applying result 19 to the numerator of $1 + L_n(z)$.

$$A_p(z, \boldsymbol{p}) = N_k(z, \boldsymbol{p}) N_g(z) + D_k(z, \boldsymbol{p}) D_g(z). \tag{4.25}$$

If $G_n(z)$ does not have any poles and zeros outside the unitary circle, condition two in result 2 is automatically satisfied. However, DT systems that have unstable poles and/or zeros, the unstable pole-zero cancellation is enforced by applying Jury's stability test to $N_k(z, \boldsymbol{p})$ and/or to $D_k(z, \boldsymbol{p})$.

Remark 2. *By restricting $D_k(\epsilon, \boldsymbol{p})$ to have only stable roots, the controller cannot have poles at $s = 0$ or $z = 1$. However, an integrator is required to guarantee zero steady-state error for reference tracking and high disturbance rejection at low frequencies. In order to allow poles at $s = 0$ or $z = 1$, we consider the following representation of the $D_k(\epsilon, \boldsymbol{p})$.*

$$D_k(\epsilon, \boldsymbol{p}) = Z_k(\epsilon) D_k^{'}(\epsilon, \boldsymbol{p}) \tag{4.26}$$

where $Z_k(\epsilon) = s^\mu$ for CT systems, $Z_k(\epsilon) = (z-1)^\mu$ for DT systems and μ is the multiplicity of the roots at $s = 0$ or $z = 1$ of $D_k(\epsilon, \boldsymbol{p})$. As a result, instead of enforcing the stability of D_k, we impose stability requirements on $D_k^{'}$. Since it is already assumed that the plant has no zeros at $s = 0$ or $z = 1$. Therefore, pole-zero cancellation between the Z_k and $N_g(\epsilon)$, can not occur.

Based on the results 17 and result 19, it is evident that the stability set $\mathcal{S}_p$ is a semi-algebraic set that contains polynomial inequalities $g_i(\boldsymbol{p}) > 0$.

4.4 Polynomial description of the set $\mathcal{P}_s$

A polynomial description of the set $\mathcal{P}_s$ is obtained by the following result.

Result 20. *For suitable variables ϕ and a set Φ, the inequalities in (4.13) can be equivalently written as*

$$h_i(\phi, \boldsymbol{p}) > 0,\ i = 1, 2,\ \forall \phi \in \Phi \tag{4.27}$$

where $h_i(\phi, \boldsymbol{p})$ are polynomial functions of both $\boldsymbol{p}$ and ϕ

Proof. Consider the following rational transfer functions

$$H_i(\epsilon, \boldsymbol{p}) = \frac{N_i(\epsilon, \boldsymbol{p})}{D_i(\epsilon, \boldsymbol{p})},\ i = 1{,}2 \tag{4.28}$$

where

$$H_1(\epsilon, \boldsymbol{p}) = S_n(\epsilon, \boldsymbol{p}) W_1(\epsilon) \tag{4.29}$$

and

$$H_2(\epsilon, \boldsymbol{p}) = T_n(\epsilon, \boldsymbol{p}) \hat{W}_2(\epsilon) \tag{4.30}$$

CT systems
In case of CT systems, $\epsilon = s$ and we replace $s = j\omega$. Now, by using the H_∞ norm definition provided in equation (1.7), we rewrite conditions (4.13) as

$$h_i(\omega, \boldsymbol{p}) = |D_i(j\omega, \boldsymbol{p})|^2 - |N_i(j\omega, \boldsymbol{p})|^2 \geq 0,\ i = 1{,}2,\ \forall \omega \in \Omega. \tag{4.31}$$

By setting $\phi = \omega$ that belongs to the given compact set $\Phi = \Omega$, constraints in equation (4.31) can be rewritten as polynomial inequalities

$$h_i(\phi, \boldsymbol{p}) > 0,\ i = 1, 2,\ \forall \phi \in \Phi. \tag{4.32}$$

DT systems
In case of DT systems, $\epsilon = z$ where $z = e^{j\omega T_s}$. Therefore, we rewrite conditions (4.13) as

$$h_i(\omega, \boldsymbol{p}) = |D_i(e^{j\omega T_s}, \boldsymbol{p})|^2 - |N_i(je^{j\omega T_s}, \boldsymbol{p})|^2 \geq 0,\ i = 1{,}2,\ \forall \omega \in \Omega. \tag{4.33}$$

By Euler's formula,

$$e^{j\omega T_s} = \cos(\omega T_s) + j \sin(\omega T_s). \tag{4.34}$$

Suppose, $a = \cos(\omega T_s)$ and $b = \sin(\omega T_s)$. Since, for DT system: $\omega \in \Omega = [0\ \ \frac{\pi}{T_s}]$, therefore,

$$z = a + jb,\ a \in [-1{,}1] \subset \mathbb{R},\ a^2 + b^2 = 1,\ b \geq 0. \tag{4.35}$$

Now, we define $\phi = [a\, b]^T$ and $\Phi = \{\phi \in \mathbb{R}^2 : -1 \leq a \leq 1,\ a^2 + b^2 = 1,\ b \geq 0\}$. Though these definitions of ϕ and Φ, inequalities in equation (4.33) can be rewritten as:

$$h_i(\phi, \boldsymbol{p}) > 0,\ i = 1, 2,\ \forall \phi \in \Phi \tag{4.36}$$

□

4.5 Polynomial description of the set $\mathcal{D}_\mathcal{F}$

Based on the results 17, result 19 and result 20, the polynomial representation of the feasible controller parameter set $\mathcal{D}_\mathcal{F}$ is given by:

$$\begin{aligned} \mathcal{D}_\mathcal{F} = \{\boldsymbol{p} \in \mathbb{R}^{n_p} |\ & h_i(\phi, \boldsymbol{p}) > 0, \quad i = 1{,}2, \quad \forall \phi \in \Phi \\ & g_k(\boldsymbol{p}) > 0, \quad k = 1{,}2{,}3, \dots \} \end{aligned} \tag{4.37}$$

where, g_k are the stability constraints for the numerator of $1 + G_n(\epsilon)K(\epsilon, \boldsymbol{p})$ in case when $G_n(\epsilon)$ has no unstable poles/zeros. However, if $G_n(\epsilon)$ has unstable poles, stability constraints for $N_k(\epsilon, \boldsymbol{p})$ are also included. Similarly, if $G_n(\epsilon)$ has unstable zeros, we add stability constraints of $D'_k(\epsilon, \boldsymbol{p})$. Thus the index k depends on the order of $N_k(\epsilon, \boldsymbol{p})$, $D_k(\epsilon, \boldsymbol{p})$, $N_g(\epsilon)$ and $D_g(\epsilon)$.

Chapter 5

Model based FOFS H_∞ mixed sensitivity control design

In this chapter, we provide three algorithms for solving the FOFS H_∞ mixed sensitivity control design problem by relaxing the feasible controller parameter set $\mathcal{D}_\mathcal{F}$ in equation (4.37). Two of these algorithms are based on the SOS approximation of the set $\mathcal{D}_\mathcal{F}$ whereas the third algorithm is a recursive algorithm based on the exchange methods.

5.1 SOS approach to FOFS H_∞ mixed sensitivity design

5.1.1 Archimedean property of the set Φ

In case of CT systems: $\Phi = \Omega = [0, +\infty)$. To be able to solve the given problem, we consider $\Phi = \Omega = [0, M]$, where M is a constant positive number significantly larger than the bandwidth of the closed-loop system. Consequently, the set Φ can be represented as:

$$\Phi = \{\phi \geq 0,\ M - \phi \geq 0\} \tag{5.1}$$

Although, (5.1) is an approximation of the $\Phi = \Omega = [0, +\infty)$. However, if M is significantly larger than the closed-loop bandwidth, the impact of this approximation on the performance of the closed-loop system is expected to be limited. The set Φ is compact and archimedean as it is closed, bounded and contains only the linear constraints.

In the case of discrete systems:

$$\Phi = \left\{\phi \in \mathbb{R}^2 : -1 \leq a \leq 1,\ a^2 + b^2 = 1,\ b \geq 0\right\} \tag{5.2}$$

where, $\phi = [a\, b]^T$, $a = \cos(\omega T_s)$ and $b = \sin(\omega T_s)$.

The set Φ in (5.2) is compact and have bounded ∞-norm, therefore it is archimedean by construction.

5.1.2 SOS relaxation of $\mathcal{P}_s$ by Putinar's positivstellensatz

Based on the result 9, the inequalities in the set $\mathcal{P}_s$ can be represented as SOS constraints according to the following result.

Result 21. *Suppose,* $\Phi = \{q_1(\phi) \geq 0, \ldots, q_m(\phi) \geq 0\}$. *Suppose,* d_1 *is the degree of* $h_1(\phi, \boldsymbol{p})$, $r_1 \in \mathbb{N}$ *and* $r_1 \geq d_1$ *then* $h_1 > 0$ *on the set* Φ *if*

$$\begin{aligned} &h_1(\phi, \boldsymbol{p}) - \sum_{\nu=1}^{m} \sigma_\nu(\phi) q_\nu(\phi) \text{ is SOS} \\ &\text{for some } \sigma_\nu(\phi) \in \Sigma^{r_1}(\phi) \end{aligned} \tag{5.3}$$

where, $\Sigma^{r_1}(\phi)$ *is the set of SOS polynomials and degree of each* $\sigma_\nu(\phi)$ *is* $r_1 - degree(q_\nu(\boldsymbol{\phi}))$.

Similarly, suppose, d_2 *is the degree of* $h_2(\phi, \boldsymbol{p})$, $r_2 \in \mathbb{N}$ *and* $r_2 \geq d_2$ *then* $h_2 > 0$ *on the set* Φ *if:*

$$\begin{aligned} &h_2(\phi, \boldsymbol{p}) - \sum_{\mu=m+1}^{2m} \sigma_\mu(\phi) q_{\mu-m}(\phi) \text{ is SOS} \\ &\text{for some } \sigma_\mu(\phi) \in \Sigma^{r_2}(\phi) \end{aligned} \tag{5.4}$$

where, $\Sigma^{r_2}(\phi)$ *is the set of SOS polynomials and degree of each* $\sigma_\mu(\phi)$ *is* $r_2 - degree(q_\mu(\boldsymbol{\phi}))$.

5.1.3 SOS relaxation of $\mathcal{P}_s$ by generalized S-procedure

By exploiting the result 10, the inequalities in the set $\mathcal{P}_s$ can be represented as SOS constraints according to the following result.

Result 22. *Suppose,* $\Phi = \{q_1(\phi) \geq 0, \ldots, q_m(\phi) \geq 0\}$. *Suppose,* d_1 *is the degree of* $h_1(\phi, \boldsymbol{p})$ *then* $h_1 \geq 0$ *if*

$$\begin{aligned} &h_1(\phi, \boldsymbol{p}) - \sum_{\nu=1}^{m} \sigma_\nu(\phi) q_\nu(\phi) \text{ is SOS} \\ &\text{for some } \sigma_\nu(\phi) \in \Sigma^{t_1}(\phi) \end{aligned} \tag{5.5}$$

where, $\Sigma^{t_1}(\phi)$ *is the set of SOS polynomials of degree* t_1 *and* t_1 *is a non-negative integer.*

Similarly, suppose, d_2 is the degree of $h_2(\phi, \boldsymbol{p})$ then $h_2 \geq 0$ if

$$\begin{aligned} &h_2(\phi, \boldsymbol{p}) - \sum_{\nu=1}^{m} \sigma_\nu(\phi) q_\nu(\phi) \text{ is SOS} \\ &\text{for some } \sigma_\nu(\phi) \in \Sigma^{t_2}(\phi) \end{aligned} \tag{5.6}$$

where, $\Sigma^{t_2}(\phi)$ is the set of SOS polynomials of degree t_2 and t_2 is a non-negative integer.

5.1.4 Construction of SDP for $\mathcal{D}_\mathcal{F}$

It is clear from the results (17-19) that stability set $\mathcal{S}_p$ is a set of positive polynomials both for CT and DT systems. Thus the positive polynomials in the set $\mathcal{S}_p$ are replaced by SOS polynomials. Since, the coefficients of the $h_i(\phi, \boldsymbol{p})$, $i = 1,2$ are polynomial functions of unknown controller parameters $\boldsymbol{p}$, therefore, the Gram matrices corresponding to h_1 and h_2 have the elements that are nonconvex in $\boldsymbol{p}$. Thus, the polynomial constraints in the Gram matrices are relaxed by using moment relaxation given in [83].

5.2 Exchange algorithm based SDP relaxation for FOFS H_∞ mixed sensitivity design

Since Φ is an infinite set, thus the set $\mathcal{D}_\mathcal{F}$ in equation (4.37) contains semi-infinite polynomials. Therefore, we can compute the unknown controller parameters by solving a semi-infinite polynomial program (SIPP). SIPP are commonly solved by three methods, namely, the discretization methods, methods based on local reduction and exchange methods (see, e.g., [81], [71], [133], [77], [53] and [168]). In this section, we will use the exchange algorithm for computing the unknown controller parameters that belong to the set $\mathcal{D}_\mathcal{F}$.

A general SIPP has the following form:

$$\begin{aligned} &\min_{x \in X} f(x) \\ &s.t. \quad g(x, y) \geq 0, \quad \forall y \in Y \end{aligned} \tag{5.7}$$

where, X and Y are compact semialgebraic sets, and $f(x)$ and $g(x, y)$ are polynomials. Typically, the exchange algorithm consists of the following four steps.

(a) *Initialization*: Suppose $Y_k \subset Y$. set $k = 0$ and choose some random $y_0 \in Y$ and select $Y_0 = \{y_0\}$.

(b) *Upper level Program*: For k^{th} iteration, compute $x^k \in X$ by solving the following optimization problem.

$$\begin{aligned} &\min_{x \in X} f(x) \\ &s.t. \quad g(x, y) \geq 0, \quad \forall y \in Y_k \end{aligned}$$

(c) *Lower level Program*: For k^{th} iteration, compute $y^k \in Y$ by solving the following optimization problem.

$$\min_{y \in Y} g(x^k, y)$$

(c) *Stopping criteria*: if $g(x^k, y^k) \geq 0$, stop. Else, $Y_{k+1} = Y_k \cup y^k$ and go to step 2.

Most of the exchange algorithms for solving semi-infinite polynomial programs converge locally. On the other hand, algorithms with guaranteed global convergence require strong assumptions such as convexity or linearity (see, e.g., [134],[101]). Two exchange algorithms based on semi-definite relaxations for solving the SIPP problem are proposed in [101]. In this section, we will compute the unknown controller parameters by using the algorithm 1, which is based on the results presented in [101]. As discussed earlier, the set Φ is a compact set for CT and DT systems. The compactness of $\mathcal{S}_p$, can be achieved by restricting the controller variables to a Euclidean ball by adding a redundant constraint similar to equation (2.13).

Algorithm 1 An SDP exchange algorithm for model based FOFS H_∞ controller design

1: Suppose, $\Phi_k \in \Phi$. Set $k = 0$ and choose some random $\phi_0 \in \Phi$ and select $\Phi_0 = \{\phi_0\}$.

2: For k^{th} iteration, apply moment relaxation given in [83] to solve

$$(\mathcal{Q}_k) : \begin{cases} h_i(\phi, \boldsymbol{p}) > 0, & i = 1,2, \quad \forall \phi \in \Phi_k \\ g_k(\boldsymbol{p}) > 0, & k = 1,2,3,\ldots \end{cases}$$

The global optimal solutions are extracted by extraction algorithm given in [28]. Suppose, $\mathcal{S}_k = \{\boldsymbol{p}_1^k, ..., \boldsymbol{p}_\ell^k\}$ be the set of the global minimizers of problem $(\mathcal{Q}_k)$.

3: Set $\Phi_{k+1} = \Phi_k$. For $i = 1, ..., \ell$, do the following
a) Use moment relaxation given in [83] to solve

$$(\mathcal{O}_i^k) : \quad \mathcal{F}_i^k := [\min_{\phi \in \Phi} h_1(\boldsymbol{p}_i^k, \phi), h_2(\boldsymbol{p}_i^k, \phi)]^T.$$

b) If all the elements of $\mathcal{F}_i^k(\boldsymbol{p}_i^k, \phi_i^k))$ are positive then stop. Otherwise select only those elements of $\mathcal{F}_i^k$ which are negative and choose corresponding global minimizers.
c) Let $T_i^k = \{\Phi_{i,j}^k, j = 1, ..., ti^k\}$ be the set of global minimizers of $(\mathcal{O}_i^k)$ for which elements of $\mathcal{F}_i^k$ are negative. Update $\Phi_{k+1} = \Phi_{k+1} \bigcup T_i^k$

4: If $k > k_{max}$, stop. Otherwise $k = k + 1$ and go to step 2.

Result 23. *Suppose that $\mathcal{S}_p$ is compact. If at each step k,*
(a) sub-problems $(\mathcal{Q}_k)$ and $(\mathcal{O}_i^k)$ are solved globally,
(b) intermediate results $\mathcal{S}_k$ and at least one T_i^k are nonempty, then either Algorithm 1 stops with solutions in a finite number of iterations or for any sequence $\{\boldsymbol{p}^k\}$ with $\boldsymbol{p}^k \in \mathcal{S}_k$, there exists at least one limit point as k increases and each of them solves the SIPP.

The proof of the result 23 can be found in [101].

5.3 Comparison of the proposed algorithms

In the previous section, three methods are presented for computing the unknown controller parameters $\boldsymbol{p}$ by using convex relaxation. We call Putinar's positivstellensatz based SOS relaxation of the set $\mathcal{D}_\mathcal{F}$ as method 1, the generalized S-procedure based SOS relaxation of the set $\mathcal{D}_\mathcal{F}$ as method 2 and algorithm 1 as method 3. In this section, we provide a comparison of these methods.

5.3.1 CT systems

Method 1 provides the necessary and sufficient conditions for the positivity of h_1 and h_2 over the set Φ. However, this method requires high order SOS polynomials for SOS relaxation of the set $\mathcal{P}_s$ and therefore it is computationally expensive, especially for high order plants with complex structure controllers .

Method 2 provides only the sufficient conditions for the positivity of h_1 and h_2 over the set Φ. This method is computationally efficient compared to the method 1 as it requires low order SOS polynomials for SOS relaxation of the set $\mathcal{P}_s$.

The computational complexity of method 3 can be higher than method 1 and method 2 for lower order plants with simpler controllers. Since, method 3 is a recursive algorithm based on the exchange algorithm therefore it can solve the mixed sensitivity control design problem more efficiently for higher order plants with complex structure controllers.

5.3.2 DT systems

For DT systems, method 1 has the highest computational complexity among the three methods proposed in this section. This is because it requires to solve high dimension Gram matrices associated with the set $\mathcal{P}_s$. The dimension of Gram matrices corresponding to polynomials $h_1(\phi, \boldsymbol{p}) - \sum_{\nu=1}^{m} \sigma_\nu(\phi) q_\nu(\phi)$ and $h_2(\phi, \boldsymbol{p}) - \sum_{\mu=m+1}^{2m} \sigma_\mu(\phi) q_{\mu-m}(\phi)$ in equations((5.5) and (5.6)), respectively, increases due to the following reasons.

- In DT systems, the set ϕ contains two elements and replacing $z^n = (a + jb)^n$ result in increased number of terms in the polynomials $h_1(\phi, p)$ and $h_2(\phi, p)$, compared to CT systems.
- Requirement of high order SOS polynomials in method 1 increases the number of terms in polynomials $\sum_{\nu=1}^{m} \sigma_\nu(\phi) q_\nu(\phi)$ and $\sum_{\mu=m+1}^{2m} \sigma_\mu(\phi) q_{\mu-m}(\phi)$.

For DT systems, the computational complexity of method 2 is lower than method 1, but it is still high. The reduction in the computational complexity is due to the requirement of low order SOS polynomials for SOS relaxation of the set $\mathcal{P}_s$.

For DT systems, method 3 has the lowest computational complexity compared to other methods, as it solves the SIPP iteratively using the exchange algorithm.

Chapter 6

Simulation examples and experimental results

6.1 Simulation example1: CT controller design

Consider the following CT LTI SISO system.

$$G_n(s) = \frac{1000}{s^2 + 70s + 1000} \tag{6.1}$$

The system is subjected to the multiplicative uncertainty described by the following frequency domain filter.

$$W_u(s) = \frac{0.5(s + 52)}{s + 98} \tag{6.2}$$

The goal is to design a PID controller

$$K(s, \boldsymbol{p}) = \frac{c_1 s + c_2}{s} \tag{6.3}$$

such that

$$\begin{aligned} \|S_n(s)W_1(s)\|_\infty &\leq 1 \\ \|T_n(s)\hat{W}_2(s)\|_\infty &\leq 1 \end{aligned} \tag{6.4}$$

where,

$$W_1(s) = \frac{0.03341s^2 + 0.852s + 7.518}{0.06667s^2 + s}, \tag{6.5}$$

$$W_2(s) = 0.00353s^2 + 0.09002s + 0.7943 \tag{6.6}$$

and $\boldsymbol{p} = [c_1, c_2]^T$. $W_u(s)$ and $W_2(s)$ are plotted in the figure 6.1. It is clear from the figure 6.1 that $|W_2(j\omega)|$ is greater than $|W_u(j\omega)|$ for all frequencies, thus we select

$$\hat{W}_2(s) = W_2(s). \tag{6.7}$$

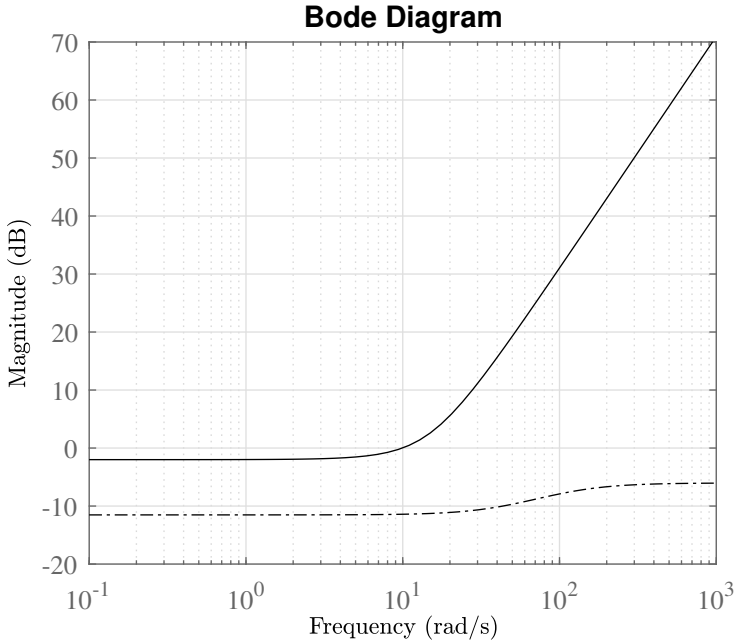

Figure 6.1: Comparison between $|W_2{}^{-1}(j\omega)|$ (solid) and $|W_u(j\omega)|$ (dashed)

Now, we compute $\boldsymbol{p} = [c_1, c_2]^T$ by all the three methods proposed in the chapter 5. We have chosen $\Omega = [0,10^4]^T$. The constraints in the stability set are obtained by using Routh's Hurwitz criteria. The highest degree of the polynomial $h_1(\omega, \boldsymbol{p})$ with respect to ω is 8 and the highest degree of the polynomial $h_2(\omega, \boldsymbol{p})$ with respect to ω is 6. For method 1, we choose $r_1 = r_2 = 9$ such that the degree of each SOS polynomial in equation (5.3) and equation (5.4) is 8. For method 2, we choose SOS polynomials of degree 1, that is, $t_1 = t_2 = 1$. For method 1 and method 2, non-convex polynomial constraints in the Gram matrices are relaxed by moment relaxation of order 1. For method 3, we use moment relaxation of order 3 for the sub-problem $(\mathcal{Q}_k)$ and moment relaxation of order 6 for the sub-problem $(\mathcal{O}_i^k)$. It is worth mentioning that, for method 3, a redundant constraint $10000 - c_1^2 - c_2^2 \geq 0$ is also added to the stability set for compactness.

For all three methods, we solve the controller design problem by using YALMIP ([78]) and MOSEK ([115]). We perform all the simulations on a PC running on 64 bit Windows 10 platform, equipped with Intel core $i7 - 7500$ CPU and 8 GB RAM. For each method, simulation time, the controller parameters extracted from the feasible controller parameter set and the corresponding $\|S_n(s)W_1(s)\|_\infty$ and

$\|T_n(s)\hat{W}_2(s)\|_\infty$ are reported in the table 6.1. For method 3, algorithm 1 converges in 2 iterations.

It can be seen from the table 6.1 that in all cases at all frequencies (i) $|S_n(j\omega)|$ is smaller than $|W_1^{-1}(j\omega)|$, and (ii) $|T_n(j\omega)|$ is smaller than $|W_2^{-1}(j\omega)|$. Thus for all three methods, the closed-loop system is robustly stable while achieving the nominal performance.

Table 6.1: Simulation results for model-based CT control design

	Parameters	Time (s)	H_∞ mixed sensitivity norms
Method 1	$c_1 = 0.1043$, $c_2 = 7.5236$	2.94	$\|S_n(s)W_1(s)\|_\infty = 0.9992$, $\|T_n(s)\hat{W}_2(s)\|_\infty = 0.7943$
Method 2	$c_1 = 0.1038$, $c_2 = 7.5235$	0.70	$\|S_n(s)W_1(s)\|_\infty = 0.9992$, $\|T_n(s)\hat{W}_2(s)\|_\infty = 0.7943$
Method 3	$c_1 = 0.0896$, $c_2 = 7.5178$	7.00	$\|S_n(s)W_1(s)\|_\infty = 0.9995$, $\|T_n(s)\hat{W}_2(s)\|_\infty = 0.7943$

6.2 Simulation example2: DT controller design

Consider the following DT LTI SISO system

$$G_n(z) = \frac{3z + 2.25}{4z^2 - 2.8z + 1} \tag{6.8}$$

which is subjected to multiplicative uncertainty characterized by the following frequency domain transfer function.

$$W_u(z) = \frac{0.3944z^2 - 0.143z - 0.05305}{z^2 + 0.5162z - 0.3177} \tag{6.9}$$

The aim is to design a DT robust PI controller

$$K(z, \boldsymbol{p}) = k_p + \frac{k_i}{z - 1}, \tag{6.10}$$

such that $\|S_n(z)W_1(z)\|_\infty \leq 1$ and $\|T_n(z)\hat{W}_2(z)\|_\infty \leq 1$, where

$$W_1(z) = \frac{0.606z^2 - 0.96z + 0.3875}{(z - 0.7787)(z - 1)}, \tag{6.11}$$

$$W_2(z) = \frac{z^2 - 1.254z + 0.4595}{0.1636z + 0.1261}. \tag{6.12}$$

The unknown controller parameter vector is $\boldsymbol{p} = [k_p, k_i]^T \in R^2$. From Figure 6.2, we see that $|W_2(z)|$ is greater than $|W_u(z)|$ for all the frequencies, thus we choose

$$\hat{W}_2(z) = W_2(z). \tag{6.13}$$

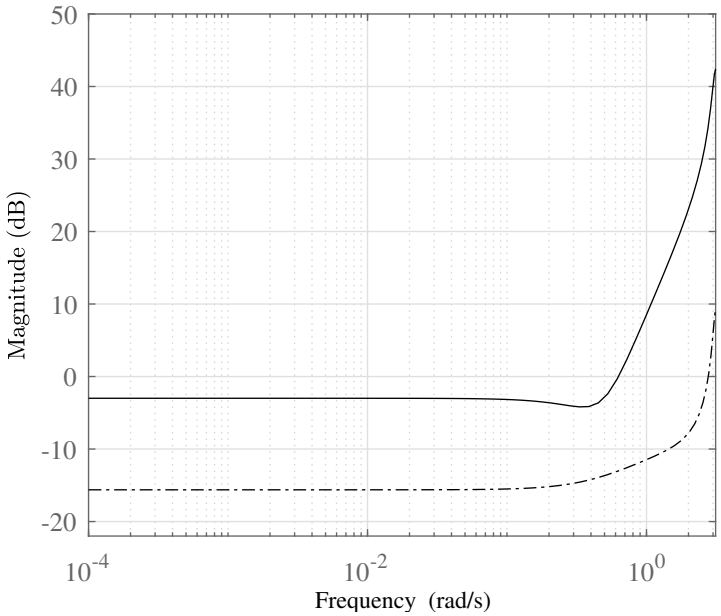

Figure 6.2: Comparison between $|W_u(e^{j\omega})|$ (dotted) and $|W_2(e^{j\omega})|$ (solid).

We will design the PI controller by method 2 and method 3 described in the chapter 5.

6.2.1 Controller design by Method 2

We choose $t_1 = t_2 = 1$ for SOS relaxation of the set $\mathcal{P}_s$. The constraints in the stability set are obtained by the Jury's method. The positivity test of each non-convex polynomial constraint in the stability set is replaced by SOS constraints. Non-convex polynomial constraints in the Gram matrices are relaxed by moment relaxation of order 2. The controller design problem is solved by using YALMIP ([78]) and MOSEK ([115]). The simulation is performed on the HPC@polito, equipped with 128GB RAM. HPC@polito is a project of Academic Computing within the Department of Control and Computer Engineering at the Politecnico di Torino. The simulation took approximately 4 hours and the optimization problem converged with $k_p = 0.1480$ and $k_i = 0.1266$. The graphical comparisons between $|S_n(z)|$ and $|W_1(z)|$ is reported in figure 6.3. Similarly, the graphical comparisons between $|T_n(z)|$ and $|W_2(z)|$ is reported in figure 6.4. It is clear from Figures 6.3 and 6.4 that

the closed-loop system is robustly stable while achieving the desired performance specifications. Numerically, $\|S_n(z)W_1(z)\|_\infty = 0.8725$ and $\|T_n(z)\hat{W}_2(z)\|_\infty = 0.99$.

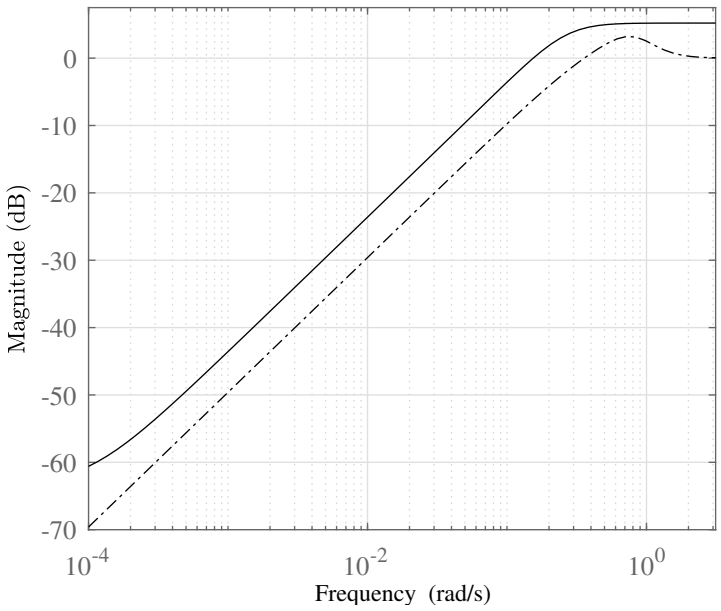

Figure 6.3: Comparison between $|W_1^{-1}(e^{j\omega})|$ (solid) and $|S_n(e^{j\omega})|$ (dotted).

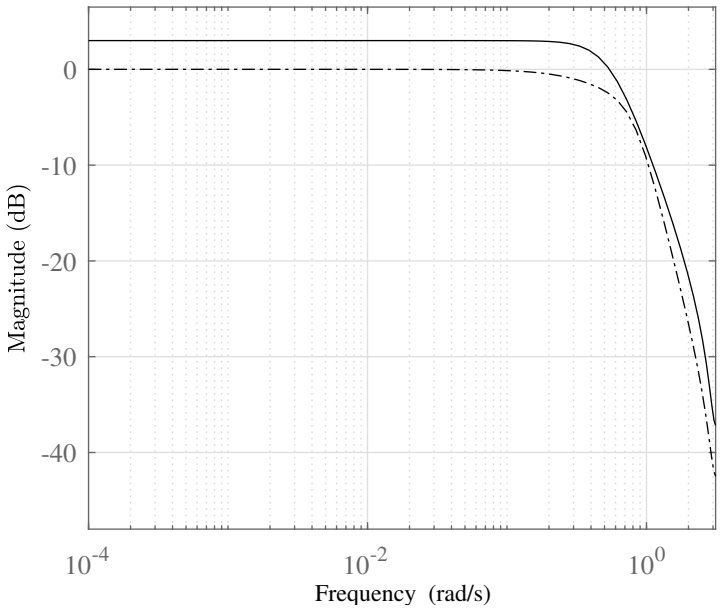

Figure 6.4: Comparison between $|\hat{W}_2^{-1}(e^{j\omega})|$ (solid) and $|T_n(e^{j\omega})|$ (dotted).

6.2.2 Controller design by Method 3

The constraints in the stability set are obtained by the Jury's method. A redundant constraint $10000-(k_p^2+k_i^2)\geq 0$ is added to the stability set for compactness. We use moment relaxation of order 5 for both sub-problems $(\mathcal{Q}_k)$ and $(\mathcal{O}_i^k)$. The controller design problem is solved by using YALMIP ([78]) and MOSEK ([115]). The simulation is performed on a PC running on 64 bit Windows 10 platform, equipped with Intel core $i7-7500$ CPU and 8 GB RAM. The optimization problem converged in 50 seconds in 4 iterations. The controller parameters extracted from the feasible controller parameter set are $k_p = 0.0182$ and $k_i = 0.0934$. Sensitivity and complementary sensitivity functions along-with their corresponding frequency domain weighting filters are plotted in figures (6.5 and 6.6). It is clear from these figures that at all frequencies $|S_n(z)| < |W_1^{-1}(z)|$ and $|T_n(z)| < |W_2^{-1}(z)|$. Thus, the closed-loop system is robustly stable and the controller achieves desired performance specifications. Numerically, $\|S_n(z)W_1(z)\|_\infty = 0.8831$ and$\|T_n(z)\hat{W}_2(z)\|_\infty = 0.7096$.

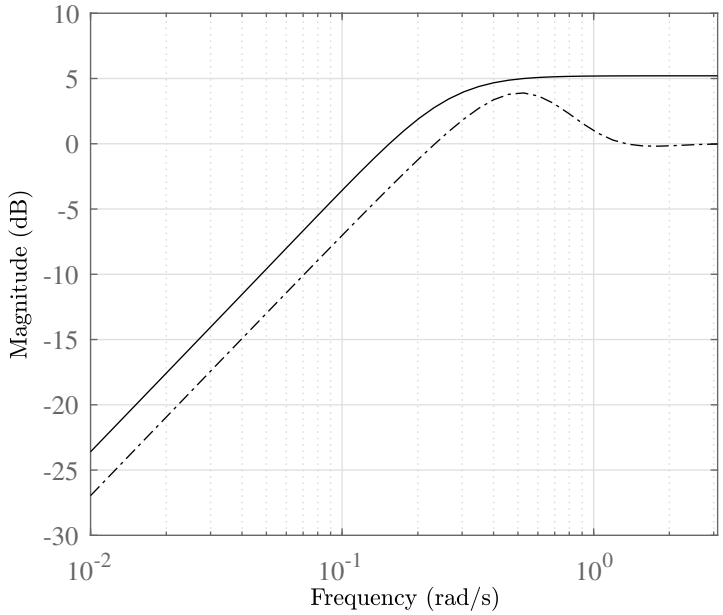

Figure 6.5: Comparison between $|W_1^{-1}(e^{j\omega})|$ (solid) and $|S_n(e^{j\omega})|$ (dotted).

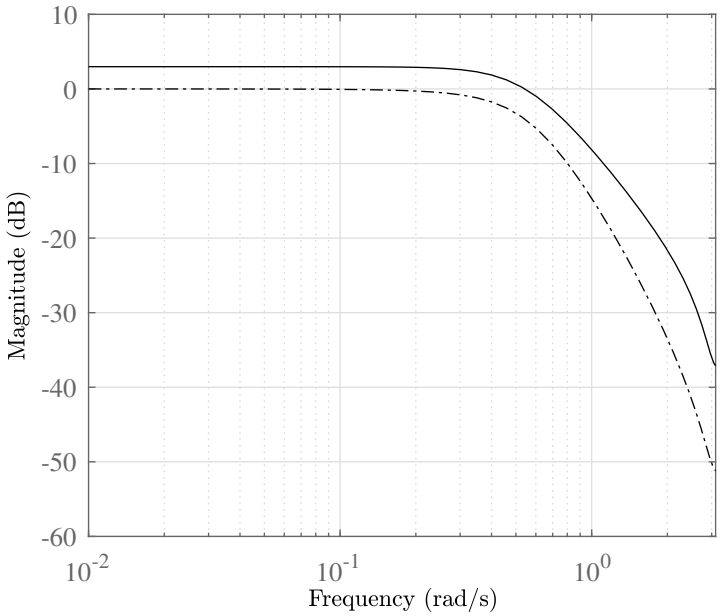

Figure 6.6: Comparison between $|\hat{W}_2^{-1}(e^{j\omega})|$ (solid) and $|T_n(e^{j\omega})|$ (dotted).

6.3 Experimental example

In this section, we use method 2 to design FOFS H_∞ mixed sensitivity controller for the magnetic levitation system shown in the figure 6.7.

Figure 6.7: Magnetic levitation system.

The control loop of the magnetic levitation system is shown in figure 6.8, where $\omega(t)$ is the reference signal in volts, $K(s)$ is the controller, K_T is the transconductance amplifier that transforms the voltage signal into the current signal and $u(t)$ is the current through an electromagnet coil. The magnetic field generated by the current exerts a force on the ball to balance the gravity force. An optical transducer measures the ball position and produced the output voltage signal $y(t)$. Further details on the considered system can be found in the book book [22].

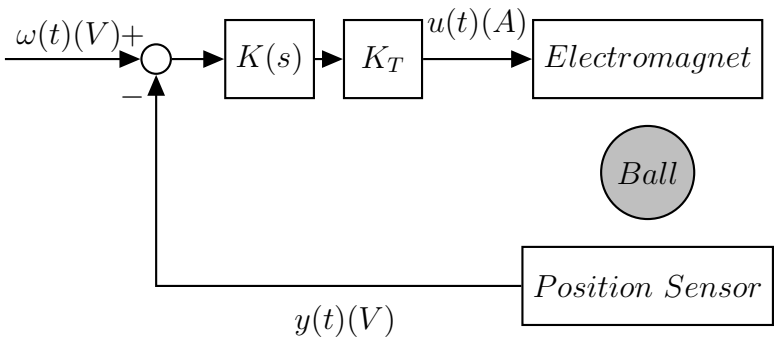

Figure 6.8: Control of Magnetic Levitation System

Magnetic levitation systems are highly non-linear unstable systems. In order to design a low-order fixed structure controller, a linearized model of the magnetic levitation system in 6.7 is obtained around a suitable equilibrium point and is given by

$$G_n(s) = \frac{Y(s)}{U(s)} = \frac{-7044}{(s - 29.68)(s + 29.68)} \tag{6.14}$$

where $U(s)$ and $Y(s)$ are the Laplace transform of the input and output voltage signals, respectively. The nominal plant in the equation (6.14) is subjected to multiplicative uncertainty bounded by the following frequency domain weighting filter

$$W_u(s) = \frac{0.1993s^2 + 6.852s + 55.96}{s^2 + 46.15s + 429.5}. \tag{6.15}$$

The goal is to design a FOFS controller

$$K(s, \boldsymbol{p}) = \frac{c_1 s^2 + c_2 s + c_3}{c_4 s^2 + s}, \tag{6.16}$$

where $p = [c_1, c_2, c_3, c_4]^T \in R^4$ is the vector of unknown parameters. Moreover, for a square wave reference signal $w(t)$ with period 2 s, duty-cycle 50% and amplitude 0.1 V, the closed-loop system must satisfy the following nominal specifications: (i) rise time $t_r \leq 0.015$ s, (ii) overshoot $\hat{s} \leq 25\%$, and (iii) zero steady-state tracking error for a step command. Since the controller has an integrator, therefore zero steady-state error for the step reference is implicitly achieved. The above-mentioned

time domain specifications are translated to the frequency domain weighting filters $W_1(s)$ and $W_2(s)$ through the methodology provided in [95].

$$W_1(s) = \frac{0.004206s^2 + 1.073s + 94.64}{s(0.006667s + 1)} \tag{6.17}$$

$$W_2(s) = 2.524e{-}06s^2 + 0.002145s + 0.631 \tag{6.18}$$

The constraints in the set $\mathcal{S}_p$ are obtained by applying Routh's stability criterion to the numerator of $1 + G(s)K(s, \boldsymbol{p})$. To avoid unstable pole-zero cancellation between the plant and the controller, we consider stable $N_k(s, \boldsymbol{p})$ and $D_k^{'}(s, \boldsymbol{p})$, where

$$N_k(s, \boldsymbol{p}) = c_1 s^2 + c_2 s + c_3 \tag{6.19}$$

and

$$D_k^{'}(s, \boldsymbol{p}) = c_4 s + 1 \tag{6.20}$$

Stability constraints for $N_k(s, \boldsymbol{p})$ and $D_k^{'}(s, \boldsymbol{p})$ are obtained according to Ruth Hurwitz criterion. It is worth mentioning that these constraints will be added to the set $\mathcal{S}_p$.

The graphical comparison between $W_2(s)$ and $W_u(s)$ is provided in the figure 6.9. It can be clearly seen from the figure 6.9 that for all frequencies $|W_2(s)| > |W_u(s)|$, therefore, we select

$$\hat{W_2}(s) = W_2(s). \tag{6.21}$$

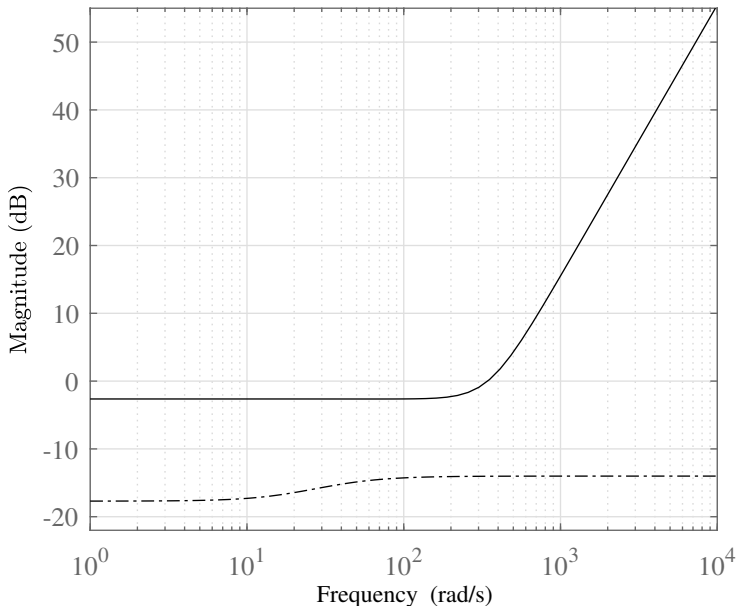

Figure 6.9: Comparison between $|W_u(j\omega)|$(dotted) and $|W_2(j\omega)|$ (solid).

We also choose $t_1 = t_2 = 0$ for SOS relaxation of the set $\mathcal{P}_s$. The positivity test of each nonconvex polynomial constraint in the stability set is replaced by SOS constraints. Non-convex polynomial constraints in the Gram matrices are relaxed by moment relaxation of order 2. The controller design problem is solved by using YALMIP ([78]) and MOSEK ([115]). The simulation is performed on a PC running on 64 bit Windows 10 platform, equipped with Intel core $i7-7500$ CPU and 8 GB RAM. The optimization problem is converged in approximately 3 minutes. The controller extracted from the feasible controller parameters set is

$$K(s) = \frac{-0.0205s^2 - 1.20232s - 12.0}{0.0011s^2 + s}. \tag{6.22}$$

The controller achieves the nominal performances as, for all frequencies, (i) $|S_n(j\omega)|$ is smaller than $|W_1^{-1}(j\omega)|$ (see Figure 6.10), and (ii) $|T_n(j\omega)|$ is smaller than $|W_2^{-1}(j\omega)|$ (see Figure 6.11). Numerically,

$$\|S_n(j\omega)W_1(j\omega)\|_\infty = 0.99 \tag{6.23}$$

and

$$\|T_n(j\omega)W_2(j\omega)\|_\infty = 0.8750. \tag{6.24}$$

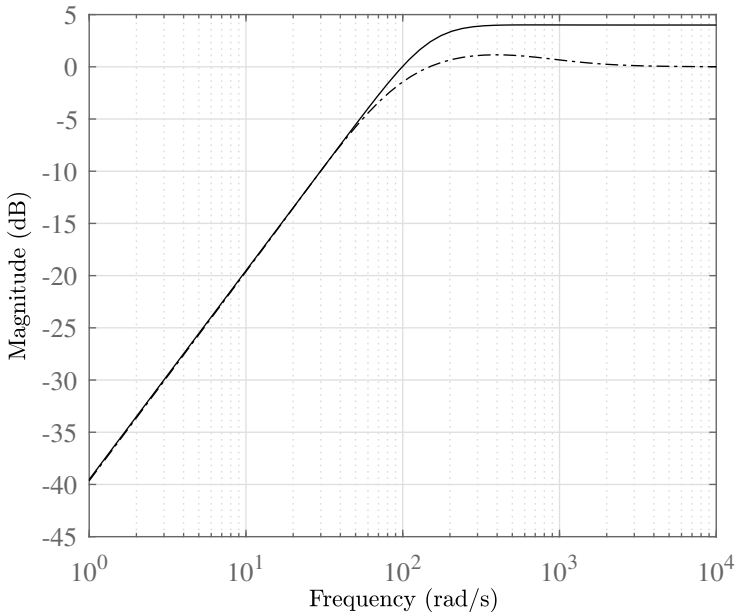

Figure 6.10: Comparison between $|W_1^{-1}(j\omega)|$ (solid) and $|S_n(j\omega)|$ (dotted).

In figure 6.12, we provide the comparison of closed-loop time-domain responses between the linearized system $G_n(s)$ and the real plant. As pointed out earlier,

reference $w(t)$ is a square with amplitude 0.1V and frequency 0.5 Hz. The linear system $G_n(s)$ achieves the time domain requirements as both the rise time $t_r \approx 0.00928$ s and the overshoot $\hat{s} \approx 23.02\%$. However, with the designed controller the overshoot on the actual plant is $\hat{s} \approx 35\%$. The large overshoot is due to the modeling error resulting from the linearization of the actual nonlinear plant. However, despite this modeling error, the designed controller is able to stabilize the unstable nonlinear plant and is also able to achieve the desired rise time $t_r \approx 0.011$ s.

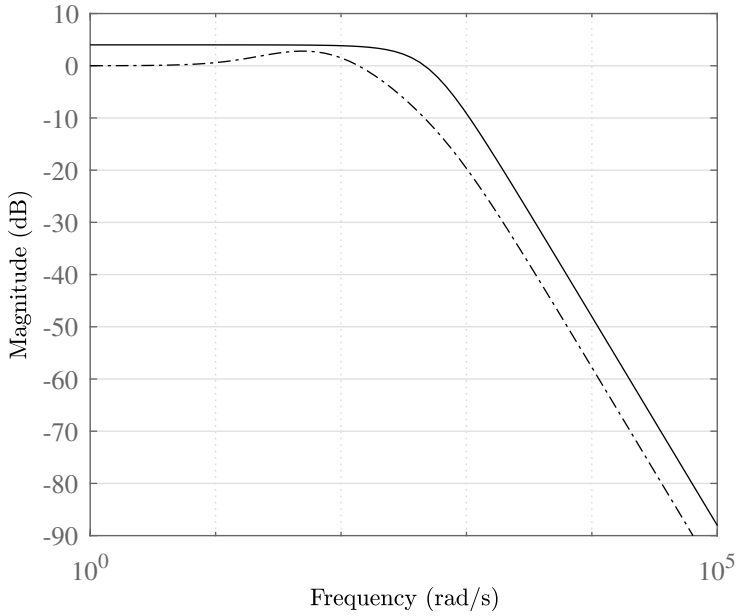

Figure 6.11: Comparison between $|W_2^{-1}(j\omega)|$ (solid) and $|T_n(j\omega)|$ (dotted).

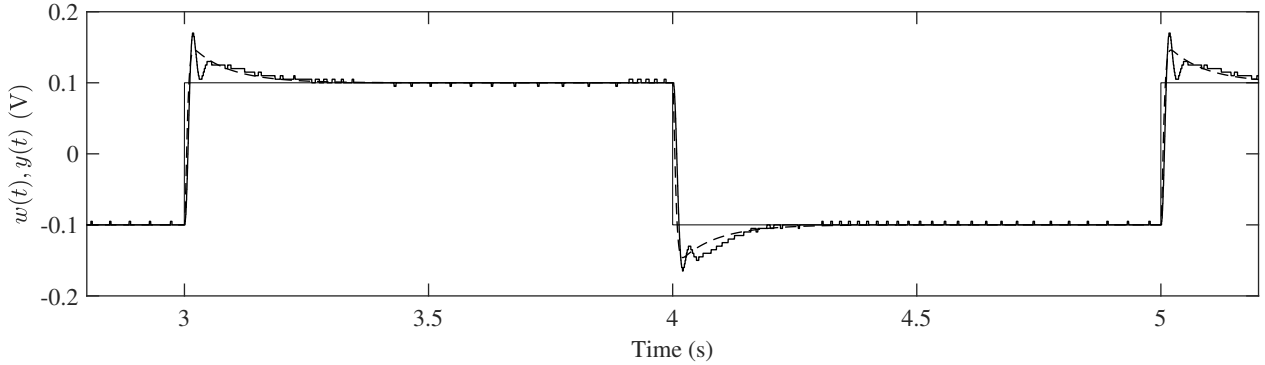

Figure 6.12: Magnetic levitation system response to square wave reference signal: reference $w(t)$ (solid square-wave), magnetic levitation system output $y(t)$ (solid) and linearized $G_n(s)$ system output (dashed) responses.

Chapter 7

Conclusions

In this section, we have proposed convex relaxation algorithms for designing model-based FOFS H_∞ mixed sensitivity controllers both for CT and DT systems. First, we define the feasible controller parameter set as a semi-algebraic set of all the controller parameters that guarantee robust stability and fulfillment of nominal performance. We then translate the constraints in the feasible controller parameter set to polynomials in unknown controller parameters and frequency. The problem of designing the FOFS H_∞ mixed sensitivity controllers is then reformulated as the non-emptiness test of the feasible controller parameter set. It is worth mentioning that the feasible controller parameter set is a non-convex set and thus the FOFS H_∞ control design problem is NP-hard to be solved. To compute the parameters of the FOFS controller, the feasible controller parameter set is relaxed by using recent results from the field of polynomial optimization, reviewed in Chapter 2.

We have provided three algorithms for the convex relaxation of the feasible controller parameter set. The first algorithm uses Putinar's positivstellensatz for relaxing the feasible controller parameter set. This algorithm is a single-shot algorithm based on SOS relaxation and it provides the inner approximation of the feasible controller parameter set. The computational complexity of this algorithm is low only for low-order CT systems with lower-order controllers. In the second algorithm, SOS relaxation of the feasible controller parameter set is achieved by exploiting the generalized S-procedure. This algorithm also solves the FOFS H_∞ mixed sensitivity control problem in a single shot and provides the inner approximation of the feasible controller parameter set. The computational complexity of this method is high for DT systems. The third algorithm is based on the exchange method and solves the optimization problems iteratively using moment relaxation. This method provides the outer approximation of the feasible controller parameter set. In comparison to the other two methods, this method is computationally efficient for DT systems and high-order CT systems with higher-order controllers.

The main advantages of the proposed algorithms compared to existing methods are:

(i) The BMI-based local algorithms, HIFOO and *Hinfstruct* provide only local solutions and thus can typically trap in local minima, whereas the proposed algorithms look for controller parameters in a relaxed convex set.

(ii) In contrast to the BMI-based global algorithms, the interval arithmetic-based algorithms, and the convex algorithms for special structure controllers such as PI and PID controllers, the proposed algorithms do not require any special structure of the plant and/ or controller for computing the parameters of the FOFS mixed sensitivity H_∞ controller that belong to a relaxed convex set.

Finally, we provide two simulation examples and one experimental application to show the efficiency and comparison of the proposed algorithms on both CT and DT systems.

Part II

Direct data-driven FOFS H_∞ mixed sensitivity control design

Chapter 8

Introduction

The control system for a plant can be designed in two ways, namely, model-based control and direct data-driven control. In model-based control, a model of the plant is typically developed by using system identification methods. This model is then used for controller design. In direct data-driven control, the controller is directly designed from the experimental data.

In model-based control, the model of a dynamic system plays a pivotal role in the overall performance of the feedback control system. The complexity of the model obtained from system identification is crucial as for simpler models, model estimation and controller synthesis are easier. On the other hand, building higher-order complex models may require large experimental data and computational effort. Moreover, system analysis and control system design and implementation tend to be complex for higher-order models. Thus in industry, low-order models are preferred. However, approximation of plant dynamics with a lower-order model leads to model uncertainty which can degrade the performance of the control loop. Control synthesis by using process data eliminates the issues associated with the modeling of a dynamic process. A survey on the difference between model-based control and direct data-driven control is presented in [171], where the authors state that building a model for a dynamic system is an approximation of the true system and unmodeled dynamics always exist in model-based control. As a result, model-based control methods are inherently less robust and unsafe for practical applications. On the contrary, for linear time-invariant systems, the parametric uncertainties and the unmodeled dynamics are irrelevant in direct data-driven control where the only source of uncertainty comes from the measurement process.

8.1 Overview of existing direct data-driven control techniques

This section provides an overview of existing direct data-driven control design techniques. Data-driven control synthesis techniques are broadly categories as: (i) model-reference control, (ii) predictive control and (iii) robust control. Here we provide only a brief description of each method.

8.1.1 Model Reference Control

Model-reference Adaptive Control (MRAC)

MRAC [72] is one of the first approaches to designing direct data-driven controllers. It is an online method that adjusts the controller parameters by minimizing the error between the reference signal and the actual output. Further details on MRAC can be found in [73].

Virtual Reference Feedback Tuning (VRFT)

The VRFT approach was originally proposed for SISO systems in [113]. This technique requires the time-domain input-output data experimentally collected from the plant. It is an offline method that can compute the direct data-driven controller in a single shot. Closed-loop stability for VRFT is addressed in [90] and [3]. The extension of VRFT to MIMO systems is provided in [137] and for linear time-varying systems in [136]. The issue of performance robustness is addressed in [52] and [139] by applying scenario optimization tools. Automatic tuning of the direct data-driven controller in the VRFT framework is developed in [44]. In the VRFT approach, the optimal choice of the reference model and select controller class without prior knowledge of the plant is not trivial. The papers [31] and [165] provide methods for the selection of reference models. The paper [138] addresses the selection of the controller class.

Iterative Correlation-based Tuning (ICbT)

ICbT [9] is an offline iterative approach for direct data-driven control synthesis. This method is based on the correlation approach and implements the concepts of system identification. A non-iterative version of this method is presented in [91] where sufficient conditions for closed-loop stability are also developed. The extension of ICbT to MIMO systems is provided in [100].

Iterative Feedback Tuning (IFT)

IFT is an offline method first introduced in 1994 by Hjalmarsson et al. in [59]. A detailed discussion on IFT and its applications is provided in papers [60] and [58], and the references therein. IFT has two main drawbacks, one is the requirements of multiple experiments, and the other is that stability is not guaranteed. The papers,[144] and [65] provide some results on robust stability conditions.

Unfalsified Control (UC)

UC [108] is an online direct data-driven control synthesis method that identifies a controller belonging to a set of candidate controllers known as an unfalsified controller set. A controller is said to be falsified by the measurements if it violates the desired performance specification when inserted in the closed loop. Otherwise, the controller is unfalsified. A virtual reference for the falsification procedure is obtained by inverting the controller at the current iteration. A controller from the unfalsified set that satisfies the desired performance is selected at each iteration. Various switching methods are available in the literature to select a controller from the unfalsified controller set (see, e.g., [163], [110]). A new direct data-driven technique based on the unfalsified control is presented in [46]. This approach requires only one experiment and two reference models. The stability of unfalsified adaptive switching control in noisy environments is studied in [47].

All model-reference based schemes require special care as minimization based on desired reference model can lead to poor stability and robustness.

8.1.2 Predictive data-driven control

Model-Free Adaptive Control (MFAC)

MFAC, introduced in [169], is an online direct data-driven control method for a class of unknown non-affine nonlinear systems. It does not require any explicit physical model of the plant or any stability analysis used in the control system design. MFAC implements a linearization data modeling method through a pseudo-partial derivative or pseudo-gradient vector. Therefore stability analysis only depends on the measured input-output data of the controlled plants. Further details on MFAC can be found in [170].

Data Driven Model Predictive Control

Classical model predictive control (MPC) is a prediction-based control that relies on the dynamic model of the plant. Direct data-driven MPC uses input-output data instead of a model of the process. A subspace approach based on

direct data-driven MPC is presented in [16] whereas data-driven MPC that uses implicit model description based on behavioral systems theory and past measured trajectories is proposed in [20].

8.1.3 Robust data-driven control

Model-based robust control is a popular method that deals with uncertainties, noise and disturbances. Mostly robust control problem is solved through H_∞ framework where desired performance specifications and uncertainty are formulated as weighting norms on the mixed sensitivity functions. In classical H_∞ control, the optimization problem is solved through linear matrix inequalities (LMI) (see, e.g., [124, 123]) or on the algebraic Riccati equation (see, e.g., [94, 76]). However, controllers obtained through these methods have higher order and may be impossible to implement. Any additional constraint on the order or structure of the controller makes the optimization problem non-convex and thus difficult to solve. Many techniques are available in the literature to solve this nonconvex problem ([75], [121] and [164], just to cite a few).

Many frequency domain direct data-driven techniques are also available in the literature to design FOFS controllers that guarantee closed-loop stability and performance. Some of these techniques provide global optimal solutions while others can solve optimization problems locally.

Global frequency domain methods for FOFS direct data-driven control design

One of the earlier frequency domain direct data-driven techniques is [98] where a complete set of stabilizing PID controllers are obtained directly from the frequency response of the plant without the need for any identified model. For closed-loop stability, the relative degree of the plant and its number of right-half plane (RHP) zeros and poles are estimated from the frequency response. The resulting optimization problem for computing the controller's parameters is convex as PID controllers are linear in unknown parameters. This approach also ensures performance measures such as gain margin, phase margin, and H_∞ performance specifications. Based on this method, the design of fixed-order controllers is proposed in [63] whereas the design of fixed structure robust controllers is presented in [64]. In [63] and [64], convexity of H_∞ optimization is achieved by fixing the poles of the controller a priori.

A data-driven approach for designing fixed-order controllers in a mixed-sensitivity loop-shaping framework is proposed in [135]. It is a convex optimization technique, where the Youla–Kučera parameter is first derived directly from a set of input-output data. A fixed-order controller is then identified from the same input-output data. However, this technique is limited only to stable LTI plants and can not

ensure a specific controller structure.

Design of robust fixed-order H_∞ controller for LTI SISO plants through convex optimization is proposed in [8]. This method translates stability conditions and performance requirements to a set of linear constraints on the Nyquist diagram of the loop function by considering a linearly parameterized controller. However, the approximation of nonconvex robust performance constraints by linear constraints introduces conservatism that depends on the desired open-loop transfer function choice. This method treats low-order and high-order controllers differently. Higher-order controllers are linearly parameterized using orthogonal basis functions. On the other hand, linear parameterization of low-order controllers is achieved by fixing the poles of the controller before design. For implementation purposes, high-order controllers are approximated by low-order controllers by model order reduction methods. However, this may cause degradation of the performance and even instability in some cases.

Design of robust fixed order H_∞ controllers for LTI SISO systems via convex optimization is proposed in [6]. This approach requires the collection of frequency domain data from the coprime factors of the plant. Moreover, necessary and sufficient conditions for closed-loop stability are derived through Nyquist stability criteria. Convexity of the stability constraints is achieved through linear parameterization of the coprime factors of the controller. A linear approximation of the performance constraints is achieved through a stable transfer function that keeps the Nyquist plot of the weighted sensitivity function in the RHP. It is important to note that the optimization problem converges to a globally optimal solution only for high-order controllers. In the case of low order controllers, the choice of basis significantly affects the convergence of the optimization problem. Although a practical procedure for choosing the basis functions is proposed in the paper, optimal selection still remains an open problem.

A method based on the loop-shaping for designing fixed structure H_∞ controllers both for SISO and MIMO systems is presented in [38]. This approach uses multiple line constraints in the Nyquist diagram to achieve closed-loop stability and performance. The resulting feasible controller constraints are multilinear for linearly parameterized controllers. However, for special controllers, these constraints become linear.

In [32], a new direct data-driven approach based on convex optimization to design two degree of freedom robust fixed-order H_∞ controller is proposed. In this approach, the convexity of stability constraints is obtained through linear parameterization of the controller using orthonormal basis functions. On the other hand, the convexity of the objective function is achieved through desired loop gain, which is a function of the desired complementary sensitivity function. One major drawback of the proposed approach is that the resulting control problem is sub-optimal.

Local frequency domain methods to design FOFS direct data-driven controllers

In [13], a method to design low order fixed structure direct data-driven controllers is proposed. This approach is an extension of the work presented in [6]. In this approach, nonconvex optimization problem is solved by a new particle swarm optimization (PSO) algorithm for unknown controller parameters and optimal selection of the basis functions parameters.

An alternative formulation of the problem of fixed-order H_∞ controllers is proposed in [5] where, by exploiting the Youla parameterization of the set of stabilizing controllers, the controller is designed by solving a nonconvex optimization problem. Although approaches based on nonconvex optimization may work adequately in general, convergence of a noncovex optimization problem to a global optimal solution is not always guaranteed.

Uncertainty modeling in robust data-driven control

In direct data-driven control, frequency-domain uncertainty is modeled by probabilistic (see, e.g., [8] and [6]), or deterministic methods (see, e.g., [32]). In [6], uncertainty weighting filters for coprime factors of an uncertain plant subjected to additive uncertainty, are computed from the co-variance of the estimates for given confidence of interval. This method requires a large set of frequency-domain data to be collected from the plant at each frequency. In [32], the optimal uncertainty model for multiplicative unstructured uncertainty is computed based on the concept of the Chebyshev center of a set of points. This method also requires a large frequency-domain data set to be collected from the plant at each frequency.

8.2 Research Objective

The objective of this research is to provide a method for designing FOFS direct data-driven controllers such that the global optimal solution to H_∞ mixed sensitivity control problem is obtained. The existing convex methods for FOFS direct data driven H_∞ control, use linearly parameterized controllers to get the convex constraints for stability. Linear parameterization is achieved either by fixing the poles of the controller a priori or by using orthonormal basis functions. Furthermore, convexity on H_∞ constraints is obtained through some approximations. The methods that use the orthonormal basis for linear parameterization of the controller, do not converge to the global optimal solution for low order fixed structure controllers. In this research, instead of introducing such limitations/approximations, we propose a convex relaxation method to solve the H_∞ control problem such that global optimal solution is achieved. To apply convex relaxation, FOFS H_∞ control problem is formulated as a polynomial optimization problem. Convex relaxation methods

relax the polynomial optimization problem into an SDP which can be solved by the readily available softwares.

8.2.1 Contribution

The major highlights of this research are given below.

- FOFS H_∞ mixed sensitivity direct data-driven controllers are designed such that neither the controller transfer function nor its coprime factors are linearly parameterized. In fact user can select any controller, non linear in unknown parameters such that the numerator and the denominator are linear functions of the controller parameters to be designed.
- Necessary and sufficient conditions for closed-loop stability are derived in the direct data-driven framework. These conditions are developed based on the concepts of positive real functions and Nyquist stability.
- A one-shot convex relaxation-based algorithm for robust FOFS H_∞ mixed sensitivity direct data-driven control design is provided. This algorithm is based on assumptions that the weighting filter for the unstructured multiplicative uncertainty and frequency response samples for the nominal plant are available.
- An iterative convex relaxation-based algorithm for robust FOFS H_∞ mixed sensitivity direct data-driven control design is provided. In this algorithm, the control design problem is formulated as a SIPP in uncertainty under the assumption that uncertainty is additive, unknown, bounded, and belongs to a given semi-algebraic set. The SIPP is then solved iteratively through the exchange method by using semidefinite relaxations. Typically, in direct data-driven control the estimation of the frequency domain bound for unstructured uncertainty requires many frequency response samples to be collected from the plant at each frequency. Because of the SIPP formulation, this algorithm require only one frequency response sample for each frequency to design direct data-driven robust controllers.

The results presented in this section of the thesis will be the subject of a journal paper currently in preparation.

Chapter 9

Description of the plant and the controller

In this chapter, we first provide some elementary results on coprime factorization. Interested readers can find further details on the coprime factorization in the book [85]. We then present all the necessary class of models and controllers for the design of FOFS H_∞ mixed sensitivity direct data-driven controllers. The linear plant is represented in the coprime form which is needed to develop some important theoretical results that will be presented in the subsequent chapters. The controller to be designed is assumed to belong to a given class such that the numerator and the denominator of the controller are linear in unknown parameters. Two types of uncertainties are presented in this chapter. In the first type, a frequency domain bounding function is used for describing unstructured uncertainty. The second type of uncertainty is assumed to be unknown, bounded and belongs to a given semi-algebraic set.

9.1 Coprime factorization

Consider a rational transfer function $\mathcal{G}(s)$ such that

$$\mathcal{G}(s) = \mathcal{N}(s)\mathcal{D}^{-1}(s). \tag{9.1}$$

Suppose d_n is the degree of the numerator and d_m is the degree of the denominator.

Definition 11 (**Proper transfer function**). *The transfer function $\mathcal{G}(s)$ is said to be proper if and only if $d_m \geq d_n$.*

Definition 12 (**Improper transfer function**). *The transfer function $\mathcal{G}(s)$ is said to be improper if and only if $d_m \leq d_n$.*

Definition 13 (**Strictly proper transfer function**). *The transfer function $\mathcal{G}(s)$ is said to be strictly proper if and only if $d_m > d_n$.*

Definition 14 (**biproper transfer function**). *The transfer function $\mathcal{G}(s)$ is said to be biproper if and only if $d_m = d_n$.*

Definition 15 (**Relative degree**). *The relative degree $r_{\mathcal{G}}$ of the transfer function $\mathcal{G}(s)$ is defined as:*

$$r_{\mathcal{G}} = d_m - d_n. \tag{9.2}$$

9.1.1 Coprime factors

Suppose, $\mathcal{X}(s)$ and $\mathcal{Y}(s)$ are the coprime factors of a rational transfer function $\mathcal{G}(s)$. Thus, $\mathcal{G}(s)$ can be written as:

$$\mathcal{G}(s) = \mathcal{X}(s)\mathcal{Y}^{-1}(s). \tag{9.3}$$

The coprime factors $\mathcal{X}(s)$ and $\mathcal{Y}(s)$ have the following properties (see, e. g., [85]):

1. both $\mathcal{X}(s)$ and $\mathcal{Y}(s)$ are stable and proper transfer functions.
2. they must follow the Bezout's identity which is satisfied if $\mathcal{X}(s)$ and $\mathcal{Y}(s)$ have no common zero in $\Re[s] \geq 0$ and at $s = \infty$.

We provide the following result based on the above mentioned properties of the coprime factors.

Result 24 (**Condition for coprimeness**). *If $\mathcal{X}(s)$ and $\mathcal{Y}(s)$ are the coprime factors of a rational transfer function $\mathcal{G}(s)$ then either $\mathcal{X}(s)$ or $\mathcal{Y}(s)$ must be a bi-proper transfer function.*

9.2 Plant representation

Suppose $X_n(s)$ and $Y_n(s)$ be the coprime factors of a CT LTI SISO plant $G_n(s)$. The representation of $G_n(s)$ in terms of coprime factorization is given by:

$$G_n(s) = X_n(s)Y_n^{-1}(s). \tag{9.4}$$

The coprime representation in terms of the frequency response of the CT plant is obtained by replacing $s = j\omega$.

$$G_n(j\omega) = X_n(j\omega)Y_n^{-1}(j\omega). \tag{9.5}$$

Similarly, a DT LTI SISO plant $G_n(z)$ in terms of its coprime factors $X_n(z)$ and $Y_n(z)$, is represented as follows.

$$G_n(z) = X_n(z)Y_n^{-1}(z). \tag{9.6}$$

For DT systems, coprime factorization in terms of the frequency response of the plant is obtained by replacing $z = e^{j\omega}$.

$$G_n(e^{j\omega}) = X_n(e^{j\omega})Y_n^{-1}(e^{j\omega}). \tag{9.7}$$

9.2.1 Formulation of coprime factors

In case of stable CT systems, we choose $X_n(j\omega) = G_n(j\omega)$ and $Y_n(j\omega) = 1$ and frequency response samples are directly obtained by performing an open-loop experiment on the plant.

In case of an unstable CT plant, a stabilizing controller is needed to properly formulate $X_n(j\omega)$ and $Y_n(j\omega)$. In this work, set of closed loop frequency domain data is acquired according to scheme shown in figure 9.1, where $G_n(s)$ is an unstable plant, $K_s(s)$ is an initial stabilizing controller, r_1 is the reference signal, u_1 is the control input, $m_1(j\omega)$ and $m_2(j\omega)$ are the measurements. Co-prime factors $X_n(j\omega)$ and $Y_n(j\omega)$ are computed as follows:

$$\begin{aligned} X_n(j\omega) &= m_1(j\omega)m_2^{-1}(j\omega) \\ &= \frac{G_n(j\omega)}{1 + G_n(j\omega)K_s(j\omega)} \ \forall\omega \end{aligned} \tag{9.8}$$

$$\begin{aligned} Y_n(j\omega) &= u_1(j\omega)m_2^{-1}(j\omega) \\ &= (1 + G_n(j\omega)K_s(j\omega))^{-1} \ \forall\omega \end{aligned} \tag{9.9}$$

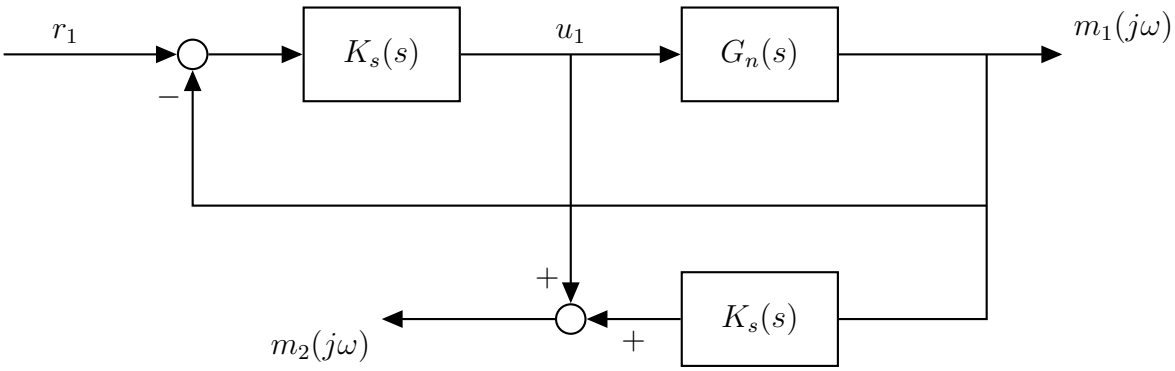

Figure 9.1: Data acquisition for coprime factors

From equations (9.8) and (9.9), it is evident that:

1. $X_n(s)$ and $Y_n(s)$ are stable transfer functions as $K_s(s)$ is a stabilizing controller.

2. $X_n(s)$ is a proper transfer function as degree of $1+G_n(s)K_s(s)$ is greater than or equal to the degree of $G_n(s)$.

3. $Y_n(s)$ is a biproper transfer function under the assumption that the $K_s(s)$ and $G_n(s)$ are the proper transfer functions.

4. $G_n(j\omega) = X_n(j\omega)Y_n^{-1}(j\omega)$

Thus, $X_n(s)$ and $Y_n(s)$ are coprime factors of $G_n(s)$.

If $K_s(s)$ is known to be a bi-proper transfer function then frequency response of the coprime factors can also be obtained according to figure 9.2, where $G_n(s)$ is an unstable plant, $K_s(s)$ is an initial stabilizing controller, r_1 is the reference signal, $m_1(j\omega)$ and $m_2(j\omega)$ are the measurements.

$$\begin{aligned} X_n(j\omega) &= m_1(j\omega) r_1^{-1}(j\omega) \\ &= \frac{G_n(j\omega)K_s(j\omega)}{1 + G_n(j\omega)K_s(j\omega)} \ \forall\omega \end{aligned} \tag{9.10}$$

and

$$\begin{aligned} Y_n(j\omega) &= m_2(j\omega) r_1^{-1}(j\omega) \\ &= \frac{K_s(j\omega)}{1 + G_n(j\omega)K_s(j\omega)} \ \forall\omega \end{aligned} \tag{9.11}$$

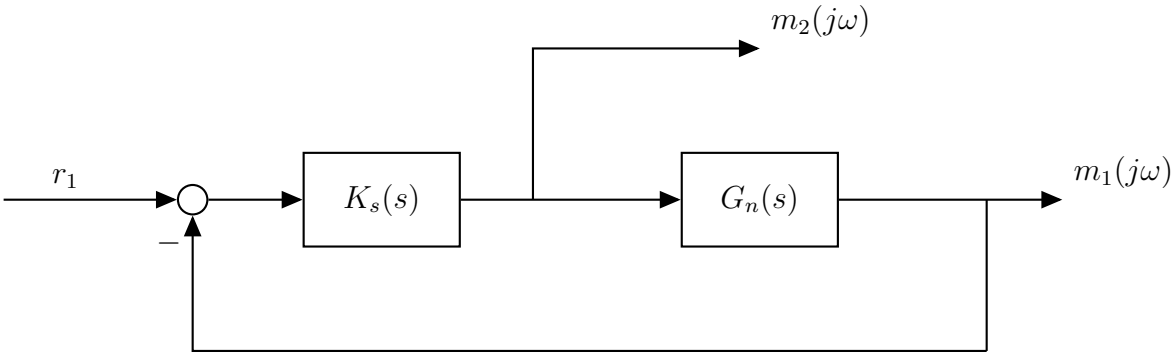

Figure 9.2: Data acquisition for coprime factors when $K_s(s)$ is a bi-proper

For DT systems, coprime factors can be formulated in the same way as discussed above.

9.3 Acquisition of the data

In data-driven settings, we assume that the transfer function of the plant is not available and that the controller is designed by only relying on a set of input-output frequency domain data collected experimentally from the stable plant or coprime factors of an unstable plant. The most commonly used method for the frequency domain data acquisition is the frequency sweep method. Two types of frequency domain data can be obtained from the plant (or coprime factors of the plant) by frequency sweep method.

- Gain-Phase data
- Real-Imaginary data

Gain-Phase data can be measured by using simple equipment such as an oscilloscope. Once available, Gain-Phase data are translated to Real-Imaginary data using Euler's formula. Real-Imaginary data can directly be measured from the open loop (stable plants) or closed loop experiment (unstable plants). One popular method of measuring Real-Imaginary data is so-called dual-phase demodulation method. In this method, a reference signal is generated by the internal oscillator is applied to the device under test and the output of the device is measured. By using the frequency domain mixer, two signals are generated. The first signal is obtained by multiplying the measured signal with a reference signal whereas the second signal is produced by multiplying 90° phase-shifted reference signal with the measured signal. The outputs of the mixer are passed through low-pass filters to reject 2ω component and the noise. The effect of the residual noise (unknown but bounded) as uncertainty is discussed in the section 9.6 . The filtered signals are the real and imaginary parts of the input signal. In this way, by changing the frequency of the reference signal, frequency response of the plant can be measured over desired frequency set Ω_d.The number of frequency points in Ω_d is selected in order to trade off between the accuracy of the frequency response description and the practical feasibility of the experiment. Although selecting an appropriate set of frequency points is still an open problem. However, for practical applications, frequency points can be chosen logarithmically, equally spaced, sets of equally spaced frequencies with different increments or on the basis of available information about the plant such as resonance frequencies and desired closed loop bandwidth, etc.

For the purpose of completeness, we present general guidelines for collecting the data from the plant or its coprime factors.

i Select $\Omega_d = \{\omega_1, \omega_2, \ldots, \omega_n\}$ such that Ω_d contains sets of equally spaced frequencies with different increments, ω_1 is a reasonably small frequency and ω_n is a sufficiently large frequency.

ii Measure the data at the starting frequency.

iii Go to next frequency and again measure the data.

iv Repeat step(iii) until no further information can be gathered at high frequencies.

v Check for data points where there is a significant change in the data (resonance points). Collect more data near those frequencies.

vi Update Ω_d based on step (iv) and step (v).

The major advantage of the above-mentioned frequency sweep method is the higher signal-to-noise ratios (SNR) since the energy of the signal is concentrated at a single frequency for any given time instant. The drawback of this method is the

longer measurement time which can be crucial for some applications. Therefore in such applications, frequency response function (FRF), which is the transfer function measurement on a discrete frequency grid Ω_d, can be computed using periodic or random excitations (see e. g., [130] and [147]). For the computation of the FRF, the measurements can be given in the time domain data set: $\{u(t_k), y(t_k), t_k = 1,2,\ldots,N_s\}$ where, $u(t_k)$ is the input, $y(t_k)$ is the output and N_s is the total number of samples. A discrete fourier transform of the input and output signals is then used to estimate the FRF. It is important to point out that periodic or random signal excitations can excite multiple frequencies at the same time, therefore reducing the measurement time significantly compared to the frequency sweep method. However, frequency resolution depends on the number of data samples acquired from the experiment. For the estimation of the FRF, the effect of the noise as uncertainty is discussed in the section 9.6.

9.4 Class of controllers

Assume that $\mathcal{K}_{Cf}$ is the class of FOFS stabilizing CT LTI controllers described by the transfer function

$$K(s,\rho) = \frac{N(s,\rho)}{D(s,\rho)} = \frac{\sum_{i=0}^{d_n} \beta_i(\rho)\ s^i}{s^{d_m} + \sum_{j=0}^{d_m-1} \alpha_j(\rho) s^j}. \tag{9.12}$$

Similarly, for DT systems, $\mathcal{K}_{Df}(z,\rho)$ is the class of LTI controllers described by the following transfer function.

$$K(z,\rho) = \frac{N(z,\rho)}{D(z,\rho)} = \frac{\sum_{i=0}^{d_n} \beta_i(\rho)\ z^i}{z^{d_m} + \sum_{j=0}^{d_m-1} \alpha_j(\rho) z^j} \tag{9.13}$$

For equations ((9.12) - (9.13)):

- we denote the unknown vector of controller parameters by $\rho \in \mathbb{R}^{n_p}$ such that $n_p = d_n + d_m + 1$.
- The coefficients, $\alpha_j(\rho)$ and $\beta_i(\rho)$, are linear in ρ.
- The controller is a proper transfer function.
- Numerator and the denominator of the controller are stable polynomials of degree d_n and d_m respectively.

It's worth mentioning that the chosen controller class is very general and flexible. As a matter of fact, one can select any LTI controller with FOFS by setting some of the controller's parameters to zero. Furthermore, because the numerator and denominator coefficients depend linearly on ρ, the controller can be nonlinear in ρ.

Remark 3. *At a given frequency ω, both $G_n(j\omega)$ and $G_n(e^{j\omega})$ are just complex numbers. Thus, in direct data-driven framework where frequency domain data acquired from the plant is used to synthesize controllers, difference in the CT and DT is trivial. Therefore,in the rest of this section, we present results only for CT systems which are equally valid for DT systems.*

9.5 Sensitivity functions

For unity feedback control structure, expressions for sensitivity and complementary sensitivity functions are given by:

$$\begin{aligned} S(j\omega) &= (1 + G_n(j\omega)K(j\omega))^{-1} \\ &= \frac{D(j\omega)Y_n(j\omega)}{N(j\omega)X_n(j\omega) + D(j\omega)Y_n(j\omega)}, \end{aligned} \tag{9.14}$$

$$\begin{aligned} T(j\omega) &= G_n(j\omega)K(j\omega)(1 + G_n(j\omega)K(j\omega))^{-1} \\ &= \frac{N(j\omega)X_n(j\omega)}{N(j\omega)X_n(j\omega) + D(j\omega)Y_n(j\omega)} \end{aligned} \tag{9.15}$$

9.6 Class of uncertainties

9.6.1 Frequency domain weighting bound representation of unstructured uncertainty

Consider the feedback control system shown in the figure 9.3, where $G_n(s)$ is the nominal plant, $K(s)$ is the controller, r is the reference signal, u is the control input, y is the measured output and z_1 and z_2 are the controlled outputs associated to the assigned performance requirements.

Suppose $G_p(s)$ is an uncertain plant, then the set of perturbed plants are represented as follows.

$$\Pi : G_p(s) = G_n(s)(1 + W_u(s)\Delta(s)) \tag{9.16}$$

where $W_u(s)$ is an uncertainty weight with bounded infinity norm and $\Delta(j\omega)$ is an unknown stable transfer function that satisfies $|\Delta| \leq 1$.

Multiplicative uncertainty weight $W_u(s)$ can be computed according to the following equation.

$$W_u(j\omega) \geq \max_{G_p \in \Pi} \left| \frac{G_p(j\omega)}{G_n(j\omega)} - 1 \right| \ \forall\omega \tag{9.17}$$

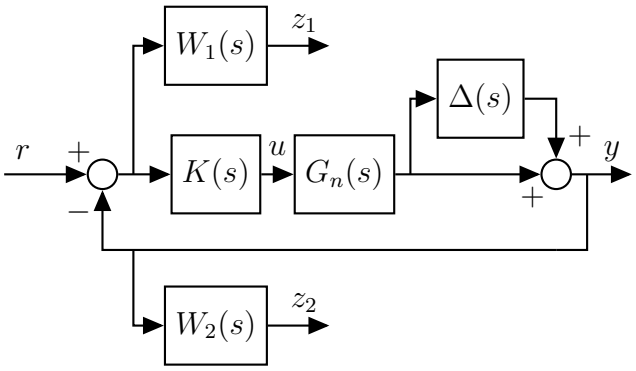

Figure 9.3: Block diagram of feedback system

Computation of Multiplicative uncertainty weight

Suppose, the perturbed plant $G_p(s)$ is represented in terms of the coprime factors $X_p(s)$ and $Y_p(s)$ such that $G_p(s) = X_p(s)Y_p^{-1}(s)$. Then equation (9.17) can be rewritten as follows:

$$W_u(j\omega) \geq \max_{G_p \in \Pi} \left| \frac{X_p(j\omega)Y_n(j\omega)}{Y_p(j\omega)X_n(j\omega)} - 1 \right| \ \forall \omega \tag{9.18}$$

For frequency sweep method, we collect N_u frequency response samples from the plant (or its coprime factors) for each $\omega \in \Omega_d$. In case of FRF method, data from the plant is collected by performing N_u independent experiments and estimation of FRF corresponding to each experiment is carried out with same frequency grid Ω_d.

The nominal coprime factors can be computed by taking the average of the experimental data for each $\omega \in \Omega_d$, that is,

$$\begin{aligned} X_n(j\omega) &= \frac{1}{N_u} \sum_{i=1}^{N_u} X_{pi}(j\omega) \\ Y_n(j\omega) &= \frac{1}{N_u} \sum_{i=1}^{N_u} Y_{pi}(j\omega) \end{aligned} \tag{9.19}$$

Finally, at each $\omega \in \Omega_d$, compute

$$\ell_i(\omega) = \left| \frac{G_{pi}(j\omega)}{G_n(j\omega)} - 1 \right|, \ i = 1,2,\ldots,N_u. \tag{9.20}$$

and

$$\overline{L}(\omega) = \max \ell_i(\omega), \ i = 1,2,\ldots,N_u. \tag{9.21}$$

A rational transfer function $W_u(j\omega)$ is obtained by fitting a curve to $\overline{L}(\omega)$ in the frequency domain. By using the same procedure, a frequency domain weighting filter for unstructured additive uncertainty can also be computed.

Remark 4. *In this subsection, the nominal frequency response is computed as an average of the obtained frequency responses for the computation of the multiplicative uncertainty weight. In principle, the nominal frequency response should be computed such that the size of the uncertainty for the given data set is minimized. However, computation of the optimal nominal frequency response would require a solution of a complex problem. On the contrary, although not optimal, one way of computing the nominal frequency response is to take the average of the obtained frequency responses at each frequency.*

Remark 5. *For the FRF, the uncertainty weight can be computed as a stochastic bound. The use of stochastic uncertainty weights is not new in direct data-driven control (see e.g., [6]). However, stochastic uncertainty weights can guarantee the robustness and performance only within a given probability level.*

9.6.2 Unknown and bounded uncertainty

One drawback of the method presented above, for computing a frequency domain bound for unstructured uncertainty is that it requires collection of many frequency response sample from the plant at each frequency (or performing multiple experiments in case of FRF estimation), which may not be trivial in some applications. On the other hand, robust direct data-driven controllers can be designed by collecting only one frequency response sample from the plant at each frequency under the assumption that the uncertainty is unknown and bounded (UB) and belongs to a given semi algebraic set.

Assume that UB additive uncertainty, that belongs to a given semi-algebraic set, corrupts the frequency response samples gathered from the coprime factors of the plant.

$$\begin{aligned} \tilde{X}(j\omega) &= X_n(j\omega) + \eta_{\alpha 1} + j\eta_{\beta 1} \quad \forall \omega \in \Omega_c \\ \tilde{Y}(j\omega) &= Y_n(j\omega) + \eta_{\alpha 2} + j\eta_{\beta 2} \quad \forall \omega \in \Omega_c \end{aligned} \tag{9.22}$$

where,

1. $\eta_{\alpha 1}$ and $\eta_{\beta 1}$ are the uncertainties in the real and imaginary parts of the coprime factor $X_n(j\omega)$.

2. $\eta_{\alpha 2}$ and $\eta_{\beta 2}$ are the uncertainties in the real and imaginary parts of the coprime factor $Y_n(j\omega)$.

We assume that

$$[\eta_{\alpha 1}, \eta_{\beta 1}] \in \mathcal{D}_{\eta 1}, \tag{9.23}$$

$$[\eta_{\alpha 2}, \eta_{\beta 2}] \in \mathcal{D}_{\eta 2} \tag{9.24}$$

and $\mathcal{D}_{\eta 1}$ and $\mathcal{D}_{\eta 2}$ are given semi-algebraic set which are defined below.

$$\mathcal{D}_{\eta 1} = \Big\{\phi_1 \in \mathbb{R}^2 : \phi_1 = [\eta_{\alpha 1}, \eta_{\beta 1}]^T;\ \eta_{\alpha 1} \in [\underline{\eta}_{\alpha 1} \quad \overline{\eta}_{\alpha 1}],\ \eta_{\beta 1} \in [\underline{\eta}_{\beta 1} \quad \overline{\eta}_{\beta 1}],\ \mathcal{L}_{1i}(\eta_{\alpha 1}, \eta_{\beta 1}) \geq 0\ i = 1,2,..r_1\Big\} \tag{9.25}$$

$$\mathcal{D}_{\eta 2} = \Big\{\phi_2 \in \mathbb{R}^2 : \phi_2 = [\eta_{\alpha 2}, \eta_{\beta 2}]^T;\ \eta_{\alpha 2} \in [\underline{\eta}_{\alpha 2} \quad \overline{\eta}_{\alpha 2}],\ \eta_{\beta 2} \in [\underline{\eta}_{\beta 2} \quad \overline{\eta}_{\beta 2}],\ \mathcal{L}_{2i}(\eta_{\alpha 2}, \eta_{\beta 2}) \geq 0,\ i = 1,2,..r_2\Big\} \tag{9.26}$$

where,

1. each $\mathcal{L}_{1i}(\eta_{\alpha 1}, \eta_{\beta 1})$ is a polynomial function of $\eta_{\alpha 1}$ and $\eta_{\beta 1}$.
2. each $\mathcal{L}_{2i}(\eta_{\alpha 2}, \eta_{\beta 2})$ is a polynomial function of $\eta_{\alpha 2}$ and $\eta_{\beta 2}$.

For a unified representation of the uncertainty, we assume that $\Phi = [\phi_1, \phi_2]^T$ and $U = \mathcal{D}_{\eta 1} \bigcup \mathcal{D}_{\eta 2}$.

Remark 6. *This study considers a semi-algebraic set representation of additive uncertainty. In cases when Real-Imaginary frequency domain data is collected directly from the plant, the corresponding uncertainty is more likely to be interval. However, when Gain-Phase data with interval uncertainty is collected from the plant and then translated to Real-Imaginary data, uncertainty will be semi-algebraic.*

Chapter 10

Stability and performance in direct data-driven framework

In this chapter we first provide some basic results on positive real systems. These results will then be used in driving the stability conditions in direct data-driven control framework. A comprehensive discussion on positive real systems is provided in [79], [69] and [109]. In this chapter we also provide controller parameter sets for nominal stability and nominal performance in direct data-driven framework. In the end, we provide controller parameter sets for robust stability and robust performance; both for unstructured multiplicative uncertainty and UB uncertainty.

10.1 Positive real functions

Consider a rational transfer function $\mathcal{G}(s)$.

Definition 16 (**Positive real functions**). *A rational transfer function $\mathcal{G}(s)$ is positive real (PR) if and only if $\Re[\mathcal{G}(s)] \geq 0$ for all $\Re[s] \geq 0$, where $\Re[.]$ stands for real of $[.]$.*

Result 25 (**Conditions for PR**). *A rational transfer function $\mathcal{G}(s)$ is PR if and only if*

1. *$\mathcal{G}(s)$ is marginally stable, that is, it has no poles in the right half plane.*
2. *any pure imaginary pole of $\mathcal{G}(s)$ is a non-repetitive pole and the associated residual is non-negative. The residual for a finite pole $s = j\omega$ is calculated as follows:*
$$\lim_{s \to j\omega} (s - j\omega)\mathcal{G}(s).$$
3. *$\Re[\mathcal{G}(j\omega)] > 0 \ \ \forall$ real ω.*

Definition 17 (**Strictly positive real functions**). *A transfer function $\mathcal{G}(s)$ is strictly positive real (SPR) if it is PR and there exist $\epsilon_R > 0$ such that*

$$\Re[\mathcal{G}(s - \epsilon_R)] > 0. \tag{10.1}$$

Result 26 (**Conditions for SPR**). *A rational transfer function $\mathcal{G}(s)$ is SPR if and only if*

1. *$\mathcal{G}(s)$ is hurwitz.*
2. *$\Re[\mathcal{G}(j\omega)] > 0 \ \ \forall$ real ω.*
3. *$\mathcal{G}(j\omega - \epsilon_R) + \mathcal{G}^T(-j\omega - \epsilon_R) > 0 \quad \forall$ real ω.*

A rational transfer function $\mathcal{G}(s)$ with relative degree zero is SPR if and only if

1. *$\mathcal{G}(s)$ is hurwitz.*
2. *$\Re[\mathcal{G}(j\omega)] > 0 \ \ \forall$ real ω.*

Definition 18 (**Weakly Strictly positive real functions**). *A rational transfer function $\mathcal{G}(s)$ is weakly strictly positive real (WSPR) if and only if*

1. *$\mathcal{G}(s)$ is hurwitz.*
2. *$\Re[\mathcal{G}(j\omega)] > 0 \ \ \forall$ real ω.*

Result 27 (**Conditions for WSPR**). *A rational transfer function $\mathcal{G}(s)$ is WSPR if and only if*

1. *it is stable, i.e., it has no poles in $Re[s] \geq 0$.*
2. *The relative degree of $\mathcal{G}(s)$ is one, zero or minus one.*
3. *$\Re[\mathcal{G}(j\omega)] > 0 \ \ \forall$ real ω.*

Result 28 (**Inverse of WSPR**). *A rational transfer function $\mathcal{G}(s)$ is WSPR if and only if $\mathcal{G}^{-1}(s)$ is WSPR.*

10.2 Nominal Stability (NS)

In this section, we derive a set of constraints that guarantee nominal internal stability of the feedback control system in direct data-driven framework.

Definition 19 (**NS**). *The closed-loop is nominal stable if the controller internally stabilizes the nominal plant in figure 9.3.*

Constraints for NS will be derived based on the following 4 Theorems.

Theorem 1. *If the coprime factors of a rational transfer functions $G_n(s)$ are $X_n(s)$ and $Y_n(s)$ then $Y_n(s)$ is always a bi-proper transfer function.*

Proof. We assume that the coprime factor $X_n(s)$ has numerator $N_{Xn}(s)$ and denominator $D_{Xn}(s)$. We further assume that the coprime factor $Y_n(s)$ has numerator $N_{Yn}(s)$ and denominator $D_{Yn}(s)$. Then the plant $G_n(s)$ can be represented as follows:

$$G_n(s) = \frac{N_{Xn}(s)D_{Yn}(s)}{N_{Yn}(s)D_{Xn}(s)} \tag{10.2}$$

Result 24 states that either $X_n(s)$ or $Y_n(s)$ is a biproper transfer function. We first assume that $Y_n(s)$ is a biproper transfer function which means

$$deg[N_{Yn}(s)] = deg[D_{Yn}(s)], \tag{10.3}$$

where $deg[\cdot]$ stands for degree of $[\cdot]$.

As $G_n(s)$ is a proper transfer function, therefore,

$$deg[D_{Xn}(s)] \geq deg[N_{Xn}(s)]. \tag{10.4}$$

Hence, $X_n(s)$ is a proper transfer function. So, we can say that if $Y_n(s)$ is a biproper transfer function then $X_n(s)$ is always a proper transfer function.

Now, we assume that $X_n(s)$ is a biproper transfer function, therefore,

$$deg[N_{Xn}(s)] = deg[D_{Xn}(s)]. \tag{10.5}$$

It is evident from equation (10.2) that $G_n(s)$ is a proper transfer function if and only if

$$deg[N_{Yn}(s)] \geq deg[D_{Yn}(s)]. \tag{10.6}$$

From the definition of the coprime factors, we know that $Y_n(s)$ is a proper transfer function. Therefore,

$$deg[N_{Yn}(s)] \not> deg[D_{Yn}(s)]. \tag{10.7}$$

Thus

$$deg[N_{Yn}(s)] = deg[D_{Yn}(s)]. \tag{10.8}$$

Hence, $Y_n(s)$ is a biproper transfer function. □

Theorem 2. *If the coprime factors of a rational transfer functions $G_n(s)$ are $X_n(s)$ and $Y_n(s)$, and the numerator and denominator of the controller $K(s)$ are $N(s)$ and $D(s)$. Then the relative degree of $N(s)X_n(s) + D(s)Y_n(s)$ is always $-d_m$ where d_m is the degree of the controller's denominator.*

Proof. Suppose, $N_{Xn}(s)$ and $D_{Xn}(s)$ be the numerator and denominator of the coprime factor $X_n(s)$. Similarly, $N_{Yn}(s)$ and $D_{Yn}(s)$ be the numerator and denominator of the coprime factor $Y_n(s)$. Then

$$N(s)X_n(s) + D(s)Y_n(s) = \frac{N_{Xn}(s)D_{Yn}(s)N(s) + N_{Yn}(s)D_{Xn}(s)D(s)}{D_{Xn}(s)D_{Yn}(s)}. \tag{10.9}$$

As, $K(s)$ is a proper transfer function and $Y_n(s)$ is a bi-proper transfer function. Therefore,

$$deg[N(s)] \leq deg[D(s)] \qquad \text{and} \qquad deg[N_{Yn}(s)] = deg[D_{Yn}(s)]. \tag{10.10}$$

Hence,

$$deg[N_{Yn}(s)D_{Xn}(s)D(s)] \geq deg[N_{Xn}(s)D_{Yn}(s)N(s)]. \tag{10.11}$$

Therefore,

$$\begin{aligned} deg[N_{Xn}(s)D_{Yn}(s)N(s) + N_{Yn}(s)D_{Xn}(s)D(s)] &= deg[N_{Yn}(s)D_{Xn}(s)D(s)] \\ &= deg[D_{Xn}D_{Yn}(s)(s)D(s)]. \end{aligned} \tag{10.12}$$

Hence, the relative degree of $N(s)X_n(s) + D(s)Y_n(s)$ is

$$\text{Relative } deg[N(s)X_n(s) + D(s)Y_n(s)] = -deg[D(s)] = -d_m. \tag{10.13}$$

□

Theorem 3 (**Necessary and sufficient conditions for stability**). *Given a plant and the frequency response of its coprime factors $X_n(s)$ and $Y_n(s)$, the controller $K(s,\rho)$ stabilizes the given plant if and only if*

(i) $\Re\Big[(N(j\omega,\rho)X_n(j\omega) + D(j\omega,\rho)Y_n(j\omega))F_s(j\omega,\zeta)\Big] > 0 \quad \forall\, \omega \in \Omega$

where,

$$F_s(s,\zeta) = [\prod_{k=1}^{q}(\zeta_k s + 1)]^{-1}$$

is a strictly stable and proper transfer function, $\zeta \in \mathbb{R}_+^q$ are the unknown poles of the $F_s(s,\zeta)$ and $q \in \mathbb{N}$ can take any value ($d_m - 1$,d_m,$d_m + 1$).

(ii) $N(s,\rho)$ and $D^{'}(s,\rho)$ are hurwitz, where

$$D^{'}(s,\rho) = \begin{cases} D(s,\rho), & \text{if } D(s,\rho) \text{has no integrator} \\ D(s,\rho)/s^{n_i}, & \text{otherwise} \end{cases}$$

where, n_i is specify n_i integrators.

Proof. The characteristic polynomial for the plant $G_n(s) = X_n(s)Y_n^{-1}(s)$ and the controller $K(s) = N(s,\rho)D^{-1}(s,\rho)$ is:

$$\mathcal{P}_c(s,\rho) = 1 + G_n(s)K(s,\rho) = \frac{N(s,\rho)X_n(s) + D(s,\rho)Y_n(s)}{D(s,\rho)Y_n(s)} \tag{10.14}$$

For closed loop stability, we check the roots of the numerator of the $\mathcal{P}_c(s,\rho)$. Suppose,

$$\mathcal{P}_N(s,\rho) = N(s,\rho)X_n(s) + D(s,\rho)Y_n(s). \tag{10.15}$$

Result 27 states that the transfer function $\mathcal{P}_N(s,\rho)$ is WSPR if its relative degree is (-1, 0 or 1). From Theorem 2 we know the relative degree of $\mathcal{P}_N$, which is $-d_m$. Thus, in order to achieve the relative degree of $\mathcal{P}_N$ equal to (-1, 0 or 1), we need an additional strictly stable and strictly proper rational transfer function. We name this function $F_s(s,\zeta)$ which can be selected as:

$$F_s(s,\zeta) = [\prod_{k=1}^{q}(\zeta_k s + 1)]^{-1}$$

where q can take any value (d_{m-1}, d_m, d_{m+1}).
Now, we define

$$\mathcal{P}_s(s,\rho,\zeta) = \Big\{N(s,\rho)X_n(s) + D(s,\rho)Y_n(s)\Big\}F_s(s,\zeta). \tag{10.16}$$

Since, $X_n(s)$ and $Y_n(s)$ are strictly stable functions therefore $\mathcal{P}_s(s,\rho,\zeta)$ is also a strictly stable function. By construction, the relative degree of $\mathcal{P}_s(s,\rho,\zeta)$ is (-1, 0 or 1).

By result 2 the closed-loop system is stable if and only if

(i) the numerator of $\mathcal{P}_s(s,\rho,\zeta)$ is hurwitz.

(ii) there is no unstable pole-zero cancellation between plant and controller and transfer functions.

If $N(s,\rho)$ and $D^{'}(s,\rho)$ are hurwitz polynomials then there is no unstable pole-zero cancellation between plant and controller.

Now, we provide conditions under which numerator of $\mathcal{P}_s(s,\rho,\zeta)$ is a hurwitz polynomial. As stated before, $\mathcal{P}_s(s,\rho,\zeta)$ is a strictly stable transfer function with relative degree equal to (-1, 0 or 1). By result 27 $\mathcal{P}_s(s,\rho,\zeta)$ is WSPR if and only if

$$\Re\Big[(N(j\omega,\rho)X_n(j\omega) + D(j\omega,\rho)Y_n(j\omega))F_s(j\omega,\zeta)\Big] > 0 \quad \forall\omega \in \Omega. \tag{10.17}$$

By Result 28, $\mathcal{P}_s^{-1}(s,\rho,\zeta)$ is also WSPR. Hence, the numerator of $\mathcal{P}_s(s,\rho,\zeta)$ is a hurwitz polynomial.
Thus, the closed-loop system is stable. □

Proof of Theorem 3 using the Nyquist plot

Proof. The phase $\phi_{\mathcal{G}}$ of a rational transfer function $\mathcal{G}$ when the Nyquist plot intersects the imaginary axis is given by:

$$\phi_{\mathcal{G}} = 90^\circ + 180N_i$$

where, N_i is an integer. Thus, for a given transfer function $\mathcal{G}$ if

$$r_{\mathcal{G}} > 1 \text{ or } r_{\mathcal{G}} < -1,$$

where $r_{\mathcal{G}}$ is the relative degree of the transfer function $\mathcal{G}$, then the Nyquist plot will always move to the left half-plane (LHP). For a strictly stable transfer function $\mathcal{G}$, even if the relative degree is -1,0,1, the Nyquist can still move to the LHP. This is due to the fact that the relative degree of $\{-1,0,1\}$ dictates the Nyquist plot to stay in the RHP only at $\omega \to \infty$. Infact, at lower frequencies, $\phi_{\mathcal{G}}$ can be less than -90° or greater than 90°. Thus the Nyquist plot of a strictly stable transfer function $\mathcal{G}$ stays in the RHP if and only if:

- $r_{\mathcal{G}} = \{-1,0,1\}$.
- $\Re\{\mathcal{G}\} > 0 \; \forall \; \omega$.

If $\mathcal{G}$ is strictly stable and satisfies both of the above conditions then, the denominator of $\mathcal{G}$ is hurwitz as any RHP zero will force the Nyquist plot into the LHP, hence, violating the second condition.

In Theorem 3, we need to prove that the denominator of $(N(s,\rho)X_n(s) + D(s,\rho)Y_n(s))$ is a hurwitz polynomial. We already know that

- $(N(s,\rho)X_n(s) + D(s,\rho)Y_n(s))$ is a strictly stable polynomial by construction.
- the relative degree of $(N(s,\rho)X_n(s) + D(s,\rho)Y_n(s))$ is $-d_m$ by Theorem 2.

By introducing a strictly stable transfer function $F_s(s,\zeta)$, we have restricted the relative degree of the $(N(s,\rho)X_n(s) + D(s,\rho)Y_n(s))F_s(s,\zeta)$ to $\{-1,0,1\}$. Thus, the closed-loop is stable if and only if

$$\Re\Big[(N(j\omega,\rho)X_n(j\omega) + D(j\omega,\rho)Y_n(j\omega))F_s(j\omega,\zeta)\Big] > 0 \quad \forall\omega \in \Omega \tag{10.18}$$

where $N(s,\rho)$ and $D^{'}(s,\rho)$ are the stable polynomials. □

Remark 7. *In equation (10.16), we have used a strictly stable transfer function $F_s(s,\zeta)$. This is equivalent of having a controller $K_F(s,\rho,\zeta)$ instead of the controller $K(s,\rho)$, where*

$$K_F(s,\rho,\zeta) = \frac{N(s,\rho)F_s(s,\zeta)}{D(s,\rho)F_s(s,\zeta)}$$

From the above equation, it is clear that $K_F(s,\rho,\zeta) = K(s,\rho)$. Thus, if $K_F(s,\rho,\zeta)$ stabilizes a stable plant then $K(s,\rho)$ also stabilizes that plant. It is important to note that replacing $K(s,\rho)$ with $K_F(s,\rho,\zeta)$ has no effect on sensitivities functions.

$$\begin{aligned} S_{F_s}(j\omega) =& \frac{D(j\omega)Y_n(j\omega)F_s(j\omega,\zeta)}{F_s(j\omega,\zeta)(N(j\omega)X_n(j\omega)+D(j\omega)Y_n(j\omega))} \\ &= \frac{D(j\omega)Y_n(j\omega)}{N(j\omega)X_n(j\omega)+D(j\omega)Y_n(j\omega)} \\ &= S(j\omega) \end{aligned} \tag{10.19}$$

$$\begin{aligned} T_{F_s}(j\omega) =& \frac{F_s(j\omega,\zeta)N(j\omega)X_n(j\omega)}{F_s(j\omega,\zeta)(N(j\omega)X_n(j\omega)+D(j\omega)Y_n(j\omega))} \\ &= \frac{N(j\omega)X_n(j\omega)}{N(j\omega)X_n(j\omega)+D(j\omega)Y_n(j\omega)} \\ &= T(j\omega) \end{aligned} \tag{10.20}$$

Now, we provide an alternative theorem for the closed-loop stability of the strictly stable systems. Later we will also show that this theorem is equivalent to Theorem 3 for strictly stable systems. Since, $F_s(j\omega,\zeta)$ introduced additional unknowns ζ, this new theorem provides stability conditions for strictly stable systems without additional unknowns that may reduce the computational complexity in some situations.

Theorem 4 (**Stability conditions for strictly stable plants**). *Suppose the frequency response of a strictly stable plant $G_n(s)$ is available then the controller $K(s,\rho)$ guarantees the nominal internal stability of the closed loop if and only if*

(i) $\Re\Big[\Big\{G_n(j\omega)N(j\omega,\rho)+D(j\omega,\rho)\Big\}(D^{-1}(j\omega,\rho)\Big] > 0 \quad \forall\omega\in\Omega$

(ii) $N(s,\rho)$ *and* $D^{'}(s,\rho)$ *are hurwitz, where*

$$D^{'}(s,\rho) = \begin{cases} D(s,\rho), & \text{if } D(s,\rho) \text{has no integrator} \\ D(s,\rho)/s^{n_i}, & \text{otherwise} \end{cases}$$

and n_i is specify n_i integrators.

Proof. Suppose $\mathcal{P}_{ss}(s,\rho)$ is the characteristic polynomial for a strictly stable plant $G_n(s)$.

$$\mathcal{P}_{ss}(s,\rho) = 1 + G_n(s)K(s,\rho) = \frac{G_n(s)N(s,\rho)+D(s,\rho)}{D(s,\rho)} \tag{10.21}$$

The closed loop system is stable if and only if

- $G_n(s)N(s,\rho) + D(s,\rho)$ is a hurwitz polynomial.
- there is no unstable pole-zero cancellation between the plant and the controller while forming the loop function.

Since, we are considering the class of controllers for which $N(s,\rho)$ and $D^{'}(s,\rho)$ are hurwitz polynomials. Thus, there is no unstable pole-zero cancellation between the plant and the controller. Result 2 states that the controller $K(s,\rho)$ internally stabilizes the plant $G_n(s)$ if the sensitivity function $S(s,\rho)$ is BIBO stable. Since, both the controller and the plant doesn't have any RHP zero, therefore, the BIBO stability is guaranteed by:

$$\|S(j\omega,\rho)\|_\infty < \infty. \tag{10.22}$$

By replacing the $K(s,\rho) = N(s,\rho)D^{-1}(s,\rho)$, equation (10.22) can equivalently be written as:

$$\left\| \frac{D(j\omega,\rho)}{G_n(j\omega)N(j\omega,\rho) + D(j\omega,\rho)} \right\|_\infty < \infty. \tag{10.23}$$

By using the definition of the H_∞-norm, (10.23) can be rewritten as:

$$\left| \frac{G_n(j\omega)N(j\omega,\rho) + D(j\omega,\rho)}{D(j\omega,\rho)} \right| > 0 \quad \forall\omega \in \Omega \tag{10.24}$$

Since,

$$\Re\Big[\frac{G_nN(\rho) + D(\rho)}{D(\rho)}\Big](j\omega) \leq \Big|\frac{G_nN(\rho) + D(\rho)}{D(\rho)}\Big|(j\omega), \tag{10.25}$$

therefore, closed-loop system is internally stable if and only if

$$\Re\Big[\Big\{G_n(j\omega)N(j\omega,\rho) + D(j\omega,\rho)\Big\}(D^{-1}(j\omega,\rho)\Big] > 0 \quad \forall\omega \in \Omega. \tag{10.26}$$

□

Remark 8. *By equations (10.17) and (10.26), Theorem 3 and 4 are equivalent if* $F_s(s,\zeta) = D^{-1}(s,\rho)$, $X_n(s) = G_n(s)$ *and* $Y_n(s) = 1$.

Remark 9. *In the rest of this section, we will use Theorem 3 only for the closed-loop stability of unstable and marginally stable plants, whereas Theorem 4 will be applied to ensure the closed-loop stability of the strictly stable plants.*

10.2.1 Stability of the controller

For CT systems, stability of the controller's numerator and denominator is achieved by using the Routh hurwitz criteria. For DT systems, stability of $N(z,\rho)$ and $D^{'}(z,\rho)$ is ensured by using the Jury stability test. Here, we provide stability of only for CT controller which can straight forwardly be extended to the DT controllers as well.

From the controller structure provided in equation(9.12), it is clear that $D^{'}(s,\rho)$ is a hurwitz polynomial if and only if, all the coefficients in the first column of the Routh table are positive. For polynomial $N(s,\rho)$, sign of coefficients in the first column of Routh's table is dictated by the dc values of (10.17) and (10.26).

$$N_0(\rho)X_{n0} + D_0(\rho)Y_{n0} > 0 \tag{10.27}$$

$$\frac{G_{n0}N_0(\rho) + D_0(\rho)}{D_0^{'}(\rho)} > 0 \tag{10.28}$$

where, (i) X_{n0} and Y_{n0} are the dc value of the coprime factors, (ii) $N_0(\rho)$ and $D_0(\rho)$ are the dc gain of $N(s,\rho)$ and $D(s,\rho)$, (iii) G_{n0} is the dc gain of the plant, and (iv) $D_0^{'}(\rho)$ is the dc gain of $D^{'}(s,\rho)$.

10.2.2 Controller parameter set for nominal stability

Definition 20 (**Stabilizing Controller Parameter Set**). *A stabilizing controller parameter set*

$$\mathcal{S} = \{\rho \in \mathbb{R}^{n_p} | K(s,\rho) \text{ internally stabilizes } G_n(s)\} \tag{10.29}$$

is the set of all the parameters of the controller that guarantee the internal stability of the nominal plant $G_n(s)$ in figure 9.3.

For stable plants, ρ is unknown whereas, ρ and ζ are unknown for unstable and marginally stable plants. Thus, for the unified representation of the nominal stability, we define

$$\xi = [\rho, \zeta]^T$$

and

$$\mathcal{F}_{NS}(j\omega,\xi) = \begin{cases} \mathcal{F}_{NS1}(j\omega,\xi), & \text{for unstable and marginally stable systems} \\ \mathcal{F}_{NS2}(j\omega,\xi), & \text{for stable systems} \end{cases} \tag{10.30}$$

where,

$$\mathcal{F}_{NS1}(j\omega,\xi) = \Re\Big[\Big(N(j\omega,\rho)X_n(j\omega) + D(j\omega,\rho)Y_n(j\omega)\Big)F_s(j\omega,\zeta)\Big] \tag{10.31}$$

$$\mathcal{F}_{NS2}(j\omega,\xi) = \Re\Big[\Big(G_n(j\omega)N(j\omega,\rho) + D(j\omega,\rho)\Big)(D^{-1}(j\omega,\rho)\Big]. \tag{10.32}$$

Suppose, $g(\rho)$ be the set of constraints that ensure the stability of $N(s,\rho)$ and $D(s,\rho)$, then the set $\mathcal{S}$ can be redefined as:

$$\begin{aligned}\mathcal{S}_\Omega = \{&\rho \in \mathbb{R}^{n_p}, \zeta \in \mathbb{R}_+^q : \mathcal{F}_{NS}(j\omega,\xi) > 0 \ \forall\omega \in \Omega,\\ &g(\rho) > 0.0\}\end{aligned} \tag{10.33}$$

In direct data-driven framework, frequency response of the plant or its coprime factors is obtained for a set finite frequencies Ω_d. Therefore, the set $\mathcal{S}_\Omega$ must be redefined for finite frequencies set.

$$\begin{aligned}\mathcal{S}_{\Omega_d} = \{&\rho \in \mathbb{R}^{n_p}, \zeta \in \mathbb{R}_+^q : \mathcal{F}_{NS}(j\omega,\xi) > 0 \ \forall\omega \in \Omega_d,\\ &g(\rho) > 0.0\}\end{aligned} \tag{10.34}$$

Since the set $\mathcal{S}_{\Omega_d}$ is the same for both unstable and marginally stable plants, therefore in the rest of the section, the term unstable plants will be used both for marginally stable and unstable plants. Similarly, strictly stable plants will be referred as stable plants.

10.3 Nominal Performance (NP)

Definition 21 (**NP**). *The closed loop system in figure 9.3 achieves the nominal performances if:*

$$\begin{aligned}\|S(s,\rho)W_1(s)\|_\infty &< \gamma\\ \|T(s,\rho)W_2(s)\|_\infty &< \gamma\end{aligned} \tag{10.35}$$

where, $\gamma \leq 1$.

Definition 22 (**NP Controller Parameter Set**). *A performance controller parameter set*

$$\begin{aligned}\mathcal{P} = \{&\rho \in \mathbb{R}^{n_p} | \|S(s,\rho)W_1(s)\|_\infty \leq \gamma,\\ &\|T(s,\rho)W_2(s)\|_\infty \leq \gamma,\\ &\}\end{aligned} \tag{10.36}$$

is the set of all the controller parameters that guarantees the nominal performance of the plant $G_n(s)$ *given in figure 9.3.*

Based on definitions of H_∞-norm in equation (1.7), sensitivity function in equation (9.14) and complementary sensitivity function in equation (9.15), $\mathcal{P}$ can be rewritten as follows.

$$\begin{aligned}\mathcal{P}_\Omega = \{&\rho \in \mathbb{R}^{n_p} \\ &\gamma_1 |N(j\omega,\rho)X_n(j\omega) + D(j\omega,\rho)Y_n(j\omega)|^2 - |W_1(j\omega)D(j\omega,\rho)Y_n(j\omega)|^2 \geq 0 \quad \forall \omega \in \Omega, \\ &\gamma_1 |N(j\omega,\rho)X_n(j\omega) + D(j\omega,\rho)Y_n(j\omega)|^2 - |W_2(j\omega)N(j\omega,\rho)X_n(j\omega)|^2 \geq 0 \quad \forall \omega \in \Omega \\ \}\end{aligned} \tag{10.37}$$

where, $\gamma_1 = \gamma^2$.

In direct data-driven framework $\mathcal{P}_\Omega$ is rewritten as:

$$\begin{aligned}\mathcal{P}_{\Omega_d} = \{&\rho \in \mathbb{R}^{n_p} \\ &\gamma_1 |N(j\omega,\rho)X_n(j\omega) + D(j\omega,\rho)Y_n(j\omega)|^2 - |W_1(j\omega)D(j\omega,\rho)Y_n(j\omega)|^2 \geq 0 \quad \forall \omega \in \Omega_d, \\ &\gamma_1 |N(j\omega,\rho)X_n(j\omega) + D(j\omega,\rho)Y_n(j\omega)|^2 - |W_2(j\omega)N(j\omega,\rho)X_n(j\omega)|^2 \geq 0 \quad \forall \omega \in \Omega_d \\ \}\end{aligned} \tag{10.38}$$

10.4 Robust stability and performance under unstructured multiplicative uncertainty

10.4.1 Robust Stability (RS)

Definition 23 (RS). *The closed-loop system is robustly stable if the controller internally stabilizes every plant belonging to* Π *in equation* (9.16).

By using result 3, the uncertain plant $G_p(s)$ is robustly stable if the nominal sensitivity function $S(s,\rho)$ is stable and

$$\|T(s,\rho)W_u(s)\|_\infty \leq \gamma. \tag{10.39}$$

where, $\gamma \leq 1$.

Based on definitions of H_∞-norm in equation (1.7) and complementary sensitivity function in equation (9.15), equation (10.39) can be rewritten as given by.

$$\gamma_1 |N(j\omega,\rho)X_n(j\omega) + D(j\omega,\rho)Y_n(j\omega)|^2 - |W_u(j\omega)N(j\omega,\rho)X_n(j\omega)|^2 \geq 0 \quad \forall \omega \in \Omega \tag{10.40}$$

In data-driven framework, RS can be redefined as:

$$\gamma_1 |N(j\omega,\rho)X_n(j\omega) + D(j\omega,\rho)Y_n(j\omega)|^2 - |W_u(j\omega)N(j\omega,\rho)X_n(j\omega)|^2 \geq 0 \quad \forall \omega \in \Omega_d \tag{10.41}$$

Definition 24 (**Robust stabilizing Controller Parameter Set**). *A robust stabilizing controller parameter set*

$$\mathcal{R}_s = \{\rho \in \mathbb{R}^{n_p} | K(s,\rho) \text{ internally stabilizes } G_p(s)\} \tag{10.42}$$

is the set of all the parameters of the controller that guarantee the robust stability of the uncertain plant $G_p(s)$ in figure 9.3.

The set $\mathcal{R}_s$ can alternatively be rewritten as:

$$\begin{aligned}\mathcal{R}_{\Omega_d} =& \{\rho \in \mathbb{R}^{n_p}, \zeta \in \mathbb{R}_+^q : \mathcal{F}_{NS}(j\omega,\xi) > 0 \ \forall \omega \in \Omega_d, \\ & \gamma_1 |N(j\omega,\rho)X_n(j\omega) + D(j\omega,\rho)Y_n(j\omega)|^2 - |W_u(j\omega)N(j\omega,\rho)X_n(j\omega)|^2 \geq 0 \quad \forall \omega \in \Omega_d, \\ & g(\rho) > 0.0\}\end{aligned} \tag{10.43}$$

10.4.2 Robust Performance

Definition 25 (**Robust Performance (RP)**). .
The closed loop system achieves the robust performance if the performance objectives are satisfied for every plant belonging to Π in equation (9.16).

The closed loop system in figure 9.3 achieves RP if NP and RS are achieved by a factor of 2 (e.g., [85]), that is,

$$\|S(s,\rho)W_1(s)\|_\infty < 0.5 \tag{10.44}$$

and

$$|T(s,\rho)W_u(j\omega)\|_\infty < 0.5. \tag{10.45}$$

Based on definitions of H_∞-norm in equation (1.7) and RP in equations ((10.44)-(10.45)), we define the following RP controller parameter set.

Definition 26 (**RP Controller Parameter Set**). *A RP controller parameter set*

$$\begin{aligned}\mathcal{P}_R = \{\rho \in \mathbb{R}^{n_p} | & \|S(s,\rho)W_1(s)\|_\infty \leq 0.5, \\ & \|T(s,\rho)W_u(j\omega)\|_\infty \leq 0.5, \\ & \}\end{aligned} \tag{10.46}$$

is the set of all the parameters of the controller that guarantee the robust performance of the uncertain plant $G_p(s)$ in figure 9.3.

The RP controller parameter set can alternative be defined as:

$$\begin{aligned}\mathcal{P}_{R\Omega} = \{&\rho \in \mathbb{R}^{n_p} \\ &0.25|N(j\omega,\rho)X_n(j\omega) + D(j\omega,\rho)Y_n(j\omega)|^2 - |W_1(j\omega)D(j\omega,\rho)Y_n(j\omega)|^2 \geq 0 \;\; \forall\omega \in \Omega, \\ &0.25|N(j\omega,\rho)X_n(j\omega) + D(j\omega,\rho)Y_n(j\omega)|^2 - |W_u(j\omega)N(j\omega,\rho)X_n(j\omega)|^2 \geq 0 \;\; \forall\omega \in \Omega \\ \}\end{aligned} \tag{10.47}$$

In direct data-driven framework, $\mathcal{P}_{R\Omega}$ can be alternatively rewritten as:

$$\begin{aligned}\mathcal{P}_{R\Omega_d} = \{&\rho \in \mathbb{R}^{n_p} \\ &0.25|N(j\omega,\rho)X_n(j\omega) + D(j\omega,\rho)Y_n(j\omega)|^2 - |W_1(j\omega)D(j\omega,\rho)Y_n(j\omega)|^2 \geq 0 \;\; \forall\omega \in \Omega_d, \\ &0.25|N(j\omega,\rho)X_n(j\omega) + D(j\omega,\rho)Y_n(j\omega)|^2 - |W_u(j\omega)N(j\omega,\rho)X_n(j\omega)|^2 \geq 0 \;\; \forall\omega \in \Omega_d \\ \}\end{aligned} \tag{10.48}$$

10.5 Robust stability and robust performance for UB uncertainty

Definition 27. *If frequency response samples are collected from the coprime factors of a plant are subjected to UB uncertainty described by equations (9.22)-(9.26) then the closed-loop system will be robustly stable if*

$$\mathcal{F}_{RS}(j\omega,\xi,\Phi) = \Re\Big[\Big(N(j\omega,\rho)\tilde{X}(j\omega,\phi_1)+D(j\omega,\rho)\tilde{Y}(j\omega,\phi_2)\Big)F_s(j\omega,\zeta)\Big] > 0 \quad \forall\Phi \in U \text{ and } \forall\omega \in \Omega_d \tag{10.49}$$

where, for stable systems, $F_s(j\omega,\zeta) = D^{-1}(j\omega,\rho)$, $\tilde{X}(j\omega,\phi_1) = \tilde{G}(j\omega,\phi_1)$ *and* $\tilde{Y}(j\omega,\phi_2) = 1$.

Definition 28. *A system subjected to UB uncertainty described by equations (9.22)-(9.26) achieves the closed loop robust performance if*

(i) $W_1(j\omega)\tilde{S}(j\omega,\Phi) \leq \gamma \;\; \forall\Phi \in U$, *and*

(ii) $W_2(j\omega)\tilde{T}(j\omega,\Phi) \leq \gamma \;\; \forall\Phi \in U$

where, $\gamma \leq 1$,

$$\tilde{S}(j\omega,\Phi) = \frac{D(j\omega,\rho)\tilde{Y}(j\omega,\phi_2)}{N(j\omega,\rho)\tilde{X}(j\omega,\phi_1) + D(j\omega,\rho)\tilde{Y}(j\omega,\phi_2)} \tag{10.50}$$

$$\tilde{T}(j\omega,\Phi) = \frac{N(j\omega,\rho)\tilde{X}(j\omega,\phi_1)}{N(j\omega,\rho)\tilde{X}(j\omega,,\phi_1) + D(j\omega,\rho)\tilde{Y}(j\omega,\phi_2)} \tag{10.51}$$

Based on the definitions of $\tilde{S}(j\omega, \Phi)$ and $\tilde{T}(j\omega, \Phi)$ provided in the equations (10.50) and (10.51), the RP conditions for UB uncertainty can equivalently be written as:

$$\begin{aligned}\mathcal{F}_{W1}(j\omega, \rho, \Phi) =& \gamma_1 |N(j\omega, \rho)\tilde{X}(j\omega, \phi_1) + D(j\omega, \rho)\tilde{Y}(j\omega, \phi_2)|^2 - |W_1(j\omega)D(j\omega, \rho)\tilde{Y}(j\omega, \phi_2)|^2 > 0 \\ & \forall \Phi \in U \text{ and } \forall \omega \in \Omega_d \\ \mathcal{F}_{W2}(j\omega, \rho, \Phi) =& \gamma_1 |N(j\omega, \rho)\tilde{X}(j\omega, \phi_1) + D(j\omega, \rho)\tilde{Y}(j\omega, \phi_2)|^2 - |W_2(j\omega)N(j\omega, \rho)\tilde{X}(j\omega, \phi_1)|^2 > 0 \\ & \forall \Phi \in U \text{ and } \forall \omega \in \Omega_d \end{aligned} \tag{10.52}$$

For stable plants, RP conditions are obtained by replacing $\tilde{X}(j\omega, \phi_1) = \tilde{G}(j\omega, \phi_1)$ and $\tilde{Y}(j\omega, \phi_2) = 1$ in equation (10.52).

Remark 10. *It is important to mention that in this chapter (and in the rest of this section), the conditions for stability, robust stability and robust performance are posed for a discrete set of frequencies as the data from the plant is obtained for a finite frequencies set Ω_d. This is based on the assumptions that a good experiment was performed for the acquisition of the data and the number of frequencies in Ω_d are sufficient for describing the true behaviour of the plant. These assumptions are reasonable in a sense that the similar type of assumptions are also made in any black-box identification technique used for identifying the model of the plant.*

It is worth mentioning that many interesting results in the field of scenario based optimization are available for gridding the infinite constraints using a randomization approach such that the violation probability approaches zero when the number of samples goes to infinity (see e. g., [48], [140], [141] and [154]). The use of randomized approach for choosing frequencies in Ω_d will be the subject of the future work.

Chapter 11

Design of FOFS H_∞ controller in direct data-driven framework

In this chapter we consider the design of FOFS H_∞ direct data-driven controllers for the following problems.

(1) Problem 1: NS and NP.

(2) Problem 2: RS and NP for unstructured multiplicative uncertainty.

(3) Problem 3: RS and RP for unstructured multiplicative uncertainty.

(4) Problem 4: RS and RP for UB uncertainty.

Based on the results from the previous chapter, all four problems of direct data-driven control design are first formulated as polynomial optimization problems which are then solved by suitable convex relaxation methods.

11.1 Design of FOFS H_∞ direct data-driven controller for NS and NP

Based on the definition of $\mathcal{S}_{\Omega_d}$ and $\mathcal{P}_{\Omega_d}$, the feasible controller parameter set (FCPS) for NP and NS is given by:

$$\mathcal{D}_N = \mathcal{S}_{\Omega_d} \cap \mathcal{P}_{\Omega_d} \tag{11.1}$$

That controller parameters that ensures the NS and NP are computed by solving the following the polynomial optimization problem.

$$\xi^* = \arg \min_{\xi \in \mathcal{D}_N} \ \gamma_1 \tag{11.2}$$

where, $\gamma_1 = \gamma^2$. As the constraints in FCPS given in equation(11.1) are nonconvex polynomials in ξ, solving the problem in the equation (11.2) is NP-hard. To obtain a globally optimal solution, we provide the following algorithm for solving the optimization problem in equation (11.2).

Algorithm 2 SDP relaxation of FCPS

(i) Apply moment relaxation given in [83] to relax the nonconvex FCPS into a SDP by choosing a suitable relaxation order.

(ii) Solve the SDP by YALMIP ([78]) and MOSEK ([115]).

(iii) Extract the global optimal solution (or solutions, if there are many solutions) by extraction algorithm given in [28].

11.2 Design of robust FOFS H_∞ controller for unstructured multiplicative uncertainty

11.2.1 Design of robust FOFS H_∞ controller for RS and NP

Based on the definitions of $\mathcal{R}_{\Omega_d}$ and $\mathcal{P}_{\Omega_d}$, the FCPS for achieving the RS and NP in direct data-driven framework can be written as:

$$\begin{aligned}\mathcal{D}_R = \{&\rho \in \mathbb{R}^{n_p}, \zeta \in \mathbb{R}^q_+ :, \mathcal{F}_S(j\omega, \xi) > 0 \ \forall \omega \in \Omega_d, \\ &\gamma_1 |N(j\omega,\rho)X(j\omega) + D(j\omega,\rho)Y(j\omega)|^2 - |W_1(j\omega)D(j\omega,\rho)Y(j\omega)|^2 \geq 0 \ \forall \omega \in \Omega_d, \\ &\gamma_1 |N(j\omega,\rho)X(j\omega) + D(j\omega,\rho)Y(j\omega)|^2 - |W_u(j\omega)N(j\omega,\rho)X(j\omega)|^2 \geq 0 \ \forall \omega \in \Omega_d \\ &g(\rho) > 0.0\}.\end{aligned} \tag{11.3}$$

where, $\gamma_1 = \gamma^2$.

The controller parameters for RS and NP are computed by solving to the following problem.

$$\xi^* = \arg \min_{\xi \in \mathcal{D}_R} \ \gamma_1 \tag{11.4}$$

The FCPS $\mathcal{D}_R$ contains the nonconvex polynomials in ξ therefore the optimization problem in equation (11.4) is NP-hard and difficult to solve. Thus, we use algorithm 2 for solving the optimization problem in equation (11.4).

11.2.2 Design of robust FOFS H_∞ controller for RS and NP

According to definitions of the sets $\mathcal{S}_{\Omega_d}$ and $\mathcal{P}_{R\Omega_d}$, the FCPS for RS and RP is defined as:

$$\mathcal{D}_P = \mathcal{S}_{\Omega_d} \cap \mathcal{P}_{R\Omega_d}. \tag{11.5}$$

The controller parameters for RS and RP are obtained according to the following problem.

$$\xi^* = \arg\min_{\xi \in \mathcal{D}_P} \ \gamma_1 \tag{11.6}$$

where, $\gamma_1 = \gamma^2$.

Since the polynomial optimization problem in equation (11.6) is nonconvex in ξ therefore, we use algorithm 2 for solving the optimization problem in equation (11.6).

Remark 11. *It is important to mention that the controller computed for each of the problem* 1*, problem* 2 *and problem* 3 *will be different for the proposed method and the methods presented in ([6] and [13]), even if the desired controller has no unknown parameter in the denominator. This is due to the difference in the adopted methodologies. For example in ([6] and [13]), the constraint*

$$\gamma_1 |N(j\omega,\rho)X(j\omega) + D(j\omega,\rho)Y(j\omega)| \geq |W_1(j\omega)D(j\omega,\rho)Y(j\omega)| \tag{11.7}$$

is approximated by:

$$\Re\Big[\{N(j\omega,\rho)X(j\omega) + D(j\omega,\rho)Y(j\omega)\}F\Big] \geq \gamma_1^{-1} |W_1(j\omega)D(j\omega,\rho)Y(j\omega)| \tag{11.8}$$

where F, $N(j\omega,\rho)$ and $D(j\omega,\rho)$ are stable transfer functions. In [6], the controller is linearly parameterized and $F = 1$ such that the problem in (11.8) is converted into an SDP for a given frequency grid. Similarly, in [13] a nonconvex problem is solved locally for the optimal choice of the (i) controller parameters, (ii) basis function parameters for the linearly parameterized controller and, (iii) basis function parameters for the linearly parameterized F. In our approach, $N(j\omega,\rho)$ and $D(j\omega,\rho)$ are polynomials and the convexity of the FCPS is obtained by exploiting moment based convex relaxation.

It is also worth mentioning that our method has a higher computational complexity than the methods proposed in ([6] and [13]). This is due to the inherent higher computational cost associated with moment based convex relaxation.

11.3 Design of robust FOFS H_∞ controller for UB uncertainty

Based on the definitions 27 and 28, the FCPS for RS and RP for UB uncertainty can be defined as:

$$\begin{aligned}\mathcal{D}_{Rp} = \{&\rho \in \mathbb{R}^{n_p}, \zeta \in \mathbb{R}^{q}_{+},\ \Phi \in U : \\ &\mathcal{F}_{RS}(j\omega, \xi, \Phi) > 0\ \ \forall \Phi \in U \text{ and } \forall \omega \in \Omega_d, \\ &\mathcal{F}_{W1}(j\omega, \rho, \Phi) > 0\ \ \forall \Phi \in U \text{ and } \forall \omega \in \Omega_d, \\ &\mathcal{F}_{W2}(j\omega, \rho, \Phi) > 0\ \ \forall \Phi \in U \text{ and } \forall \omega \in \Omega_d, \\ &g(\rho) > 0.0\}\end{aligned} \tag{11.9}$$

It is worth mentioning that the uncertainty set U is a compact set by construction. The compactness of the stability set can be achieved by restricting the controller variables to a Euclidean ball by adding a redundant constraint similar to equation (2.13). The optimization problem for computing the controller parameters is given by:

$$\begin{aligned}&\min\ \ \gamma_1 \\ &s.t.\ \mathcal{D}_{Rp}(j\omega, \xi, \Phi) \quad \forall \Phi \in U,\ \ \forall \omega \in \Omega_d.\end{aligned} \tag{11.10}$$

where, $\gamma_1 = \gamma^2$.

The FCPS $\mathcal{D}_{Rp}$ contains nonconvex polynomials in ξ. Furthermore, the set U is an infinite set, therefore at each frequency, the FCPS $\mathcal{D}_{Rp}$ has infinite constraints in Φ. Thus, the polynomial optimization problem in equation (11.10) is a semi-infinite polynomial optimization problem (SIPP). In this work, we solve SIPP in equation (11.10) by using the algorithm 3, which is based on the results presented in [101].

Since the stability set and the uncertainty set are compact, sub-problems $(\mathcal{Q}_k)$ and $(\mathcal{O}_i^k)$ are solved globally by SDP relaxations and global optimal solutions are extracted in each iteration, therefore Algorithm 3 has a finite convergence according to result 23.

Algorithm 3 SDP relaxation of SIPP

1: Choose a random $\Phi_0 \in U$ and select $U_0 = \{\Phi_0\}$. Set $k = 0$.

2: For k^{th} iteration, apply moment relaxation given in [83] to solve

$$(\mathcal{Q}_k) : \begin{cases} \gamma_{1k}^{min} := \min \quad \gamma_1 \\ s.t.\ \mathcal{D}_{Rp}(\omega, \xi, \Phi) \quad \forall \Phi \in U_k, \ \ \forall \omega \in \Omega_d \end{cases}$$

The global optimal solutions are extracted by extraction algorithm given in [28]. Let $\mathcal{S}_k = \{\xi_1^k, ..., \xi_\ell^k\}$ be the set of the global minimizers of problem $(\mathcal{Q}_k)$.

3: Set $U_{k+1} = U_k$. For $i = 1, ..., \ell$, do the following

a) For frequency set $\Omega_d = \{\omega_1, \omega_2, \ldots, \omega_n\}$ calculate $\mathcal{F} = [\mathcal{D}_{Rp}(\omega_1, \xi_i^k, \Phi), \mathcal{D}_{Rp}(\omega_2, \xi_i^k, \Phi), \ldots, \mathcal{D}_{Rp}(\omega_n, \xi_i^k, \Phi)]^T$.

b) Use moment relaxation given in [83] to solve

$$(\mathcal{O}_i^k) : \ \mathcal{F}_i^k := \Big[\min_{\Phi \in U} \mathcal{F}(\xi_i^k, \Phi)(1), \min_{\Phi \in U} \mathcal{F}(\xi_i^k, \Phi)(2), \ldots, \min_{\Phi \in U} \mathcal{F}(\omega_n, \xi_i^k, \Phi)(3\omega_n) \Big]^T$$

c) If all the elements of $\mathcal{F}_i^k$ are positive then stop. Otherwise select only those elements of $\mathcal{F}_i^k$ which are negative and choose corresponding global minimizers.

d) Let $T_i^k = \{\Phi_{i,j}^k, j = 1, ..., ti^k\}$ be the set of global minimizers of $(\mathcal{O}_i^k)$ for which elements of $\mathcal{F}_i^k$ are negative. Update $U_{k+1} = U_{k+1} \bigcup T_i^k$.

4: If $k > k_{max}$, stop. Otherwise $k = k + 1$ and go to step 2.

Chapter 12

Simulation Examples

All the simulations in this chapter are performed on a PC running on 64 bit Windows 10 platform, equipped with Intel core $i7-7500$ CPU and 8 GB RAM.

12.1 NS and NP for a stable DT system

Consider the following nominal DT system, which is strictly stable and minimum phase.

$$G_n(z) = \frac{z + 0.43}{z^2 - 0.57z + 0.37} \tag{12.1}$$

The sampling time for $G_n(z)$ is 1 second. The nominal performance specifications are given by the frequency domain weighting filters $W_1(z)$ and $W_2(z)$,

$$W_1(z) = \frac{0.631z^2 - 1.021z + 0.4133}{z^2 - 1.819z + 0.8187} \tag{12.2}$$

$$W_2(z) = \frac{z^2 - 1.096z + 0.2231}{0.125z + 0.07612} \tag{12.3}$$

where, $W_1(z)$ is the weighting filter for sensitivity function and $W_2(z)$ is the weighting filter for the complementary sensitivity function. It is worth mentioning that $W_1(z)$ and $W_2(z)$ are designed from the time domain specifications according to the methodology presented in [95].

The goal is to design a PI-controller

$$K(z, \rho) = \frac{N(z, \rho)}{D(z, \rho)} = \frac{c_1(z - 1) + c_2}{z - 1} \tag{12.4}$$

such that the closed loop system satisfy the performance specifications $W_1(z)$ and $W_2(z)$.

First of all, we will drive the stability constraints for $N(z, \rho)$ and $D(z, \rho)$. It is clear from the equation (12.4) that $D^{'}(z, \rho) = 1$, thus there is no constraint for the

stability of $D^{'}(z,\rho)$. The condition in equation (10.27) is satisfied if $c_2 > 0$. From Jury stability test, $N(z,\rho)$ is a stable polynomial if $\{c_1 > 0,\ c_2 > 0,\ 2c_1 - c_2 > 0\}$. Thus, the constraints for the stability $N(z,\rho)$ and $D^{'}(z,\rho)$ are

$$g(\rho) = \{c_1 > 0,\ c_2 > 0,\ 2c_1 - c_2 > 0\}. \tag{12.5}$$

In this example we collect frequency response data from $G_n(z)$ at 100 logarithmically spaced frequencies between 0.001 rad/sec and 3.0903 rad/sec.

To find the parameters of the FOFS controller $K(z,\rho)$, the nominal feasible controller set $\mathcal{D}_N$ (for DT system) is constructed according to equation (11.1). By applying moment relaxation of order 4, the FCPS $\mathcal{D}_N$ is relaxed to SDP. The optimization problem in equation (11.2) is solved by using YALMIP ([78]) and MOSEK ([115]). The optimization problem converged with $\gamma = 0.9775$ n approximately 8 seconds. The global optimal solutions are extracted by extraction algorithm given in [28]. The value of γ obtained from *Hinfstruct* function of MATLAB is 0.9777.

The controller obtained is given by:

$$K(z) = \frac{0.048z + 0.04545}{z - 1} \tag{12.6}$$

It is worth mentioning that in this example the value of γ is almost same for the proposed method and the *Hinfstruct*. However, since the proposed approach uses frequency response data at the finite set of frequencies and the optimization problem is solved by using convex relaxation methods, the optimal solution for the proposed approach and the *Hinfstruct* may differ slightly in other cases.

The closed loop step response for the nominal plant is plotted in figure 12.1.

It is clear from the step response that the closed-loop system has achieved the nominal stability.

For NP, we plot $W_1(z)$ against the sensitivity function $S(z)$ in figure 12.2 and $W_2(z)$ against the complementary sensitivity function $T(z)$ in figure 12.3.

It is evident from figures (12.2-12.3) that:

1. magnitude of the $S(z)$ is smaller than the magnitude of $W_1^{-1}(z)$ at all frequencies.

2. magnitude of $T(z)$ is smaller than the magnitude of $W_2^{-1}(z)$ at all frequencies.

Thus the closed loop system achieves the nominal performances specified by the weighting filter $W_1(z)$ and $W_2(z)$.

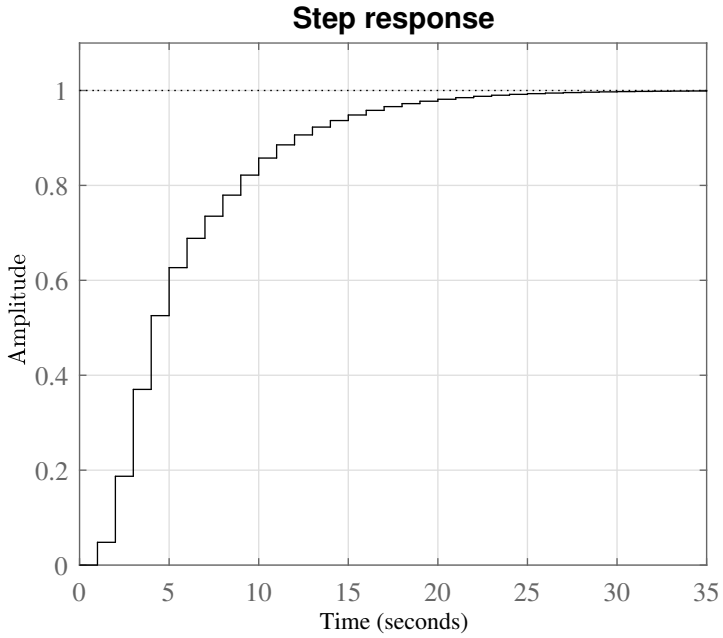

Figure 12.1: Closed-loop step response

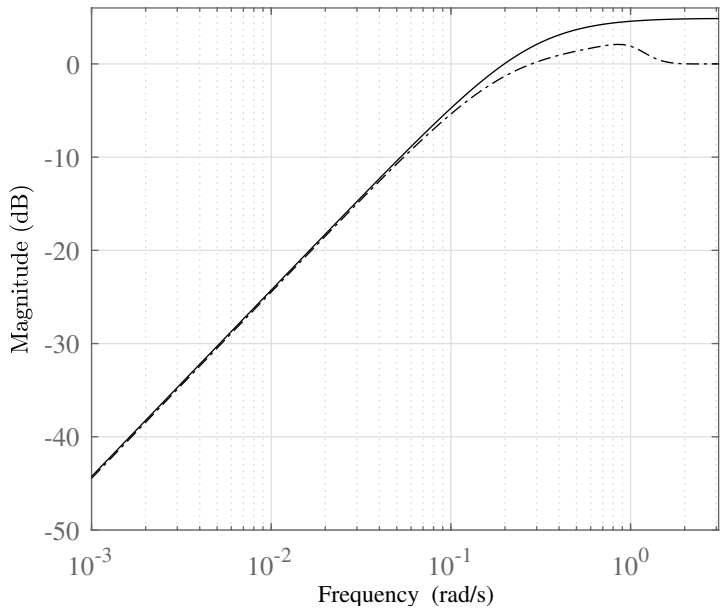

Figure 12.2: Comparison between $|{W_1}^{-1}(e^{j\omega})|$ (solid) and $|S(e^{j\omega}))|$ (dashed)

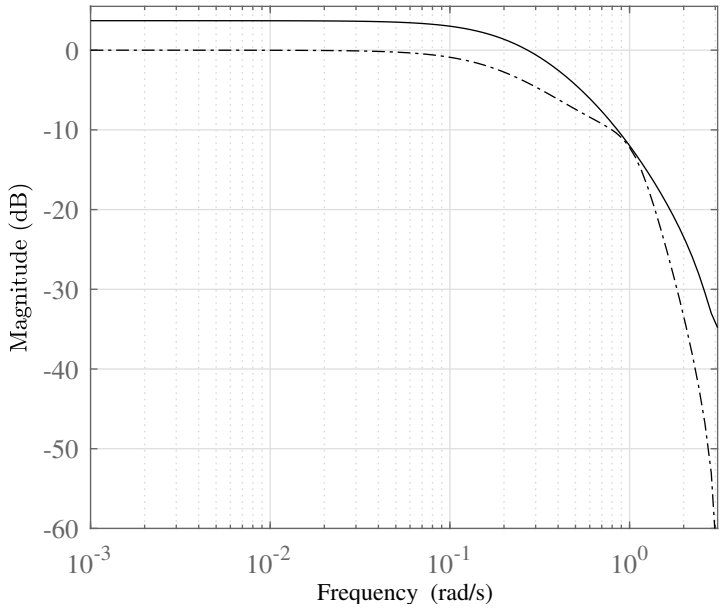

Figure 12.3: Comparison between $|W_2{}^{-1}(e^{j\omega})|$ (solid) and $|T(e^{j\omega})|$ (dashed)

12.2 RS and NP for an unstable system CT system

We consider the following uncertain plant analysed in [8].

$$G_p(s) = \frac{(s+1)(s+10)}{(s+2)(s+4)(s-1)}(1 + W_u(s)\Delta(s)) \tag{12.7}$$

where, weighting function for uncertainty is

$$W_u(s) = 0.8\frac{1.1337s^2 + 6.8857s + 9}{s+10} \tag{12.8}$$

and weighting function for the complementary sensitivity function is

$$W_1(s) = \frac{2}{(20s+1)^2}. \tag{12.9}$$

It is important to note that the $W_1(s)$ and $W_2(s)$ are same as considered in [8]. Since, the plant $G_p(s)$ is an unstable plant, therefore, an initial stabilizing controller is required to obtain the coprime factors of the plant. In this example, we consider the following stabilizing controller $K_s(s)$

$$K_s(s) = \frac{2.074s^2 + 9.702s + 6.425}{0.01s^2 + s}, \tag{12.10}$$

which is also the initial stabilizing controller used for constructing the desired open loop transfer function in [8]. The coprime factors of the plant are given by:

$$\begin{aligned} X_n(s) &= \frac{G_n(s)K_s(s)}{1+G_n(s)K_s(s)} \\ &= \frac{(s+10)(s+1)}{(s+300)(s^2+1.698s+0.8185)} \end{aligned} \tag{12.11}$$

$$\begin{aligned} Y_n(s) &= \frac{K_s(s)}{1+G_n(s)K_s(s)} \\ &= \frac{(s+4)(s+2)(s-1)}{(s+300)(s^2+1.698s+0.8185)} \end{aligned} \tag{12.12}$$

where,

$$G_n(s) = \frac{(s+1)(s+10)}{(s+2)(s+4)(s-1)} \tag{12.13}$$

is the nominal plant.

The objective is to design a PID controller (same as in [8])

$$K(s,\rho) = \frac{N(s,\rho)}{D(s,\rho)} = \frac{c_1 s^2 + c_2 s + c_3}{c_4 s^2 + s}, \tag{12.14}$$

such that uncertain plant $G_p(s)$ is internally stable while achieving the NP defined through $W_1(s)$.

First of all, we will drive constraints for the stability of the controller based on the Routh stability criteria. The numerator of the controller without integrator is given by:

$$D^{'}(s,\rho) = c_4 s + 1. \tag{12.15}$$

By applying Routh's criteria to $D^{'}(s,\rho)$, we get $c4 > 0$. For polynomial $N(s,\rho)$, sign of the coefficients in the first column of the Routh's table is governed by the equation (10.27), that is,

$$N_0(\rho)X_{n0} = c_3 > 0. \tag{12.16}$$

Now, by applying Routh's criteria to $N(s,\rho)$, we get $\{c_1 > 0, c_2 > 0, c_3 > 0\}$. Suppose, $g(\rho)$ be the set of constraints that ensures the stability of $N(s,\rho)$ and $D^{'}(s,\rho)$.

$$g(\rho) = \{c_1 > 0, c_2 > 0, c_3 > 0, c_4 > 0\}. \tag{12.17}$$

We assume that the data from the coprime factors of the plant is collected at the following set of frequencies.

$$\Omega_d = \{0.01 : 0.01 : 0.09,\ 0.1 : 0.1 : 0.9,\ 1 : 1 : 20,\ 20 : 5 : 200\}. \tag{12.18}$$

According to Theorem 3, $F_s(s,\zeta)$ is chosen as a first order pole:

$$F_s(s,\zeta) = \frac{1}{s+\zeta}. \tag{12.19}$$

Based on $X_n(s)$, $Y_n(s)$, $K(s,\rho)$, $g(\rho)$ and $F_s(s,\zeta)$, FCPS $\mathcal{D}_R$ is constructed according to equation (11.3). By applying moment relaxation of order 5, the FCPS $\mathcal{D}_R$ is relaxed to SDP. The optimization problem in equation (11.4) is solved by using YALMIP ([78]) and MOSEK ([115]). The global optimal solutions are extracted by extraction algorithm given in [28]. Optimization problem converged with $\gamma = 0.73$ and $\zeta = 1.8178$ in approximately 25 minutes. The value of γ obtained by *Hinfstruct* toolbox of MATLAB is 0.72, whereas the value of the γ computed by the algorithm in [8] is 0.7247. It is important to mention that the *Hinfstruct* is a model based approach and the direct comparison between the proposed technique and *Hinfstruct* is not possible. Similar, direct data-driven approach proposed in [8] is also different from the proposed technique. Thus for aforementioned techniques, the optimal value of γ may differ slightly.

The controller obtained is

$$K(s) = \frac{0.4589s^2 + 2.0082s + 3.6093}{s(0.0042s+1)}. \tag{12.20}$$

The closed loop step response for the nominal plant is plotted in figure 12.4. It is

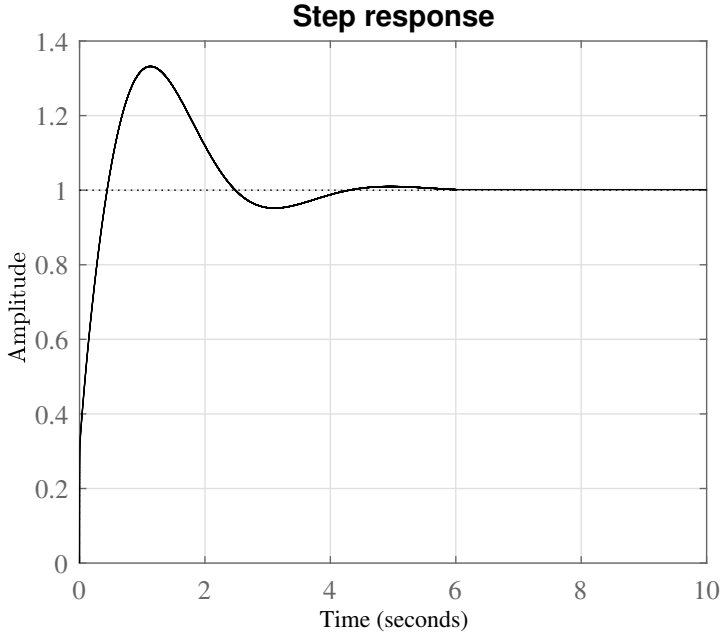

Figure 12.4: Closed-loop step response of the nominal plant

clear from the step response that the closed-loop nominal system is stable.

For RS, we plot the W_u against the complementary sensitivity function T in figure 12.5. It is clearly visible from the figure 12.5 that the magnitude of the

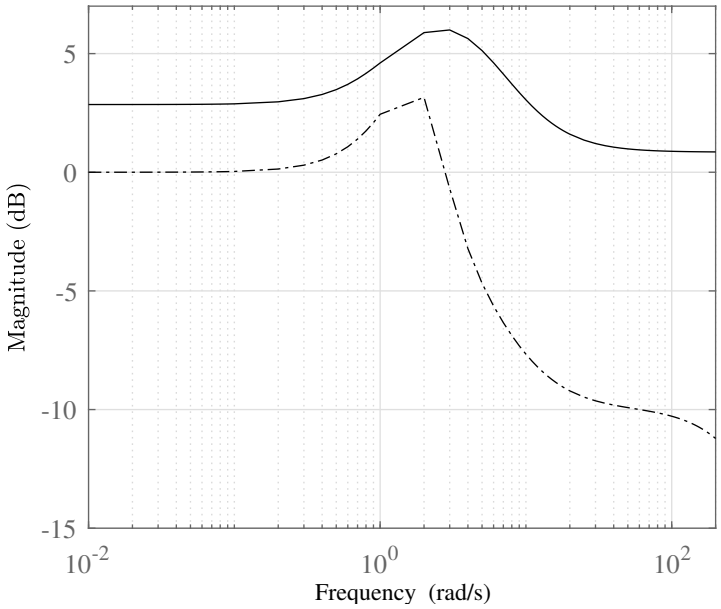

Figure 12.5: Comparison between $|{W_u}^{-1}(j\omega)|$ (solid) and $|T(j\omega)|$ (dashed)

complementary sensitivity function T is smaller than the magnitude of $W_u^{-1}(s)$ at all frequencies, thus the uncertain system $G_p(s)$ is robustly stable against the unstructured uncertainty defined by weighting function $W_u(s)$.

For NP, we plot $W_1(s)$ against the sensitivity function $S(s)$ in figure 12.6. Since, from figure 12.6, magnitude of the sensitivity function is smaller than the magnitude of $W_1^{-1}(s)$ at all frequencies, thus the closed loop system achieves the nominal performances specified by the weighting filter $W_1(s)$.

12.3 RS and RP for a stable system subjected to UB uncertainty

Consider the following strictly stable CT plant

$$G_n(s) = \frac{466.67(s+15)}{(s+7)(s+20)(s+50)}. \tag{12.21}$$

The frequency response of the plant is acquired at 120 frequencies logarithmically spaced between $10^{-1.5}$ rad/sec and $10^{2.5}$ rad/sec. The frequency response of the plant $G_n(s)$ is subjected to additive uncertainty, that is,

$$\tilde{G}(j\omega) = G_n(j\omega) + \eta_{\alpha 1} + j\eta_{\beta 1} \quad \forall \omega \in \Omega_d \tag{12.22}$$

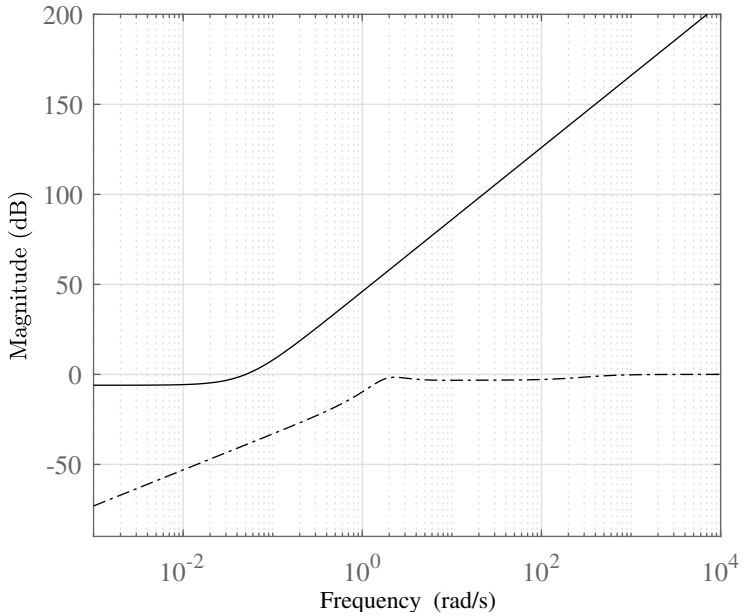

Figure 12.6: Comparison between $|W_1{}^{-1}(j\omega)|$ (solid) and $|S(j\omega)|$ (dashed)

where, $\eta_{\alpha 1}$ and $\eta_{\beta 1}$ belongs to the set Φ.

$$\begin{aligned}\Phi = \Big\{\phi_1 \in \mathbb{R}^2 : \phi_1 = [\eta_{\alpha 1}, \eta_{\beta 1}]^T;\ \eta_{\alpha 1} \in [-0.2 \quad 0.2],\\ \eta_{\beta 1} \in [-0.25 \quad 0.25],\Big\}.\end{aligned} \tag{12.23}$$

The objective is to design a PI controller

$$K(s) = \frac{N(s,\rho)}{D(s,\rho)} = \frac{c_1 s + c_2}{s} \tag{12.24}$$

such that the plant $\tilde{G}(s)$ is robustly stable while achieving the robust performance according to definition 28.

The weighting filter for $\tilde{S}(j\omega, \Phi)$ is:

$$W_1(s) = \frac{11.14s^2 + 1.782s + 0.0713}{12.5s^2 + s}.$$

Similarly, the weighting transfer function for $\tilde{T}(j\omega, \Phi)$ is

$$W_2(s) = \frac{90s^2 + 1890s + 3240}{248s + 3720}.$$

It is worth mentioning that $W_1(s)$ and $W_2(s)$ are designed according to the time domain specification.

The stability of the controller is ensured through Routh's stability criteria. Assuming that $g(\rho)$ be the set of constraints that ensures the stability of $N(s,\rho)$ and $D^{'}(s,\rho)$ then

$$g(\rho) = \{c_1 > 0, c_2 > 0\}. \tag{12.25}$$

Based on the available information, the FCPS $\mathcal{D}_{Rp}$ is constructed according to equation (11.9). Since, $\mathcal{D}_{Rp}$ is nonconvex polynomial in unknown controller parameters and semi infinite polynomial in uncertainty. The optimization problem in equation (11.10) is relaxed and solved according to Algorithm 3 by using YALMIP ([78]) and MOSEK ([115]). The optimization problem converged in 2 iterations where problem $(\mathcal{Q}_k)$ is solved with a relaxation order of 4, and each problem in $(\mathcal{O}_i^k)$ is solved with a relaxation order of 3. The optimization problem converged with $\gamma = 0.9718$ in approximately 15 minutes and the obtained controller is:

$$K(s) = \frac{0.0260s + 0.1268}{s}. \tag{12.26}$$

The closed loop step response for the nominal plant is plotted in figure 12.7. It

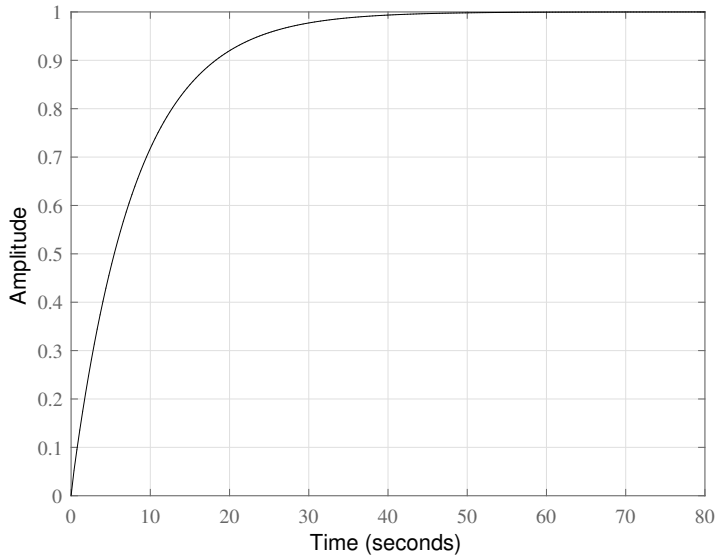

Figure 12.7: Closed-loop step response of the nominal plant

is clear from the figure figure 12.7 that the closed-loop nominal system is stable. We grid both $\eta_{\alpha 1}$ and $\eta_{\beta 1}$ into 51 equally spaced values and call this grid as Φ_g. The values of $\mathcal{F}_{RS}(j\omega, \xi, \Phi)$ in equation (10.49) are computed over the grid Φ_g for every frequency in Ω_d. The result is plotted in the figure 12.8. It is clear from the figure 12.8 that $\mathcal{F}_{RS}(j\omega, \xi, \Phi_g) > 0$ for all frequencies in Ω_d. Hence, the closed-loop system is robustly stable.

For RP: we plot $W_1(s)$ against $\tilde{S}(j\omega, \Phi_g)$ in figure 12.9; and $W_2(s)$ against $\tilde{T}(j\omega, \Phi_g)$ in figure 12.10.

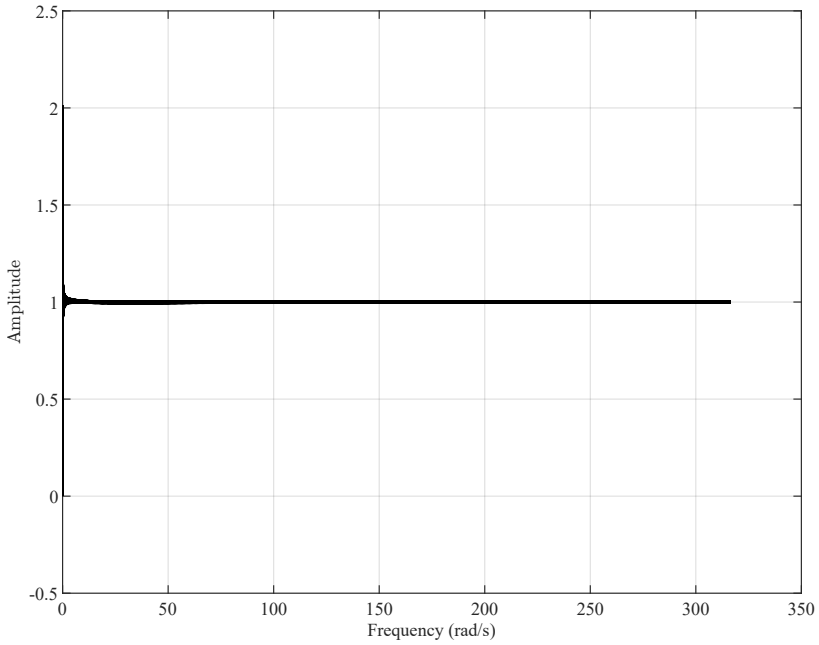

Figure 12.8: $\mathcal{F}_{RS}(j\omega, \xi, \Phi_g)$

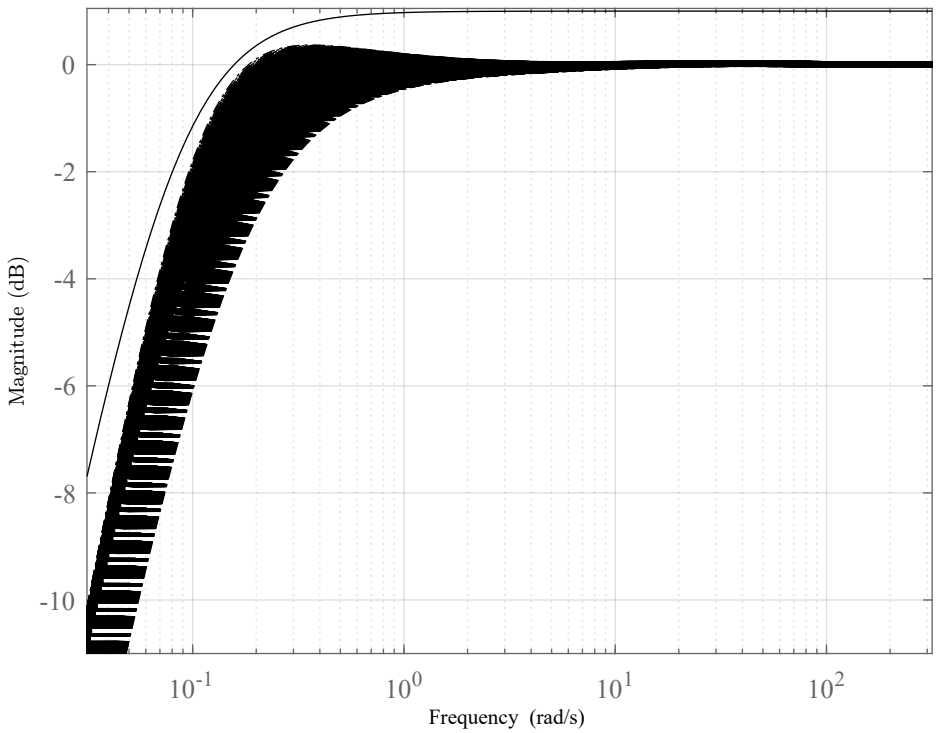

Figure 12.9: Comparison between $|{W_1}^{-1}(j\omega)|$ (solid) and $|\tilde{S}(j\omega, \Phi_g)|$ (dashed)

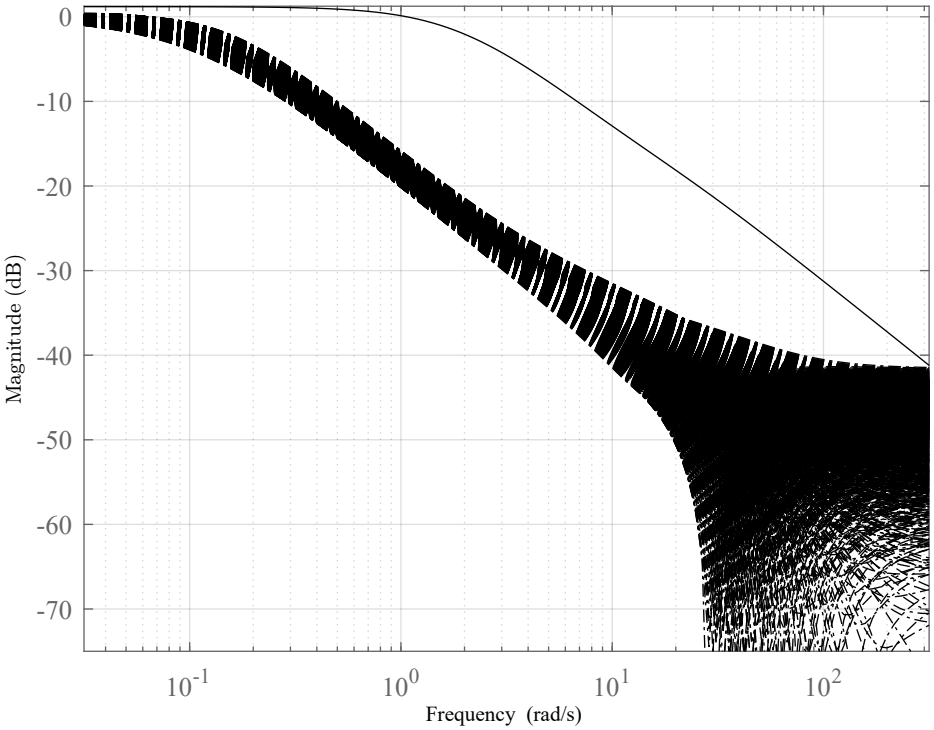

Figure 12.10: Comparison between $|{W_2}^{-1}(j\omega)|$ (solid) and $|\tilde{T}(j\omega, \Phi_g)|$ (dashed)

It is clear from the figures (12.9-12.10) that the closed system has achieved the desired robust performance.

Chapter 13

Conclusions

In this section, we have proposed a unified approach for designing robust FOFS H_∞ mixed-sensitivity direct data-driven controllers, both for CT and DT systems. The proposed method does not need any mathematical model of the plant and only requires the frequency response samples collected from the plant (for stable systems) or its co-prime factors (for the unstable system) at discrete frequencies. The problem of designing the H_∞ mixed sensitivity direct data-driven controller is reformulated as a polynomial optimization problem. The polynomial optimization problem is then relaxed to an SDP using moment relaxation.

The necessary and sufficient conditions for achieving nominal stability in the direct data-driven framework without linear parameterization of the controller are also developed in this section. It is worth mentioning that stability conditions for direct-data driven control, provided in [8] and [6], are limited to linear parameterized controllers and can only be applied in H_∞ mixed sensitivity framework. On the other hand, stability conditions developed in this section are generic and applicable to both linearly and nonlinearly parameterized controllers.

Two classes of uncertainties for designing robust FOFS H_∞ mixed-sensitivity direct data-driven controllers are considered in this section. The first uncertainty class is the unstructured uncertainty bounded by a frequency domain weighting filter. A method to compute the frequency domain weighting filter for the unstructured uncertainty is also provided in this section. However, computation of this filter requires collecting a large number of frequency response samples from the plant or its co-prime factors at each frequency. For the unstructured description of uncertainty, a single shot moment relaxation-based algorithm is provided for computing the parameters of the FOFS controller. In the second case, it is assumed that the frequency response samples collected from the plant or its co-prime factors are subjected to UB uncertainty that belongs to a given semi algebraic set. For UB uncertainty, an iterative algorithm based on the exchange method is provided to design robust FOFS H_∞ mixed-sensitivity direct data-driven controllers. It is worth mentioning that the sub-problems in the exchange algorithms are solved

globally by using moment relaxation. The main advantage of this method is that it requires only one sample of data at each frequency for computing robust FOFS direct data-driven controllers.

The main advantages of the proposed algorithms compared to existing methods are:

(i) It does not require linear parameterization of the controller or its co-prime factors.

(ii) Compared to [13] and [5], which provide only the local solutions, the proposed algorithm guarantees the globally optimal solution.

(iii) Compared to [98], [63], [64] and [8], it does not require fixing the denominator of the controller for the globally optimal solution.

(iv) In contrast to [6] which converges to a globally optimal solution only for higher-order controllers, the proposed algorithms converge to the globally optimal solution, both for low-order and high-order fixed structure controllers.

Finally, we provide three simulation examples to show the efficiency of the proposed algorithms on both CT and DT systems.

Part III

Computation of Bode envelope bounds for LTI systems effected by semialgebraic parametric uncertainty

Chapter 14

Introduction

Uncertainty in the plant's model exists for all physical systems. The parametric uncertainty in the model can come from several sources. For example, the parameters are known approximately, they may vary due to nonlinearities, they may change due to changes in the operating conditions or aging. As an example of parametric uncertainty, consider the following mass-spring-damper model.

$$G(s) = \frac{1}{ms^2 + bs + k} \tag{14.1}$$

where k is the spring constant, b is the damping and m is the mass. Suppose m is uncertain and we only know that the value of m varies from 2 to 3, then the system in (14.1) is said to be a parametric uncertain system.

Frequency domain is one of the the key tool in the linear control theory. One of the best tool in the frequency domain is the H_∞ control. Parametric uncertainty can be represented in the H_∞ framework by considering real perturbations. However, real perturbations are difficult to handle both mathematically and numerically. Typically, in the H_∞ framework, the real perturbations are replaced with complex perturbations which results in overbounding of the uncertainty set.

Many powerful graphical tools such as the Bode plot, Nyquist plot, and Nichols chart are also available in the frequency domain for the control system design and analysis. In the case of the fixed nominal plants, stability and stability margins can be computed from these graphical tools. However, it becomes much more difficult to compute the stability and stability margins for parametric uncertain plants, as the frequency response of the entire family must be available for this purpose. Loop shaping is one of the powerful methods for the control system design and it can be performed on the Bode, Nyquist, and Nichole plots. For loop shaping of the parametric uncertain plants, it is compulsory to compute the frequency response of every member of the entire family.

A significant effort through the years has been devoted towards the problem of computing Bode, Nichole and Nyquist envelopes for systems affected by parametric

uncertainty. Some of the important methodologies for computing the frequency response envelopes of different families subjected to parametric uncertainty, are given below.

14.1 Existing Methods for computing the frequency response envelopes

Many results on computing the frequency response of the parametric uncertain systems, using Kharitonov's theorem [99], Edge theorem [2] and Generalized Kharitonov's theorem [57], are available in the literature. The differences between these results are: (i) the geometric structure of the uncertainty in the parameter space and (ii) how the uncertainty enters the numerator and the denominator of the transfer function of a parametric uncertain plant. Some of the most important studies are:

14.1.1 Interval plants

An interval plant is an LTI SISO plant in which uncertainty enters the numerator and denominator of a given transfer function linearly and the uncertainty set in the coefficient space is a box. Different methods for computing the frequency response of uncertain interval plants are provided in [1],[24], [145], [11] and [118]. These methods use the results based on Kharitonov's theorem and Generalized Kharitonov's theorem to compute the Nyquist, Nichole and Bode envelopes.

14.1.2 Polytopic plants

A polytopic plant is an LTI SISO plant in which the uncertainty enters the numerator and the denominator of the transfer function linearly and the coefficient space have a polytopic structure. Based on the frequency response of the edge transfer functions, different methods for computing the frequency response of the polytopic systems are presented in [106], [17], [19], [18], [117] and [84].

14.1.3 Multilinear plants

In these LTI SISO systems, uncertainty enters multi-linearly in the numerator and the denominator of a given plant. Multilinear interval plants are the most studied plants in this family. The transfer function of a multilinear interval plant is the ratio of multilinear interval polynomials. By using the Generalized Kharitonov's theorem and the Mapping theorem, methods for computing the frequency response of the multilinear interval plants are provided in [145]. A $2q-$convex par-polygon

technique is used in [156] to compute the Bode and Nyquist envelopes of multilinear interval transfer functions that are multiples of polynomials with affine linear uncertainty.

14.1.4 Ellipsoidal plants

In ellipsoidal plants, the uncertainty enters linearly in the numerator and denominator of a given transfer function and the coefficient space is ellipsoidal. A method for the computing the Bode magnitude envelope, based on the solution to an SDP, has been presented in [167]. A complete characterization of the frequency response of ellipsoidal plants has been provided in [49].

14.1.5 Plants with nonlinear uncertainty

In these plants, the uncertainty enters nonlinearly in the numerator and denominator of a given transfer function. Different methods for computing the frequency response bounds of transfer functions whose coefficients have a nonlinear dependency on a set of uncertain parameters belonging to a given box are provided in [126], [127] and [128].

14.2 Research Objective

The objective of this research is to compute the Bode envelopes for parametric uncertain plants subjected to semialgebraic uncertainty. The main focus of the existing techniques is on the box coefficient space of uncertain parameters. However, in the last decade, new results about set-membership identification (SMI) of LTI systems from input-output data corrupted by bounded measurement errors have been presented (see, e.g.,[159], [161] and [158]). In SMI framework, the solution to the identification problem is in the form of a semialgebraic family of rational functions, that is, the coefficients of the rational functions belong to a set in the parameter space defined by polynomial constraints. Motivated from these results, computation of Bode envelopes bounds for such class of uncertain system is addressed in the proposed approach.

14.2.1 Contribution

The major highlights of this work are:

- A unified formulation is proposed for both CT and DT systems affected by semialgebraic uncertainty.

- In the proposed approach, the uncertainty can enter the rational transfer function polynomially, that is, each coefficient of the numerator and the denominator can be a polynomial function of the uncertain parameters. Furthermore, the uncertain parameters belongs to a semialgebraic set. Since, boxes, polytopes and ellipsoids are particular cases of semialgebraic sets. Therefore the proposed approach can be considered as a generalization of the techniques previously proposed for the computation of Bode plot envelopes.
- The problem of computing the Bode envelopes is formulated in terms of the solution to 4 polynomial optimization problems for each value of the frequency. Global optimal solutions to the formulated optimization problems are obtained by applying recently proposed convex relaxation techniques.

The results presented in this section are partially published in [162].

Chapter 15

Computation of Bode envelopes of LTI systems

15.1 Frequency domain representation of uncertain polynomials

Consider the following CT uncertain polynomial

$$P(s,\theta) = \theta_0 + \theta_1 s + \theta_2 s^2 + \theta_3 s^3 + \cdots + \theta_n s^n \tag{15.1}$$

where, n is the order of polynomials, $\theta = [\theta_0, \theta_1 ... \theta_n]$ is a vector of uncertain coefficients of $P(s,\theta)$.

The polynomial in equation (15.1) can be represented in the frequency domain by substituting $s = j\omega$, that is

$$P(j\omega,\theta) = \theta_0 - \omega^2\theta_2 + ... + j\{\omega\theta_1 - \omega^3\theta_3 + \dots\} \tag{15.2}$$

For a given fixed frequency ω_k, P in (15.2) can be written as the sum of real and imaginary functions.

$$P(j\omega_k,\theta) = \alpha_1(\theta) + j\beta_1(\theta) \tag{15.3}$$

where,

$$\alpha_1(\theta) = \theta_0 - \omega_k^2\theta_2 + \dots$$
$$\beta_1(\theta) = \omega_k\theta_1 - \omega_k^3\theta_3 + \dots$$

Based on the result in equation (15.3), the magnitude and the phase of the polynomial P at fixed frequency ω_k are given by:

$$|P(j\omega_k,\theta)| = |\alpha_1(\theta) + j\beta 1(\theta)| = \sqrt{\alpha_1^2(\theta) + \beta_1^2(\theta)} \tag{15.4}$$

$$\arg\left[P(j\omega_k,\theta)\right] = tan^{-1}(\frac{\beta_1(\theta)}{\alpha_1(\theta)}) \tag{15.5}$$

It is evident from the equations ((15.4)-(15.5)) that at fixed frequency ω_k:

(i) $|P(j\omega_k,\theta)|^2$ is a polynomial in uncertain parameters.

(ii) $tan(\arg[P])$ is a rational function of uncertain parameters.

Therefore, at a fixed frequency ω_k, it is possible to formulate optimization problems for the computation Bode gain and phase envelopes of the polynomial P. Now, consider the following discrete time uncertain polynomial

$$P_d(z,\theta) = \theta_0 + \theta_1 z + \theta_2 z^2 + \theta_3 z^3 + \cdots + \theta_n z^n \tag{15.6}$$

The polynomial P_d can be represented in the frequency domain by substituting the value of $z = e^{j\omega} = cos(\omega) + jsin(\omega)$ in equation (15.6), that is

$$\begin{aligned} P_d(e^{j\omega},\theta) =& \theta_0 + \theta_1 cos(\omega) + \dots \\ &+ j\{\theta_1 sin(\omega) + 2\theta_2 cos(\omega)sin(\omega) + \dots\} \end{aligned} \tag{15.7}$$

At a given frequency ω_k, polynomial P_d is given by:

$$P_d(e^{j\omega_k},\theta) = \alpha_2(\theta) + j\beta_2(\theta) \tag{15.8}$$

where,

$$\begin{aligned} \alpha_2(\theta) &= \theta_0 + \theta_1 cos(\omega_k) + ... \\ \beta_2(\theta) &= \theta_1 sin(\omega_k) + 2(\theta_2) cos(\omega_k) sin(\omega_k) + \dots \end{aligned}$$

It is evident from the equation (15.8) that at a given frequency ω_k, the gain and the phase of the polynomial P_d can be represented as polynomials of $\alpha_2(\theta)$ and $\beta_2(\theta)$. Thus, polynomial optimization problems can be formulated to compute the Bode phase and gain envelopes of P_d at ω_k.

Remark 12. *It is obvious from equations ((15.3) and (15.8)) that polynomials $P(s,\theta)$ and $P_d(z,\theta)$ have similar representation at a fixed frequency ω_k. Same is true for the CT and DT transfer functions. Therefore, polynomial optimization for the computation of Bode gain and Bode phase envelopes will be formulated only for CT system. These results are equally valid for the DT systems.*

15.2 Problem Formulation

Consider a CT LTI SISO plant described by the transfer function

$$G(s,\theta) = \frac{N(s,\theta)}{D(s,\theta)} \tag{15.9}$$

where,

$$N(s,\theta) = p_0(\theta) + p_1(\theta)s + p_2(\theta)s^2 + p_3(\theta)s^3 + \cdots + p_m(\theta)s^m, \tag{15.10}$$

$$D(s,\theta) = p_{m+1}(\theta) + p_{m+2}(\theta)s + p_{m+3}(\theta)s^2 + \cdots + p_{m+n}(\theta)s^n, \tag{15.11}$$

$n \geq m$, $\theta = \{\theta_0, \theta_1, \ldots, \theta_{m+n}\}$ is the vector of uncertain parameters, $p_0(\theta), p_1(\theta), \ldots, p_{m+n}(\theta)$ are polynomial functions of θ.

It is assumed that the coefficient vector θ belongs to a semialgebraic set $\mathcal{S}_\theta$ which is defined by ℓ polynomial equalities and / or inequalities in θ, that is,

$$\mathcal{S}_\theta = \{\theta \in R^{n+m+1};\ \ f_k(\theta) \geq 0,\ \ k = 1,2,\ldots,\ell\} \tag{15.12}$$

where, each $f_k(\theta)$ is a multivariate polynomial in θ.

The Bode gain and phase envelopes are computed at a given set of frequencies, defined as:

$$\Omega_d = \{\omega_1, \omega_2, \ldots, \omega_N\}. \tag{15.13}$$

At each $\omega_k \in \Omega_d$, the problem of computing the Bode gain and phase envelopes of an uncertain polynomial $G(s,\theta)$ boils down to solving the following 4 optimization problems.

$$\underline{G}(\omega_k) = \min_{\theta \in \mathcal{S}_\theta} |G_k(j\omega_k, \theta)| \tag{15.14}$$

$$\overline{G}(\omega_k) = \max_{\theta \in \mathcal{S}_\theta} |G_k(j\omega_k, \theta)| \tag{15.15}$$

$$\underline{\phi}(\omega_k) = \min_{\theta \in \mathcal{S}_\theta} \arg\left[G_k(j\omega_k, \theta)\right] \tag{15.16}$$

$$\overline{\phi}(\omega_k) = \max_{\theta \in \mathcal{S}_\theta} \arg\left[G_k(j\omega_k, \theta)\right]. \tag{15.17}$$

In the next section, we will propose new numerical algorithms for solving the optimization problems in (15.14), (15.15), (15.16) and (15.17).

15.3 Computation of Bode envelopes by polynomial optimization methods

Based on the result in equation (15.3), at a given frequency ω_k, uncertain system in equation (15.9) can be rewritten as:

$$G_k(j\omega_k, \theta) = \frac{\alpha_N(\theta) + j\beta_N(\theta)}{\alpha_D(\theta) + j\beta_D(\theta)} \tag{15.18}$$

where, $\alpha_N(\theta)$, $\alpha_D(\theta)$, $\beta_N(\theta)$ and $\beta_D(\theta)$ are polynomial functions of θ. For simplicity, $\alpha_N(\theta)$, $\alpha_D(\theta)$, $\beta_N(\theta)$ and $\beta_D(\theta)$ are denoted as α_N, α_D, β_N and β_D in rest of this chapter.

At given fixed frequency ω_k, the magnitude and the phase of the system in (15.9), are given by:

$$|G_k(j\omega_w, \theta)| = \frac{|\alpha_N + j\beta_N|}{|\alpha_D + j\beta_D|} = \frac{\sqrt{\alpha_N^2 + \beta_N^2}}{\sqrt{\alpha_D^2 + \beta_D^2}} \tag{15.19}$$

$$\arg\left[G_k(j\omega_i, \theta)\right] = \arctan(\frac{\beta_N}{\alpha_N}) - \arctan(\frac{\beta_D}{\alpha_D}) \tag{15.20}$$

To formulate polynomial optimization problems for the computation of the Bode envelopes, we introduce

$$\gamma_{mk} = |G_k(j\omega_k, \theta)|^2 = \frac{\alpha_N^2 + \beta_N^2}{\alpha_D^2 + \beta_D^2} \tag{15.21}$$

and

$$\gamma_{tk} = \tan(\arg\left[G_k(j\omega_k, \theta)\right]) \tag{15.22}$$

By using fundamental results of the trigonometry, equation (15.22) can be rewritten as:

$$\tan(\gamma_{tk}) = \frac{\alpha_D\beta_N - \beta_D\alpha_N}{\alpha_N\alpha_D + \beta_N\beta_D} \tag{15.23}$$

15.3.1 Computation of Bode gain envelope

At a given frequency, ω_k, $\underline{G}(\omega_k)$ and $\overline{G}(\omega_k)$ can be computed as following:

$$\underline{G}(\omega_k) = \sqrt{\underline{\gamma_{mk}}} \tag{15.24}$$

$$\overline{G}(\omega_k) = \sqrt{\overline{\gamma}_{mk}} \tag{15.25}$$

where,

$$\begin{aligned} \underline{\gamma}_{mk} = & \min \quad \gamma_{mk} \\ & s.\,t. \\ & \begin{cases} \gamma_{mk}(\alpha_D^2 + \beta_D^2) - \alpha_N^2 - \beta_N^2 = 0, \\ \theta \in \mathcal{S}_\theta \end{cases} \end{aligned} \tag{15.26}$$

$$\begin{aligned} \overline{\gamma}_{mk} = & \max \quad \gamma_{mk} \\ & s.\,t. \\ & \begin{cases} \gamma_{mk}(\alpha_D^2 + \beta_D^2) - \alpha_N^2 - \beta_N^2 = 0, \\ \theta \in \mathcal{S}_\theta \end{cases} \end{aligned} \tag{15.27}$$

15.3.2 Computation of Bode phase envelope

At a given frequency ω_k, $\underline{\phi}(\omega_k)$ and $\overline{\phi}(\omega_k)$ can be computed as following:

$$\underline{\phi}(\omega_k) = \arctan(\underline{\gamma}_{tk}) \tag{15.28}$$

$$\overline{\phi}(\omega_k) = \arctan(\overline{\gamma}_{tk}) \tag{15.29}$$

where,

$$\begin{aligned} \underline{\gamma}_{tk} = & \min \quad \gamma_{tk} \\ & s.\,t. \\ & \begin{cases} \gamma_{tk}(\alpha_N\alpha_D + \beta_N\beta_D) - \alpha_D\beta_N + \beta_D\alpha_N = 0, \\ \theta \in \mathcal{S}_\theta \end{cases} \end{aligned} \tag{15.30}$$

$$\begin{aligned} \overline{\gamma}_{tk} = & \max \quad \gamma_{tk} \\ & s.\,t. \\ & \begin{cases} \gamma_{tk}(\alpha_N\alpha_D + \beta_N\beta_D) - \alpha_D\beta_N + \beta_D\alpha_N = 0, \\ \theta \in \mathcal{S}_\theta \end{cases} \end{aligned} \tag{15.31}$$

It is known from trigonometry that $tan(\cdot)$ is discontinuous at every odd multiple of $\frac{\pi}{2}$. Therefore, at a given frequency ω_k, optimization problem (15.30) (optimization problem (15.31)) may return a false minimum (maximum) if any system in the uncertain set have a phase angle equal to odd multiples of $\frac{\pi}{2}$. Luckily, $cot(\cdot)$ is continuous at the odd multiples of $\frac{\pi}{2}$. Therefore, if the magnitude of the optimal solution of optimization problem (15.30) (optimization problem (15.31))) is very large, we can switch to an optimization problem with an objective function based on the $cot(\cdot)$. For this purpose, suppose

$$\gamma_{ck} = \cot(\arg\left[G_k(j\omega_k, \theta)\right]) \tag{15.32}$$

By applying elementary trigonometry rules, equation can be rewritten as:

$$\cot(\gamma_{ck}) = \frac{\alpha_N \alpha_D + \beta_N \beta_D}{\alpha_D \beta_N - \beta_D \alpha_N} \tag{15.33}$$

Thus, the optimization problems for computing $\underline{\phi}(\omega_k)$ and $\overline{\phi}(\omega_k)$ are given by:

$$\underline{\phi}(\omega_k) = arccot(\overline{\gamma}_{ck}) \tag{15.34}$$

$$\overline{\phi}(\omega_k) = arccot(\underline{\gamma}_{ck}) \tag{15.35}$$

where,

$$\begin{aligned} \underline{\gamma}_{ck} = & \min \quad \gamma_{ck} \\ & s.\,t. \\ & \begin{cases} \gamma_{ck}(\alpha_D \beta_N - \beta_D \alpha_N) - \alpha_N \alpha_D - \beta_N \beta_D = 0, \\ \theta \in \mathcal{S}_\theta \end{cases} \end{aligned} \tag{15.36}$$

$$\begin{aligned} \overline{\gamma}_{ck} = & \max \quad \gamma_{ck} \\ & s.\,t. \\ & \begin{cases} \gamma_{ck}(\alpha_D \beta_N - \beta_D \alpha_N) - \alpha_N \alpha_D - \beta_N \beta_D = 0, \\ \theta \in \mathcal{S}_\theta \end{cases} \end{aligned} \tag{15.37}$$

Remark 13. *Optimization problems* (15.26), (15.27),(15.30), (15.31),(15.36) *and* (15.37) *are nonconvex polynomial optimization problem. Standard nonlinear optimization tools such as Newton method, can not be applied to solve these optimization*

problem as they can typically trap in local minima. However, by applying sparse SDP relaxation methods in proposed in [103] and [68], these optimization problems can be solved to the global optimal solution. It is worth mentioning that by increasing the relaxation order, the solution of the relax SDP problem converges to the global optimal solution of the original polynomial optimization problem. Theoretically, convergence is guaranteed for relaxation order approaching infinity. However, in practice, convergence is usually fast and the global optimal solution is accurately approximated with low relaxation order, see, e.g., [104] for details.

It is important to mention that each optimization problem ((15.26), (15.27),(15.30), (15.31),(15.36) and (15.37)) is computed for every frequency in the grid Ω_d, independent of other frequencies in the grid. However, Ω_d is an approximation of the infinite frequency set $[0, +\infty)$, and is introduced for applying the SDP relaxation methods. Adding more frequency points to the frequency grid Ω_d is a trade-off between the accuracy of the frequency response and the computational cost.

For practical purposes, here we present general guidelines for the selection of the frequency grid.

(i) Select an initial frequency grid based on the Bode plots of the given transfer function for one or more (a few) fixed $\theta \in \mathcal{S}_\theta$ over a dense frequency grid.

(ii) Compute the Bode phase and gain envelopes for the initial frequency grid.

(iii) Identify the critical frequency regions, such as resonance peaks, by plotting the computed Bode envelope bounds for the initial frequency grid.

(iv) Select a new frequency grid for additional frequencies in the critical frequency regions.

(v) Compute the Bode gain and phase envelopes only for the new grid and augment them to the Bode envelopes computed for the initial grid. If N_n is the number of frequencies in the new frequency grid, then this requires the solution of $4N_n$ additional optimization problems.

(vi) Repeat the step (iii), (iv) and (v), if necessary.

Chapter 16

Simulation Examples

All the simulations in this chapter are performed on a PC running on 64 bit Windows 10 platform, equipped with Intel core $i7-7500$ CPU and 8 GB RAM.

16.1 Example 1

Consider the following CT system:

$$G_p(s) = \frac{5(s+\theta_2)}{s^2+\theta_1 s+\theta_2} \tag{16.1}$$

The interval bounds for the uncertain parameters θ_1 and θ_2 are given by:

$$\begin{aligned} 30 \leq \theta_1 \leq 60 \\ 120 \leq \theta_2 \leq 350 \end{aligned}$$

The semialgebraic set $\mathcal{S}_\theta$ for the uncertain parameters θ_1 and θ_2 is given by:

$$\begin{aligned} \mathcal{S}_\theta = \{(\theta_1,\theta_2) : 30 \leq & \theta_1 \leq 60, \quad 120 \leq \theta_2 \leq 350, \\ & \theta_2 <= 0.0852\theta_1^2 + 43.3333\}. \end{aligned} \tag{16.2}$$

The semialgebraic set $\mathcal{S}_\theta$ and the interval set are plotted in the figure 16.1.

The set of frequencies Ω_d for computing the frequency response bounds is given by:

$$\Omega_d(rad/sec) = [1:2:1000]. \tag{16.3}$$

Bode gain envelope is computed by solving the optimization problems (15.26) and (15.27) both for interval and semi-algebraic set uncertainty by using Sparse-POP software with a relaxation order of 3. The results are plotted in the figure 16.2. Bode phase envelope is computed by solving the optimization problems (15.30), (15.31),(15.36) and (15.37) both for interval and semi-algebraic set uncertainty by

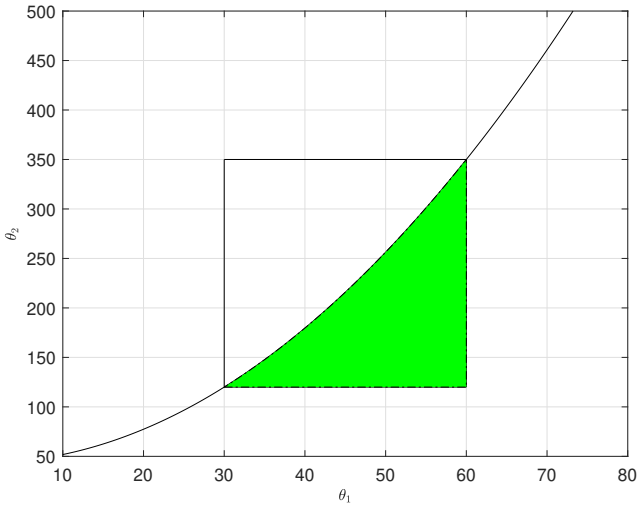

Figure 16.1: Semialgebraic region (green region) and interval region (box)

using Sparse-POP software with a relaxation order of 5. The results are plotted in the figure 16.3.

It is clear from the figures 16.2 and 16.3 that the proposed approach provide a tight bounds both for Bode gain and phase envelopes for semialgebraic uncertainty. This is due to the fact that the chosen relaxation orders, for this example, are large enough to provide tight convex bounds for the original nonconvex problem. It is also evident from the figures 16.2 and 16.3 that the semialgebraic description of the uncertainty reduces the significance amount of conservativeness introduced by the interval description of the uncertainty.

16.2 Example 2

Consider the following second order CT system:

$$G_p(s) = \frac{10(s+\theta_1)}{(s+\theta_2)^2} \tag{16.4}$$

where, θ_1 and θ_2 are the uncertain parameters. It is important to point out that the uncertainty enters polynomially in the transfer function (16.4) and the uncertain parameters, θ_1 and θ_2, belong to the following semialgebraic set.

$$\begin{aligned} \mathcal{S}_\theta = \{(\theta_1,\theta_2) : 30 \leq &\theta_1 \leq 60, \quad 120 \leq \theta_2 \leq 350, \\ &\theta_2 <= 0.0852\theta_1^2 + 43.3333\}. \end{aligned} \tag{16.5}$$

The semialgebraic set $\mathcal{S}_\theta$ is plotted in the figure the figure 16.4.

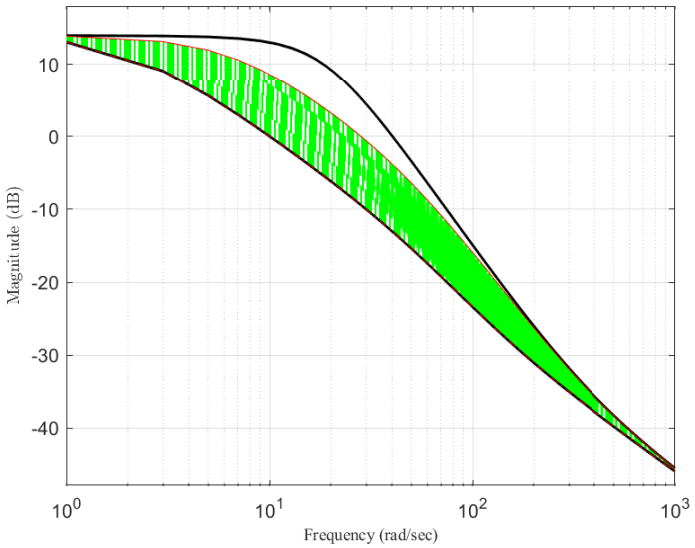

Figure 16.2: Magnitude bounds: interval description (black lines), proposed approach (red lines), envelope obtained by gridding the semialgebraic uncertainty set (green region)

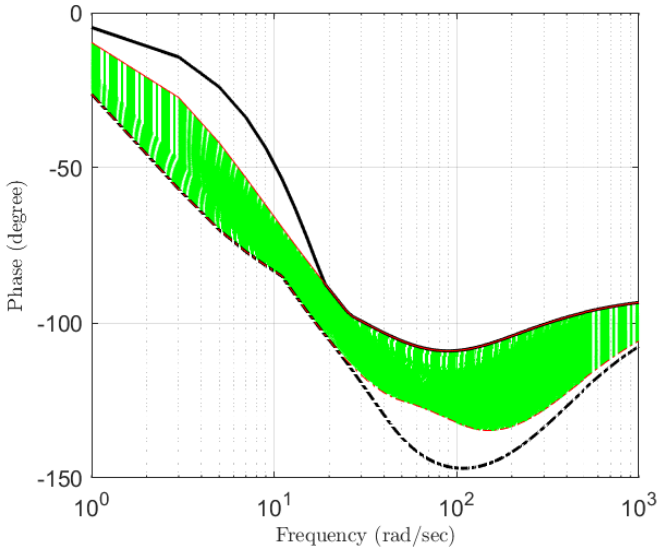

Figure 16.3: Phase bounds: interval description (black lines), proposed approach (red lines), envelope obtained by gridding the semialgebraic uncertainty set (green region)

For comparison of semialgebraic uncertainty with the interval uncertainty, the

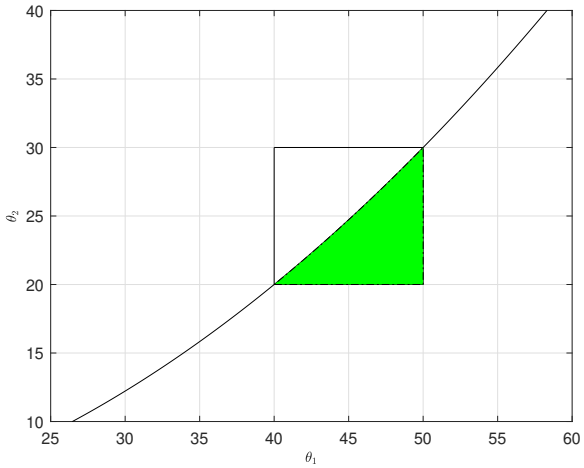

Figure 16.4: Semialgebraic region (green region) and interval region (box)

interval bounds for the uncertain parameters are given by:

$$40 \leq \theta_1 \leq 50$$
$$20 \leq \theta_2 \leq 30$$

We compute the Bode phase and gain envelopes for all the frequencies in the set Ω_d.

$$\Omega_d(rad/sec) = [1 : 3 : 200]; \tag{16.6}$$

Bode gain and phase envelopes are computed by solving the optimization problems (15.26), (15.27), (15.30), (15.31),(15.36) and (15.37) by using Sparse-POP software. A relaxation order of 4 is chosen for computation of Bode gain envelope whereas, a relaxation order of 5 is used for computation of Bode phase envelope. The Bode gain envelope is plotted in the figure 16.5, and the Bode phase envelope is plotted in the figure 16.6.

It is important to highlight that the existing techniques use the box/interval description of the uncertainty when the transfer function is a polynomial function of the uncertain parameters. However, such a description of the uncertainty can introduce the significance amount of conservativeness which is evident form the figures (16.5- 16.6). It is also clear from figures(16.5- 16.6) that the proposed approach is able to provide a tight description of actual Bode envelope, even though the transfer function is a polynomial function of uncertain parameters and uncertain parameters belong to a semialgebraic set. Thus, a significant amount of conservativeness in the Bode envelopes can be reduced by the proposed approach.

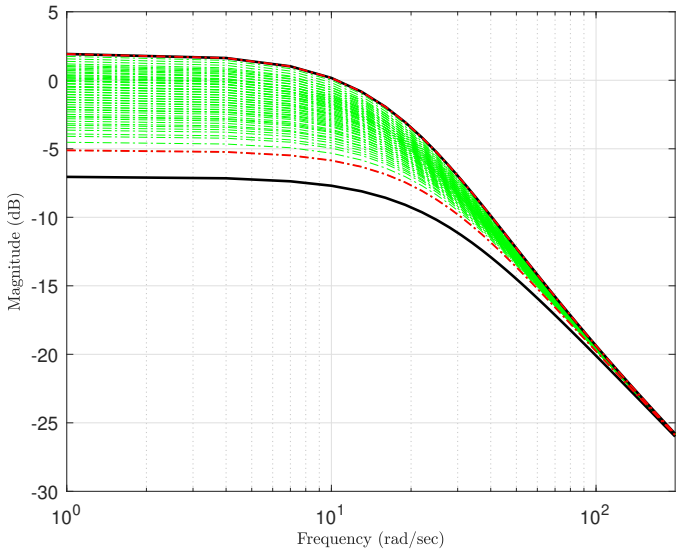

Figure 16.5: Magnitude bounds: interval description (black lines), proposed approach (red lines), envelope obtained by gridding the semialgebraic uncertainty set (green region)

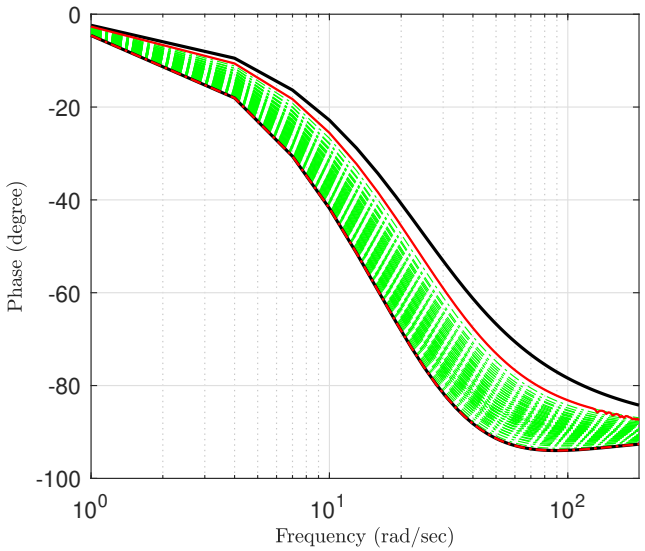

Figure 16.6: Phase bounds: interval description (black lines), proposed approach (red lines), envelope obtained by gridding the semialgebraic uncertainty set (green region)

16.3 Example 3

Consider the following DT uncertain system:

$$G_p(z) = \frac{2z + \theta_1}{4z^2 - \theta_2 z + 2} \tag{16.7}$$

It is assumed that the uncertain parameters θ_1 and θ_2 belong to the following semialgebraic set:

$$\begin{aligned} \mathcal{S}_\theta = \{(\theta_1, \theta_2) : 2 \leq & \theta_1 \leq 4 \;\; 1 \leq \theta_2 \leq 3, \\ & \theta_2^2 <= -4\theta_1^2 + 17\}, \\ & \theta_2 >= -\theta_1^2 + 5\}. \end{aligned} \tag{16.8}$$

The semialgebraic set $\mathcal{S}_\theta$ is plotted in the figure 16.7.

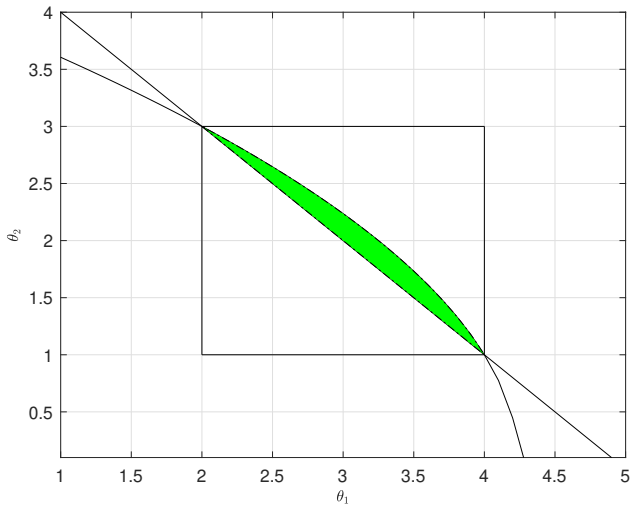

Figure 16.7: Semialgebraic region (green region) and interval region (box)

The interval bounds for the uncertain parameters are given by:

$$\begin{aligned} 2 \leq \theta_1 \leq 4 \\ 1 \leq \theta_2 \leq 3 \end{aligned}$$

Frequency response bounds are computed over a set of 100 frequencies in the range $\Omega_d(rad/sec) = [0.01,2.53]$.

Bode gain envelope is computed by solving the optimization problems (15.26) and (15.27) both for interval and semi-algebraic set uncertainty by using Sparse-POP software with a relaxation order of 4. The results are plotted in the figure 16.8. Bode phase envelope is computed by solving the optimization problems (15.30), (15.31),(15.36) and (15.37) both for interval and semi-algebraic set uncertainty by using Sparse-POP software with a relaxation order of 3. The results are plotted in the figure 16.9.

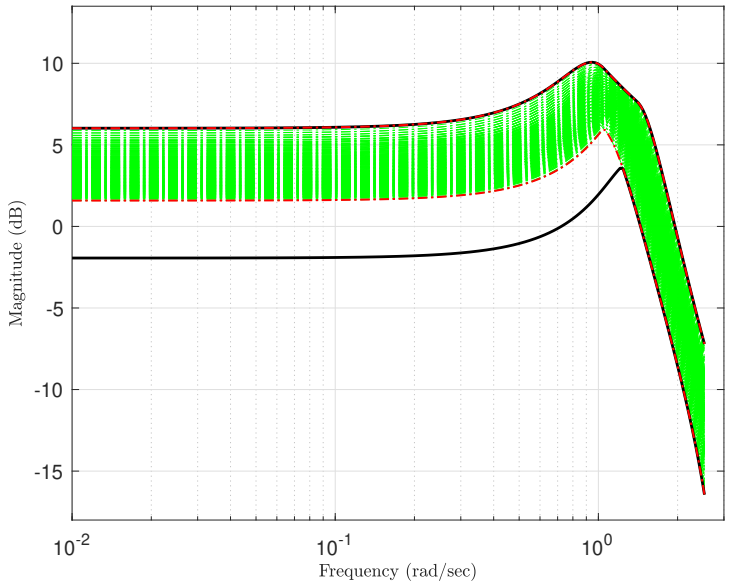

Figure 16.8: Magnitude bounds: interval description (black lines), proposed approach (red lines), envelope obtained by gridding the semialgebraic uncertainty set (green region)

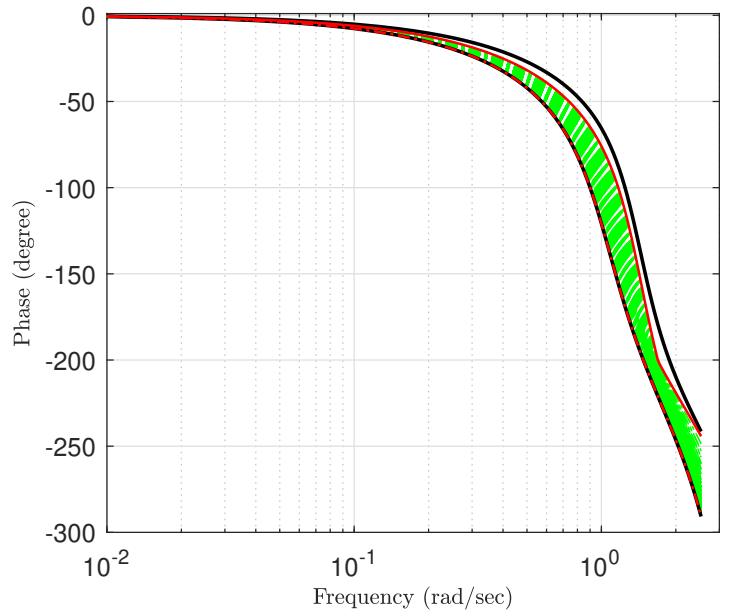

Figure 16.9: Phase bounds: interval description (black lines), proposed approach (red lines), envelope obtained by gridding the semialgebraic uncertainty set (green region)

It is evident from the figures (16.8-16.9) that:

(i) The proposed approach provides the tight bounds for Bode envelopes even for the peculiar semialgebraic structure of the parametric uncertainty affecting the system.

(ii) The Box description of the parametric uncertainty introduces conservativeness both in the Bode gain and phase envelopes which can be significantly reduced by assuming the semialgebraic description of the uncertainty.

Chapter 17

Conclusions

17.1 Conclusions

In this section, a novel approach is proposed for computing the Bode envelope bounds for uncertain LTI systems whose parameters belong to a given semialgebraic set. The problem is formulated in terms of four polynomial optimization problems and their global optimal solution are computed by exploiting sparse moment relaxation. The problem of computing the Bode plots bounds for a plant subjected to semialgebraic uncertainty is motivated from the results in SMI framework where the identified model is in the form rational functions and the coefficients of the rational functions belong to a given semialgebraic set.

In the existing techniques:

- the uncertainty can enter the numerator and the denominator of a transfer function linearly, multi-linearly or nonlinearly, and
- the coefficient space is restricted to interval, polytopic and ellipsoidal sets.

In the proposed approach, the uncertainty can enter the polynomial nonlinearly and the coefficient space is a semialgebraic set. Thus, the proposed approach generalizes previous available results. The reported simulation examples show the effectiveness of the proposed methodology in the computation of tight bounds on the Bode plots envelope.

Future works

Frequency gridding

In the design of FOFS direct data-driven control, the conditions for the stability and robustness are posed for a discrete grid of frequencies. However, the theorems and results for stability and robustness are derived for an infinite continuous set of frequencies. In future we would like to consider a random approach for the selection of the frequencies in the grid. There are some interesting results in the field of scenario based optimization about gridding a convex or nonconvex optimization problem over a finite grid and providing a bound on the violation probability of the constraints (see e. g., [48], [140], [141] and [154]). The main idea to combine the moment convex relaxation and the scenario based optimization such that stability and robustness can be guaranteed with some probability level and approaches to zero when the number of samples goes to infinity. Using these algorithms, we would like to specifically investigate the plants with many resonant modes.

Parametric robust control

In future, we will design the model-based FOFS mixed sensitivity H_∞ controllers for uncertain LTI systems subjected to semialgebraic parametric uncertainty by using convex relaxation methods.

Polynomial control system

In polynomial control system, the description of the control system is provided in terms of polynomial functions. Polynomial control systems has numerous applications as many nonlinear control problems can be modeled, transformed, or approximated by polynomial control systems. Polynomial control system can be divided into three broad categories:

1 polynomial control systems based on the qualitative behavior of polynomial systems.

2 polynomial control systems based on the algebraic nature of polynomial control systems

3 polynomial control systems based on the computational properties of polynomials.

Polynomial control systems based on the computational properties of polynomials is further divided into: (1) methods based on symbolic computations such as Grobner bases and (2) methods based on numerical computations like SDP and SOS decomposition. Thus, study of nonlinear polynomial control systems and polynomial linear parameter varying systems is the natural extension of this thesis.

List of publications

Journal papers

(J1) V. Razza, A. Salam. A Unified Framework for the H_∞ Mixed-Sensitivity Design of Fixed Structure Controllers through Putinar Positivstellensatz . Machines 2021, 9, 176. https://doi.org/10.3390/machines9080176

Conference papers

(C1) V. Cerone, S. Fosson, D. Regruto and A. Salam, "Bode envelope bounds for linear time-invariant systems affected by semialgebraic parametric uncertainty," 2020 IEEE 16th International Conference on Control and Automation (ICCA), 2020, pp. 247-252, doi: 10.1109/ICCA51439.2020.9264418.

(C2) S. M. Fosson, D. Regruto, T. Abdalla and A. Salam, "A convex optimization approach to online set-membership EIV identification of LTV systems," 2021 60th Annual Conference of the Society of Instrument and Control Engineers of Japan (SICE), 2021, pp. 1442-1447.

(C3) V. Cerone, S. M. Fosson, D. Regruto and A. Salam, "Sparse learning with concave regularization: relaxation of the irrepresentable condition," 2020 59th IEEE Conference on Decision and Control (CDC), 2020, pp. 396-401, doi: 10.1109/CDC42340.2020.9304508.

Bibliography

[1] A. C. Barlett, A. Tesi, and A. Vicino. "Frequency Response of Uncertain Systems with Interval Plants". In: *IEEE Transactions on Automatic Control* 38.6 (1993).

[2] A. C. Barlett, C. V. Hollot, and H. Lin. "Root location of an entire polytope of polynomials: it suffices to check the edges". In: *Mathematics of controls, Signals and Systems* 1 (1988), pp. 61–71.

[3] A. Dehghani et al. "Validating controllers for internal stability utilizing closed-loop data". In: *IEEE Transactions on Automatic Control* 54.11 (2009), pp. 2719–2725.

[4] A. Hassibi, J. How, and S. Boyd. "A path-following method for solving BMI problems in control". In: *Proceedings of the 1999 American Control Conference (Cat. No. 99CH36251)*. Vol. 2. 1999, pp. 1385–1389. DOI: 10.1109/ACC.1999.783595.

[5] A. J. den Hamer, S. Weiland, and M. Steinbuch. "Model-free norm-based fixed structure controller synthesis". In: *Proceedings of the 48h IEEE Conference on Decision and Control (CDC)*. , IEEE. 2009, pp. 4030–4035. DOI: 10.1109/CDC.2009.5400924.

[6] A. Karimi, A. Nicoletti, and Y. Zhu. "Robust H_∞ controller design using frequency-domain data via convex optimization". In: *International Journal of Robust Nonlinear Control* (2016).

[7] A. Karimi and G. Galdos. "Fixed-order H_∞ controller design for nonparametric models by convex optimization". In: *Automatica* 46.8 (2010), pp. 1388–1394. ISSN: 0005-1098. DOI: 10.1016/j.automatica.2010.05.019.

[8] A. Karimi and G. Galdos. "Fixed-order H_∞ controller design for nonparametric models by convex optimization". In: *Automatica* 46.8 (2010), pp. 1388–1394.

[9] A. Karimi, L. Miškovi, and D. Bonvin. "Iterative correlation-based controller tuning". In: *Int. Journal of Adaptive Control and Signal Processing* 18.8 (2004), pp. 645–664.

[10] A. Karimi, M. Kunze, and R. Longchamp. "Robust controller design by linear programming with application to a double-axis positioning system". In: *Control Engineering Practice* 15.2 (2007), pp. 197–208. ISSN: 0967-0661. DOI: 10.1016/j.conengprac.2006.06.002.

[11] A. Levkovich, E. Zeheb, and N. Cohen. "Frequency Response Envelopes of a Family of Uncertain Continuous-Time Systems". In: *IEEE TRANSACTIONS ON CIRCUITS AND SYSTEMS* 42.3 (1995).

[12] A. Nemirovskii. "Several NP-hard problems arising in robust stability analysis". In: *Mathematics of Control, Signals and Systems* 6.2 (1993), pp. 99–105.

[13] A. Nicoletti and A. Karimi. "A Data-Driven Method for Computing Fixed-Structure Low-Order Controllers With H_∞ Performance". In: *European Control Conference (ECC)* (2018), pp. 882–887.

[14] A. Sadeghzadeh, H. Momeni, and A. Karimi. "Fixed-order H_∞ controller design for systems with ellipsoidal parametric uncertainty". In: *International Journal of Control* 84.1 (2011), pp. 57–65. DOI: 10.1080/00207179.2010.540040.

[15] B. D. O. Anderson and Y. Liu. "Controller reduction: concepts and approaches". In: *IEEE Transactions on Automatic Control* 34.8 (1989), pp. 802–812. ISSN: 0018-9286. DOI: 10.1109/9.29422.

[16] B. Huang and R. Kadali. *Dynamic modeling, predictive control and performance monitoring: a data-driven subspace approach*. Springer, 2008.

[17] F.N. Bailey and C.-H. Hui. "A fast algorithm for computing parametric rational functions". In: *IEEE Transactions on Automatic Control* 34.11 (1989), pp. 1209–1212. DOI: 10.1109/9.40756.

[18] Andrew C. Bartlett. "Computation of the frequency response of systems with uncertain parameters: a simplification". In: *INT. J. Control* 57.6 (1993), pp. 1293–1307.

[19] Andrew C. Bartlett. "Nyquist, Bode, and Nichols Plots of Uncertain Systems". In: *1990 American Control Conference* (1990), pp. 2033–2037.

[20] Julian Berberich et al. "Data-Driven Model Predictive Control With Stability and Robustness Guarantees". In: *IEEE Transactions on Automatic Control* 66.4 (2021), pp. 1702–1717. DOI: 10.1109/TAC.2020.3000182.

[21] Bruce A. Francis. *A Course in H_∞ Control Theory (Lecture Notes in Control and Information Sciences)*. Springer, 1987. ISBN: 3540170693.

[22] C. Greco, M. Rulla, and L. Spagnolo. *Laboratorio sperimentale di automatica. Applicazioni di modellistica, analisi e controllo*. McGraw-Hill Education, 2003. ISBN: 978-8838660900.

[23] C. Scherer, P. Gahinet, and M. Chilali. "Multi-objective output-feedback control via LMI optimization". In: *IEEE Transactions on Automatic Control* 42.7 (1997), pp. 896–911.

[24] C. V. Hollot and R. Tempo. "On the Nyquist envelope of an interval plant family". In: *IEEE Transactions on Automatic Control* 39 (1994), pp. 391–386.

[25] C.H. Houpis, S.J. Rasmussen, and M. Garcia-Sanz. *Quantitative Feedback Theory: Fundamentals and Applications*. Second Edition. CRC Press, 2005.

[26] Chen Tongwen and Francis Bruce Allen. "Introduction to Discrete-Time H_∞-Optimal Control". In: *Optimal Sampled-Data Control Systems*. London: Springer London, 1995, pp. 171–181. ISBN: 978-1-4471-3037-6. DOI: 10.1007/978-1-4471-3037-6_7.

[27] D. Henrion. "Optimization on linear matrix inequalities for polynomial systems control". In: *Les cours du C.I.R.M.* 3.1 (2013), pp. 1–44. DOI: 10.5802/ccirm.17.

[28] D. Henrion and J.B. Lasserre. "Detecting Global Optimality and Extracting Solutions in GloptiPoly." In: *Springer* 312 (2005).

[29] D. Henrion et al. "Solving polynomial static output feedback problems with PENBMI". In: *Proceedings of the 44th IEEE Conference on Decision and Control*. IEEE. 2005, pp. 7581–7586. DOI: 10.1109/CDC.2005.1583385.

[30] D. McFarlane, K. Glover, and M. Vidyasagar. "Reduced-order controller design using coprime factor model reduction". In: *IEEE Transactions on Automatic Control* 35.3 (1990), pp. 369–373. ISSN: 0018-9286. DOI: 10.1109/9.50362.

[31] D. Selvi, D. Piga, and A. Bemporad. "Towards direct data driven model-free design of optimal controllers". In: *European Control Conference.* , IEEE. 2018, pp. 2836–2841.

[32] Ersin Daş and Selahattin Çağlar Başlamışlı. "Two degree of freedom robust data-driven fixed-order controller synthesis using convex optimization". In: *ISA Transactions* 114 (2021), pp. 291–305. ISSN: 0019-0578. DOI: https://doi.org/10.1016/j.isatra.2020.12.028. URL: https://www.sciencedirect.com/science/article/pii/S0019057820305474.

[33] Didier Henrion, Jean-Bernard Lasserre, and Johan Löfberg. "GloptiPoly 3: moments, optimization and semidefinite programming". In: *Optimization Methods and Software* 24.4-5 (2009), pp. 761–779. DOI: https://doi.org/10.1080/10556780802699201.

[34] Peter Draper. "The title of the work". In: *The title of the book*. Ed. by The editor. Vol. 4. 5. An optional note. The organization. The address of the publisher: The publisher, July 1993, p. 213.

[35] E. Artin. "Über die Zerlegung definiter Funktionen in Quadrate". In: *Mathematics Seminar University of Hamburg*. 1927, pp. 85–99.

[36] E. Grassi and K. Tsakalis. "PID controller tuning by frequency loop-shaping". In: *In Proceedings of 35th IEEE Conference on Decision and Control*. Vol. 4. 1996, pp. 4776–4781. DOI: 10.1109/CDC.1996.577667.

[37] E. Jury. "Additions to "Notes on the stability criterion for linear discrete systems"". In: *IRE Transactions on Automatic Control* 6.3 (1961), pp. 342–343.

[38] E. Solingen, J. Wingerden, and T. Oomen. "Frequency-domain optimization of fixed-structure controllers". In: *International Journal of Robust and Nonlinear Control* 28.12 (2016), pp. 3784–3805.

[39] E. Walter and L. Jaulin. "Guaranteed characterization of stability domains via set inversion". In: *IEEE Transactions on Automatic Control* 39.4 (1994), pp. 886–889. ISSN: 0018-9286. DOI: 10.1109/9.286277.

[40] E.C. Warner and J.T. Scruggs. "Iterative Convex Overbounding Algorithms for BMI Optimization Problems". In: *IFAC-PapersOnLine* 50 (1 2017), pp. 10449–10455. DOI: 10.1016/j.ifacol.2017.08.1974.

[41] Edward John. *A treatise on the stability of a given state of motion: particularly steady motion*. Macmillan and Company, 1877.

[42] F. Blanchini et al. "Characterization of PID and lead/lag compensators satisfying given H_∞ specifications". In: *IEEE Transactions on Automatic Control* 49.5 (2004), pp. 736–740. ISSN: 0018-9286. DOI: 10.1109/TAC.2004.825961.

[43] Simon Fear. *Publication quality tables in LATEX*. 2005.

[44] S. Formentin et al. "Deterministic continuous-time Virtual Reference Feedback Tuning (VRFT) with application to PID design". In: *Systems and Control Letters* 127 (2019), pp. 25–34. ISSN: 0167-6911. DOI: https://doi.org/10.1016/j.sysconle.2019.03.007.

[45] Frank H. Clarke. *Optimization and nonsmooth analysis*. Vol. 5. SIAM, 1990.

[46] G. Battistelli et al. "Direct control design via controller unfalsification". In: *International Journal of Robust and Nonlinear Control* 28.12 (2018), pp. 3694–3712.

[47] G. Battistelli et al. "Stability of unfalsified adaptive switching control in noisy environments". In: *IEEE Transactions on Automatic Control* 55.10 (2010), pp. 2424–2429.

[48] G. Calafiore and M. C. Campi. "The scenario approach to robust control design". In: *IEEE Trans. on Automatic Control* 51.5 (2006), pp. 742–753.

[49] G. Chesi et al. "A convex approach to the characterization of the frequency response of ellipsoidal plants". In: *Automatica* 38.2 (2002), pp. 249–259.

[50] G. Fiorio et al. "Robust performance design of fixed structure controllers for systems with uncertain parameters". In: *Proceedings of 32nd IEEE Conference on Decision and Control*. Vol. 4. IEEE. 1993, pp. 3029–3031. DOI: 10.1109/CDC.1993.325757.

[51] G. Galdos, A. Karimi, and R. Longchamp. "H_∞ Controller design for spectral MIMO models by convex optimization". In: *Journal of Process Control* 20.10 (2010), pp. 1175–1182. ISSN: 0959-1524. DOI: 10.1016/j.jprocont.2010.07.006.

[52] G. Rallo et al. "Vehicle stability control via VRFT with probabilistic robustness guarantees". In: *2016 IEEE 55th Conference on Decision and Control (CDC)*. 2016, pp. 7165–7170. DOI: 10.1109/CDC.2016.7799374.

[53] G. Still. "Generalized semi-infinite programming: numerical aspects". In: *Optimization* 49 (2001), pp. 223–242.

[54] G. Zames. "Feedback and optimal sensitivity: Model reference transformations, multiplicative seminorms, and approximate inverses". In: *IEEE Transactions on Automatic Control* 26.2 (1981), pp. 301–320. ISSN: 0018-9286. DOI: 10.1109/TAC.1981.1102603.

[55] Enrico Gregorio. "Installing TeX Live 2010 on Ubuntu". In: *TUGboat* 32.1 (2011), pp. 56–61.

[56] H. Anai and S. Hara. "A parameter space approach to fixed-order robust controller synthesis by quantifier elimination". In: *International Journal of Control* 79.11 (2006), pp. 1321–1330. DOI: https://doi.org/10.1080/00207170600726550.

[57] H. Chapellat and S. P. Bhattacharyya. "A generalization of Kharitonov's theorem: robust stability of interval plants". In: *IEEE Transactions on Automatic Control* 34 (1989), pp. 306–311.

[58] H. Hjalmarsson. "Iterative feedback tuning - an overview". In: *Int. Journal of Adaptive Control and Signal Processing* 16 (2002), pp. 373–395.

[59] H. Hjalmarsson, S. Gunnarsson, and M. Gevers. "A convergent iterative restricted complexity control design scheme". In: *33rd IEEE Conference on Decision and Control*. , IEEE. 1994, pp. 1735–1740.

[60] H. Hjalmarsson et al. "Iterative feedback tuning:theory and application". In: *IEEE Control Systems Magazine* (1998), pp. 26–41.

[61] H. Kwakernaak. "Mixed Sensitivity Design". In: *In Proceedings of 15th IFAC World Congress*. Vol. 35. 1. 2002, pp. 61–66. DOI: 10.3182/20020721-6-ES-1901.01236.

[62] H. Kwakernaak. "Robustness optimization of linear feedback systems". In: *The 22nd IEEE Conference on Decision and Control*. 1983, pp. 618–624. DOI: 10.1109/CDC.1983.269592.

[63] H. Parastvand and M. J. Khosrowjerdi. "Controller synthesis free of analytical model: fixed-order controllers". In: *Int. Journal of Systems Science* 46.7 (2015), pp. 1208–1221.

[64] H. Parastvand and M. J. Khosrowjerdi. "Parameterised controller synthesis for siso-lti uncertain plants using frequency domain information". In: *Int. Journal of Systems Science* 47.1 (2016), pp. 32–44.

[65] H. Prochazka et al. "Iterative feedback tuning for robust controller design and optimization". In: *Proceedings of the 44st IEEE Conference on Decision and Control*. , IEEE. 2005, pp. 3602–3607.

[66] H. Waki et al. "SparsePOP : a Sparse Semidefinite Programming Relaxation of Polynomial Optimization Problems". In: *ACM Transactions on Mathematical Software* 35.2 (2008), p. 15. DOI: http://dx.doi.org/10.1145/1377612.1377619.

[67] H. Waki et al. *SparsePOP: Sparse Semidefinite Programming Relaxation of Polynomial Optimization Problems*. Version 3.03. 2018. URL: https://sparsepop.sourceforge.io/.

[68] H. Waki et al. "Sums of squares and semidefinite programming relaxation for polynomial optimization problems with structured sparsity". In: *SIAM J. Optim.* 17.1 (2006), pp. 218–242. DOI: http://dx.doi.org/10.1137/050623802.

[69] Hassan K. Khalil. *Nonlinear systems*. 3rd. Prentice Hall, 2002, pp. 227–260.

[70] Peter Hertel. "Writing Articles with LATEX". In: (2010).

[71] Rainer Hettich. "A Review of Numerical Methods for Semi-Infinite Optimization". In: 1983.

[72] HP. Whitaker, J. Yamron, and A. Kezer. *Design of model-reference adaptive control systems for aircraft*. Technical report R-164. Cambridge, Massachusetts.: Instrumentation laboratory MIT, press, 1958.

[73] I. D. Landau et al. *Adaptive Control: Algorithms, Analysis and Applications*. Springer-Verlag, 2011.

[74] Isaac Kaminer, Pramod P. Khargonekar, and Mario A. Rotea. "Mixed H_2H_∞ control for discrete-time systems via convex optimization". In: *Automatica* 29.1 (1993), pp. 57–70. ISSN: 0005-1098. DOI: 10.1016/0005-1098(93)90174-R.

[75] J. Burke et al. “HIFOO - A MATLAB package for fixed-order controller design and H_∞ optimization”. In: *IFAC Proceedings Volumes* 39 (2006), pp. 339–344.

[76] J. C. Doyle et al. “State-space solutions to standard H_2 and H_∞ control problems”. In: *IEEE Transactions on Automatic Control* 34.8 (1989), pp. 831–847. ISSN: 0018-9286. DOI: 10.1109/9.29425.

[77] J. Elzinga and T. G.. Moore. “A central cutting plane algorithm for the convex programming problem”. In: *Math. Program.* 8 (1975), pp. 134–145.

[78] J. Löfberg. “YALMIP: A Toolbox for Modeling and Optimization in MATLAB”. In: *In Proceedings of the CACSD Conference*. IEEE. Taipei, Taiwan, 2004.

[79] J.-J. E. Slotine and W. Li. *Applied nonlinear control*. Englewood Cliffs, NJ: Prentice hall, 1991.

[80] J.V. Burke et al. “HIFOO - A Matlab package for fixed-order controller design and H_∞ optimization”. In: *IFAC Proceedings Volumes* 39.9 (2006). 5th IFAC Symposium on Robust Control Design, pp. 339–344. ISSN: 1474-6670. DOI: 10.3182/20060705-3-FR-2907.00059.

[81] J.W. Blankenship and J.E. Falk. “Infinitely constrained optimization problems”. In: *J Optim Theory Appl* 19 (1976), pp. 261–281. DOI: doi.org/10.1007/BF00934096.

[82] James V. Burke, Adrian S. Lewis, and Michael L. Overton. “A robust gradient sampling algorithm for nonsmooth, nonconvex optimization”. In: *SIAM Journal on Optimization* 15.3 (2005), pp. 751–779. DOI: https://doi.org/10.1137/030601296.

[83] Jean B. Lasserre. “Global Optimization with Polynomials and the Problem of Moments”. In: *SIAM Journal on Optimization* 11.3 (2001), pp. 796–817. DOI: 10.1137/S1052623400366802.

[84] Y. Jia. “Computing the frequency response of systems affinely depending on uncertain parameters”. In: *IEE Proceedings - Control Theory and Applications* 149.4 (2002), pp. 311–315.

[85] John C. Doyle, Bruce A. Francis, and Allen R. Tannenbaum. *Feedback Control Theory*. Macmillan Publications, 1992. ISBN: 0486469336.

[86] E.I. Jury. “On the roots of a real polynomial inside the unit circle and a stability criterion for linear discrete systems”. In: *IFAC Proceedings Volumes* 1.2 (1963). 2nd International IFAC Congress on Automatic and Remote Control: Theory, Basle, Switzerland, 1963, pp. 142–153. ISSN: 1474-6670. DOI: https://doi.org/10.1016/S1474-6670(17)69648-4.

[87] K. -. Liu, T. Mita, and H. Kimura. "Complete solution to the standard H_∞ control problem of discrete-time systems". In: *29th IEEE Conference on Decision and Control*. 1990, 1786–1793 vol.3.

[88] K. Fujisawa et al. "SDPA project: Solving large-scale semidefinite programs". In: *Journal of the Operations Research Society of Japan-Keiei Kagaku* 50.4 (2007), pp. 278–298.

[89] K. G. Murty and S. N. Kabadi. "Some NP-complete problems in quadratic and nonlinear programming". In: *Mathematical Programming* 39 (1987), pp. 117–129.

[90] K. Van Heusden, A. Karimi, and D. Bonvin. "Data-driven controller validation". In: *15th IFAC Symposium on System Identification.* , IFAC. 2009, pp. 1050–1055.

[91] K. van Heusden et al. "Data-driven model reference control with asymptotically guaranteed stability". In: *Int. Journal of Adaptive Control and Signal Processing* 25.4 (2011), pp. 331–351.

[92] K. Zhou, J. Doyle, and K. Glover. *Robust and Optimal Control*. Pearson, 1995.

[93] Keith Glover. "All optimal Hankel-norm approximations of linear multivariable systems and their $L\infty$-error bounds". In: *International Journal of Control* 39.6 (1984), pp. 1115–1193. DOI: 10.1080/00207178408933239.

[94] Keith Glover and John C. Doyle. "State-space formulae for all stabilizing controllers that satisfy an H_∞-norm bound and relations to relations to risk sensitivity". In: *Systems & Control Letters* 11.3 (1988), pp. 167–172. ISSN: 0167-6911. DOI: 10.1016/0167-6911(88)90055-2.

[95] Kemin Zhou, John C. Doyle, and Keith Glover. *Robust and Optimal Control*. Pearson, 1995. ISBN: 0134565673.

[96] M. Kojima. *Sums of squares relaxations of polynomial semidefinite programs*. 2003.

[97] L. A. Zadeh and C. A. Desoer. *Linear Systems Theory, A State Space Approach*. McGraw-Hill, New York, 1963.

[98] L. H. Keel and S. P. Bhattacharyya. "Controller synthesis free of analytical models: Three term controllers". In: *EEE Trans. on Automatic Control* 53.6 (2008), pp. 1353–1369.

[99] L. Kharitonov. "Asymptotic stability of an equilibrium position of a family of systems of linear differential equations". In: *Differential Equations* 14 (1979), pp. 1483–1485.

[100] L. Miškovi et al. "Correlation-based tuning of decoupling multivariable controllers". In: *Automatica* 43.9 (2007), pp. 1481–1494.

[101] L. Wang and F. Guo. "Semidefinite relaxations for semi-infinite polynomial programming". In: *Comput Optim Appl* 58 (2014), pp. 133–159.

[102] Leslie Lamport. *Latex*. Addison-Wesley, 1994.

[103] Jean B. Lasserre. "Convergent SDP-relaxations in polynomial optimization with sparsity". In: *SIAM J. OPTIM.* 17.3 (2006), pp. 822–843.

[104] Jean B. Lasserre. *Moments, Positive Polynomials and Their Applications*. Imperial College Press, 2010.

[105] Lee Donghwan and Hu Jianghai. "Sequential parametric convex approximation algorithm for bilinear matrix inequality problem". In: *Optimization Letters* 13.4 (2019), pp. 741–759.

[106] M. FU. "Computing the frequency response of linear systems with parametric perturbation". In: *Sytems and Control Letters* 15 (1990), pp. 45–52.

[107] M. G. Safonov, K. C. Goh, and J. H. Ly. "Control system synthesis via bilinear matrix inequalities". In: *American Control Conference, 1994*. Vol. 1. 1994, pp. 45–49. DOI: 10.1109/ACC.1994.751690.

[108] M. G. Safonov and T. C. Tsao. "The unfalsified control concept and learning". In: *IEEE Trans. on Automatic Control* 42.6 (1997).

[109] M. Hakimi-Moghaddam. "Positive real and strictly positive real MIMO systems: theory and application". In: *Int. J. Dynam. Control* 8 (2020), pp. 448–458.

[110] M. Jun and M. G.Safonov. "Controller parameter adaptation algorithm using unfalsified control theory and gradient method". In: *IFAC Proceedings Volumes* 35.1 (2002), pp. 283–287.

[111] M. Laurent. "Sums of Squares, Moment Matrices and Optimization Over Polynomials". In: *Emerging Applications of Algebraic Geometry. The IMA Volumes in Mathematics and its Applications*. Ed. by M. Putinar and S. Sullivant. Vol. 149. New York, NY: Springer, 2009, pp. 157–270. DOI: https://doi.org/10.1007/978-0-387-09686-5_7.

[112] M. Verma and E. Jonckheere. "L_∞-compensation with mixed sensitivity as a broadband matching problem". In: *Systems & Control Letters* 4.3 (1984), pp. 125–129. ISSN: 0167-6911. DOI: 10.1016/S0167-6911(84)80013-4.

[113] M.C. Campi, A. Lecchini, and S.M. Savaresi. "Virtual reference feedback tuning: A direct method for the design of feedback controllers". In: *Automatica* 38 (2002), pp. 1337–1346.

[114] Mihai Putinar. "Positive Polynomials on Compact Semi-Algebraic Sets". In: *Indiana Univ. Math. J.* 42 (3 1993), pp. 969–984. ISSN: 0022-2518.

[115] MOSEK ApS. *The MOSEK optimization toolbox for MATLAB manual, Version 9.0*. http://docs.mosek.com/9.0/toolbox/index.html. 2019.

[116] MOSEK ApS. *The MOSEK optimization toolbox for MATLAB manual. Version 8.0.* 2017. URL: https://docs.mosek.com/8.0/toolbox/index.html.

[117] N.Tan and D. P. Atherton. "Magnitude and phase envelopes of systems with affine linear uncertainty". In: *UKACC International Conference on Control '98 (Conf. Publ. No. 455)*. Vol. 2. 1998, pp. 1039–1044. DOI: 10.1049/cp:19980372.

[118] Nusret Tan. "Robust phase margin, robust gain margin and Nyquist envelope of an interval plant family". In: *Computers and Electrical Engineering* 30 (2004), pp. 153–165.

[119] O. Toker and H. Ozbay. "On the NP-hardness of solving bilinear matrix inequalities and simultaneous stabilization with static output feedback". In: *American Control Conference, 1995*. Vol. 4. AACC. 1995, pp. 2525–2526. DOI: 10.1109/ACC.1995.532300.

[120] K. Ogata. *Modern Control Engineering*. 3rd. Prentice Hall, 1997.

[121] P. Apkarian and D. Noll. "Nonsmooth H_∞ Synthesis". In: *IEEE Transactions on Automatic Control* 51.1 (2006), pp. 71–86. DOI: 10.1109/TAC.2005.860290.

[122] P. Apkarian and D. Noll. "Nonsmooth H_∞ synthesis". In: *IEEE Transactions on Automatic Control* 51.1 (2006), pp. 71–86. ISSN: 0018-9286. DOI: 10.1109/TAC.2005.860290.

[123] P. Gahinet. "Explicit controller formulas for LMI-based H_∞ synthesis". In: *Automatica* 32.7 (1996), pp. 1007–1014. ISSN: 0005-1098. DOI: 10.1016/0005-1098(96)00033-7.

[124] P. Gahinet and P. Apkarian. "A linear matrix inequality approach to H_∞ control". In: *International Journal of Robust and Nonlinear Control* 4.4 (1994), pp. 421–448. ISSN: 1099-1239. DOI: 10.1002/rnc.4590040403.

[125] P. M. M. Bongers and O. H. Bosgra. "Low order robust H_∞ controller synthesis". In: *29th IEEE Conference on Decision and Control*. 1990, 194–199 vol.1. DOI: 10.1109/CDC.1990.203575.

[126] P. S. V. Nataraj and J. J. Barve. "Reliable computation of frequency response plots for non-rational transfer functions to prescribed accuracy". In: *Reliable Computing* 9.5 (2003), pp. 373–389.

[127] P. S. V. Nataraj and S. Sondur. "Construction of bode envelopes using REP based range finding algorithms". In: *nternational Journal of Automation and Computing* 8.1 (2011).

[128] P. S. V. Nataraj and S. Sondur. "Frequency boundary of fractional order systems with nonlinear uncertainties". In: *Journal of the Franklin Institute* 350 (2013), pp. 1908–1925.

[129] Pablo A. Parrilo. "Semidefinite programming relaxations for semialgebraic problems". In: *Mathematical programming* 96.2 (2003), pp. 293–320. ISSN: 0025-5610.

[130] Rik Pintelon and Johan Schoukens. *System identification: a frequency domain approach*. John Wiley & Sons, 2012.

[131] S. Prajna, A. Papachristodoulou, and P.A. Parrilo. "Introducing SOSTOOLS: a general purpose sum of squares programming solver". In: *Proceedings of the 41st IEEE Conference on Decision and Control, 2002.* Vol. 1. 2002, pp. 741–746. DOI: 10.1109/CDC.2002.1184594.

[132] Q. T. Dinh et al. "An inner convex approximation algorithm for BMI optimization and applications in control". In: *In Proceedings of 51st IEEE Conference on Decision and Control (CDC)*. 2012, pp. 3576–3581. DOI: 10.1109/CDC.2012.6427102.

[133] R. Hettich and K.O. Kortanek. "Semi-infinite programming: theory, methods, and applications". In: *SIAM* 35 (1993), pp. 380–429.

[134] R. Hettich and K.O. Kortanek. "Semi-infinite programming: theory, methods, and applications". In: *SIAM* 35 (1993), pp. 380–429.

[135] S. Formentin and A. Karimi. "A Data-Driven Approach to Mixed-Sensitivity Control With Application to an Active Suspension System". In: *IEEE Transactions on Industrial Informatics* 9.4 (2013), pp. 2293–2300. DOI: 10.1109/TII.2012.2220556.

[136] S. Formentin and S. Savaresi. "Virtual reference feedback tuning for linear parameter-varying systems". In: *IFAC Proceedings Volumes* 44.1 (2011), pp. 10219–10224.

[137] S. Formentin, S. Savaresi, and L. Del Re. "Non-iterative direct data-driven controller tuning for multivariable systems: theory and application". In: *IET control theory and applications* 6.9 (2012), pp. 1250–1257.

[138] S. Formentin et al. "Non-parametric LPV data-driven control". In: *IFAC-PapersOnLine* 48.26 (2015), pp. 146–151.

[139] S. Formentin et al. "Robust direct data-driven controller tuning with an application to vehicle stability control". In: *International Journal of Nonlinear and Robust Control* 28 (2018), pp. 3752–3765. DOI: https://doi.org/10.1002/rnc.3782.

[140] S. Garatti and M. C. Campi. "Risk and complexity in scenario optimization". In: *Math. Program* 191 (2022), pp. 243–279. DOI: 10.1007/s10107-019-01446-4.

[141] S. Garatti, M. C. Campi, and F. A. Ramponi. "A General Scenario Theory for Nonconvex Optimization and Decision Making". In: *IEEE Transactions on Automatic Control* 63.12 (2018), pp. 4067–4078. DOI: 10.1109/TAC.2018.2808446.

[142] S. Kanev et al. "Robust output-feedback controller design via local BMI optimization". In: *Automatica* 40.7 (2004), pp. 1115–1127. ISSN: 0005-1098. DOI: 10.1016/j.automatica.2004.01.028.

[143] S. Malan, M. Milanese, and M. Taragna. "Robust Analysis and Design of Control Systems Using Interval Arithmetic". In: *Automatica* 33.7 (1997), pp. 1363–1372. ISSN: 0005-1098. DOI: 10.1016/S0005-1098(97)00028-9.

[144] S. Veres and H. Hjalmarsson. "Tuning for robustness and performance using iterative feedback tuning". In: *Proceedings of the 41st IEEE Conference on Decision and Control.* , IEEE. 2002, pp. 4682–4687.

[145] S.P. Bhattacharrya, H. Chapellat, and H. Kheel. *Robust Control, the parametric approach*. Printence Hall, 1995.

[146] S.P. Bhattacharrya, H. Chapellat, and L. H. Kheel. *Robust Control, the parametric approach*. Printence Hall, 1995.

[147] Johan Schoukens, Keith Godfrey, and Maarten Schoukens. "Nonparametric data-driven modeling of linear systems: Estimating the frequency response and impulse response function". In: *IEEE Control Systems Magazine* 38.4 (2018), pp. 49–88.

[148] A. Simonič. "A Construction of Lomonosov Functions and Applications to the Invariant Subspace Problem". In: *Pacific J. Math.* 175 (1996), pp. 257–270.

[149] A. Simonič. "An Extension of Lomonosov's Techniques to Non-Compact Operators". PhD thesis. Dalhousie University, Department of Mathematics, Statistics, & Computing Science, 1994.

[150] A. Simonič. "Grupe Operatorjev s Pozitivnim Spektrom". MA thesis. Univerza v Ljubljani, FNT, Oddelek za Matematiko, 1990.

[151] A. Simonič. "Matrix Groups with Positive Spectra". In: *Linear Algebra Appl.* 173 (1992), pp. 57–76.

[152] A. Simonič. "Notes on Subharmonic Functions". Lecture Notes, Dalhousie University, Department of Mathematics, Statistics, & Computing Science. 1991.

[153] J. F. Sturm. "Using SeDuMi 1.02, a MATLAB Toolbox for optimization over symmetric cones". In: *Optim. Methods Software* 11.12 (1999), pp. 625–653.

[154] T. Alamo, R. Tempo, and A. Luque. "On the sample complexity of probabilistic analysis and design methods". In: *Perspectives in Mathematical System Theory, Control, and Signal Processing* (2010), pp. 39–55.

[155] T. Emami, R. J. Hartnett, and J. M. Watkins. "Estimate of discrete-time PID controller parameters for H-infinity complementary sensitivity design: Autonomous sailboat application". In: *American Control Conference*. 2013, pp. 1795–1801.

[156] N. Tan. "Computation of the frequency response of multilinear affine systems". In: *IEEE Transactions on Automatic Control* 47.10 (2002), pp. 1691–1696. DOI: 10.1109/TAC.2002.803537.

[157] U. Topcu and A. Packard. "Local Stability Analysis for Uncertain Nonlinear Systems". In: *IEEE TRANSACTIONS ON AUTOMATIC CONTROL* 54.5 (2009).

[158] V. Cerone, D. Piga, and D. Regruto. "Improved parameter bounds for set-membership EIV problems". In: *International Journal of Adaptive Control and Signal Processing* 25.3 (2011), pp. 208–227.

[159] V. Cerone, D. Piga, and D. Regruto. "Set-Membership Error-in-Variables Identification Through Convex Relaxation Techniques". In: *IEEE Transactions on Automatic Control* 57.2 (2012), pp. 517–522.

[160] V. Cerone, V. Razza, and D. Regruto, "H_∞ mixed-sensitivity design with fixed structure controller through Putinar positivstellensatz". In: *American Control Conference (ACC)*. 2019, pp. 1806–1811. DOI: 10.23919/ACC.2019.8814775.

[161] V. Cerone et al. "A Unified Framework for Solving a General Class of Conditional and Robust SetMembership Estimation Problems". In: *IEEE Transactions on Automatic Control* 59.11 (2014), pp. 2897–2909.

[162] V. Cerone et al. "Bode envelope bounds for linear time-invariant systems affected by semialgebraic parametric uncertainty". In: *16th IEEE International Conference on Control and Automation (ICCA)*. 2020, pp. 247–252. DOI: 10.1109/ICCA51439.2020.9264418.

[163] V. Helvoort, B. de Jager, and M. Steinbuch. "Direct data-driven recursive controller unfalsification with analytic update". In: *Automatica* 43.12 (2007), pp. 2034–2046.

[164] V.Razza and A. Salam. "A Unified Framework for the H_∞ Mixed-Sensitivity Design of Fixed Structure Controllers through Putinar Positivstellensatz". In: *Machines* 9.8 (2021). DOI: 10.3390/machines9080176.

[165] B. Valentina and S. Formentin. "Virtual Reference Feedback Tuning with data-driven reference model selection". In: *Proceedings of the 2nd Conference on Learning for Dynamics and Control*. Vol. 120. Proceedings of Machine Learning Research. PMLR, 2020, pp. 37–45.

[166] W. Kongprawechnon and H. Kimura. "J-lossless factorization and H control for discrete-time systems". In: *International Journal of Control* 70.3 (1998), pp. 423–446. DOI: 10.1080/002071798222316.

[167] X. Bombois, M. Gevers, and G. Scorletti. "Controller validation based on an identified model". In: *Proc. of 38th Conference on Decision and Control*. 1999.

[168] Y. Tanaka, M. Fukushima, and T. Ibaraki. "A globally convergent SQP method for semi-infinite nonlinear optimization". In: *J. Comput. Appl. Math.* 23 (1988), pp. 141–153.

[169] Z. Hou. *Nonparametric models and its adaptive control theory*. Science Press, 1999.

[170] Z. Hou and S. Jin. *Model free adaptive control: theory and applications*. CRC Press, 2013.

[171] Z. Hou and Z. Wang. "From model-based control to data-driven control: Survey, classification and perspective". In: *Information Sciences* 235 (2013), pp. 3–35. DOI: https://doi.org/10.1016/j.ins.2012.07.014.

This Ph.D. thesis has been typeset by means of the TEX-system facilities. The typesetting engine was pdfLATEX. The document class was `toptesi`, by Claudio Beccari, with option `tipotesi=scudo`. This class is available in every up-to-date and complete TEX-system installation.